Fire Performance of Connections in Laminated Veneer Lumber

Submitted by

Terence Chung Biau, CHUO

Supervised by

Professor Andrew H. Buchanan
and
Associate Professor Peter J. Moss

Fire Engineering Research Thesis
February 2007

A research thesis presented to University of Canterbury in fulfilment of the thesis requirement for the degree of Master of Engineering (Fire)

School of Engineering
University of Canterbury
Department of Civil Engineering
Private Bag 4800
Christchurch, New Zealand

Acknowledgements

First of all I would like to thank my supervisors, Professor Andy Buchanan and Associate Professor Peter Moss, for their enthusiasm for the topic, ideas, support, and guidance. Thanks to Dr. Andrea Frangi for giving his opinion on the research and providing relevant information.

Many thanks to all M.E. Fire Engineering academic staff, Dr. Michael Spearpoint and Dr. Charley Fleischmann, for providing valuable opinions and criticism during regular research meetings throughout the research period.

Thanks also to Dr. Massimo Fragiacomo for his enthusiasm in Timber Engineering, support, ideas and guidance in applying experimental results into spreadsheet models based on Johansen's Equations.

To all the technical staff in College of Engineering, Civil Engineering Department at University of Canterbury, especially Robert Wilsea-Smith, who provided technical support and guidance for the use of machinery.

To Year 2005/2006 Fire Engineering fellow classmates, thank you for all the advice, opinion and help throughout the years. Thanks for giving me an unforgettable experience in university.

Lastly, I also like to express my appreciation to Carter Holt Harvey for sponsoring all the LVL required to conduct the research.

Without involvement from any party listed above, the research would not have been completed.

Abstract

The embedment strength of timber with respect to exposure temperature has not been widely studied. Some studies have suggested that the timber totally loses its embedment strength when the timber temperature reaches 300°C. This research concentrates on the embedment strength study of Laminated Veneer Lumber (LVL) timber product exposed to elevated temperatures up to 250°C using singly bolted connections.

Experiments showed that the embedment strength of LVL decreased at a constant rate from 0.08 kN/mm² to 0.025 kN/mm² once the bolt temperature increased from ambient conditions. The embedment strength was then assumed to remain at strength of 0.025 kN/mm² as the bolt temperature continues to increase from 120°C.

The difference between the estimated failure load based on Johansen's Equations and the experimental failure load for the connections tested under fire conditions was less than 30%. The estimation was based on bolt strength reduction using NZS 3404, the experimental charring rate and the experimental embedment strength. The predicted failure mode agreed with experimental for all types of connection.

Table of Contents

List of Figures

List of Tables

1 Introduction

1.1 Background

Wood is one of the oldest construction materials known and continues to be used as a construction material (Buchanan, 2002). This is because the basic characteristics of timber are useful in many structural and finishing roles in buildings. Wood has the following characteristics which other construction materials may not offer:

1. It is a renewable resource;
2. It has insulation benefits; and
3. It has excellent strength-to-weight ratio.

Most of the houses in New Zealand (NZ) have been built using timber frames because timber is readily available and is easy to work with. Timber is also used in humid and corrosive environments such as indoor swimming pools. The other reason NZ widely uses timber is because NZ's climate is ideal for growing radiata pine. The rate of forest plantation turn-over in NZ is twice the rate in other places in the world (Walker, 1993). This fact not only encourages timber as building material but also contributes significantly towards the NZ economy (NZFI, 2006).

One of the issues with these fast growing pine trees is that they are subjected to unpredictable distortion compared to the slower growing trees during the drying process. These distorted timber studs have virtually no structural benefit. Laminated Veneer Lumber (LVL), which is similar to Glue Laminated Timber (glulam), has better properties compared to the traditional sawn timber. The weakest point of each veneer layer is only one veneer layer depth and all the weakest points are randomly distributed between layers. This gives LVL virtually uniform properties along its length.

Traditional types of connections used for timber construction are screws, nails, bolts, dowels and epoxy steel rods. It is widely recognised that the weakest point in a timber construction is usually at the timber connections (Buchanan (2001) and Lau (2006)).

Therefore to ensure the reliability of the timber construction, design of timber connections is emphasized rather than the timber members.

This research was extended from the research conducted by Lau (2006). In Lau's study of bolted connections, after exposing the pre-loaded timber connections to fire condition, the drilled holes that accommodate the bolts appeared to have elongated by the action of the elevated temperature bolts (see Figure 1-1). This phenomenon is caused by either charring around the hot fastener or the softening of timber at elevated temperature which allows the timber to be crushed more easily. Therefore this led to the study in this research thesis.

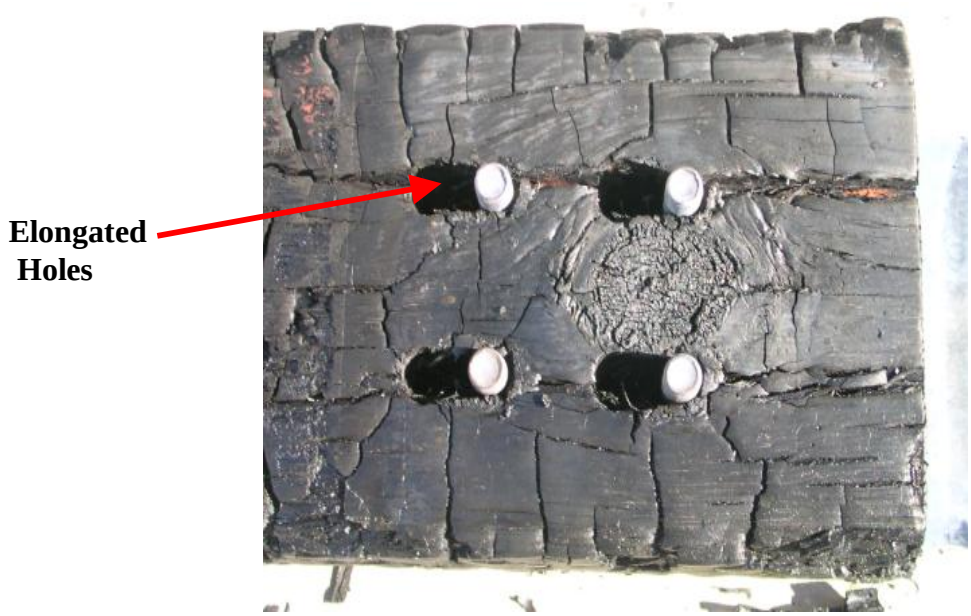

Figure 1-1: Typical consequence of timber connection after fire exposure (Lau, 2006).

1.2 Objectives of Research

The overall aim of this project is to provide fire performance information about bolted connections exposed to various uniform temperature conditions as well as standard fire curves. The connections are designed for either the bottom chord of a timber roof truss or a floor truss. The "embedment strength" of timber at elevated temperatures will also be studied. Embedment strength can be defined as the crushing force that timber can bear per unit area. The higher the embedment strength value means that the required force to crush the timber per unit area is higher. The steps to achieve this aim will be discussed as the following section.

In addition, the aims of the studies are:

1. To compare the fire performance of connections with different geometric arrangement, using wood and steel splice plates.
2. To investigate the temperature profiles of bolts and timber surfaces adjacent to bolts across the cross section of the timber structure.
3. To investigate the correlation between the constant temperature tests and fire tests.
4. To develop a simple method of predicting the load capacity of connections in timber structures.

1.3 Scope of Research

The experiments required in this research are categorised into three separate categories, namely Ambient Tests, Heated Tests and Fire Tests. With the results obtained from each experiment, the embedment strength of LVL at elevated temperature is predicted using Johansen's Equation. Each category is briefly described as below.

1. **Ambient Tests (For singly-bolted connections)**

   As the name suggested, the specimen for Ambient Test are not heated before loads are introduced to the specimen. Even though the specimen is not heated, the experiment is still carried out using the test frame holding the furnace. This test is carried out using singly-bolted connections. Singly-bolted connection will be discussed in Chapter 4. Displacement of the centre members during the testing is recorded.

2. **Heated Tests (For singly-bolted connections)**

   This test is carried out using singly-bolted connections. A pre-test heating phase of two hours at the desired furnace temperature is required for all the Heated Tests. During this two hour period, the specimen will absorb the external heat and the temperature of the whole specimen will elevate and stabilise. Temperatures at various defined spots and the displacement of the centre members are recorded.

3. **Fire Tests**

   Two different bolt arrangement types for each type of connection are exposed to real fire tests, one specimen with only one bolt and the other with multiple bolts. For a fire test, once the specimen is in place in the furnace, the specimen will be pre-loaded for 20 minutes before turning on the furnace. The temperatures at various defined spots and the displacement of the centre members are recorded.

4. **Embedment Strength Prediction**

   Based on the type of failure mode, the maximum experimental load applied at 10mm displacement and the bolt temperature obtained from the Heated Tests, the embedment strength of LVL can be calculated by implementing into the relevant Johansen's Equations.

5. **Estimation of failure load and failure mode for fire tested connections**

   The predicted failure mode and failure load for connections exposed to fire conditions can be done by substituting the experimental charring rate and the embedment strength relation obtained from the Ambient and Heated Tests into the relevant Johansen's Equations. The result of the actual failure time, failure load and failure mode were compared with the predicted results.

1.4 Outline of Thesis

Chapter 1 of this thesis gives an overview of timber usage in construction sector, together with the objectives of this research. A literature review was conducted and is summarised in Chapter 2. Literature review is undertaken prior to the experimental task of the research. Chapter 3 describes the available testing equipment that is used in the experimental section of this research. Chapter 4 describes the testing specimens as well as performing the calculations for determining the load capacity of each testing specimen. The experimental procedures are summarised in Chapter 5. Chapter 6 contains the results from all the experimental testing and is followed by the discussion of the results in Chapter 7. The experimental conclusions and recommendations for future research are included in Chapter 8.

2 Literature Review

2.1 Outline of chapter

This chapter reviews and summarizes of all topics relevant to this research. The summary can be categorised into three different sections, i.e. the reviewed information at normal conditions, the reviewed information at elevated conditions, as well as national code requirements.

2.2 Normal Conditions

2.2.1 Timber Connections

The strength and the stiffness of structural members and structural connections determine the stability and the performance of the structure (Buchanan, 2001). It is important that the structural members and the connections to perform to their best throughout the designed lifetime of the structure. This includes normal functioning conditions and low probability conditions such as earthquake and fire incidents.

According to Buchanan (2001), the timber connection strength at elevated temperature is much less easy to predict compared to that of the structural members. Therefore to ensure that the connection can perform well during a fire incident, the connections must have a better fire resistance than the main structural members. In practice, most timber connections use either metal fasteners or adhesives. Even though metal fasteners and adhesives type fasteners have competitive performance at ambient temperature, they have very different fire performance characteristics (Buchanan, 2001). Epoxy glue virtually loses all its strength when the temperature reaches 70°C and above. This means that epoxied connections lose all their strength at elevated temperature.

For a timber structure with a metal fastener connection, one may think that the behaviour of the structure connection becomes unreliable at elevated temperatures due to the natural expansion of metal. However, this may not be the most significant

concern. At high elevated temperatures, the metal will loose its strength considerably. Alongside this, the high temperature causes the timber to char and lose strength (Buchanan, 2001). The metal fastener, which is more heat conductive, will conduct the heat from the surface into the core of the connection, which enhances the softening of timber.

Some widely used metal fasteners are bolts, screws, nails and truss plates. Because bolts are the only type of fastener considered in the research, their performance will be reviewed in the following section.

2.2.2 Bolts

2.2.2.1 General

Bolts are categorised as dowel type fasteners. They are commonly made from ordinary mild steel with hexagonal heads and nuts and usually mass produced in a diameter range up to 30mm. Square headed bolts and nuts are also available commercially. Bolts are normally used for double or multiple sheared timber-to-timber joints, panel-to-timber joints or steel-to-timber joints. Bolts pass through the holes that were drilled in all members.

2.2.2.2 Practice Criteria

The thickness of each member is vital to ensure the performance of the joints. According to Timber Engineering STEP 1 (1995), the side member thickness must be at least 30mm and the main member must have minimum thickness of 40mm for a timber joint. Washers are required under any heads and nuts for tightened bolts in contact with timber member. Included in the Eurocode 5 (2004), the washer must have size length or a diameter of at least (3×d) and thickness of at least (0.3×d), where d represents the diameter of the bolt. This is to constrain the heads and nuts from embedding into the timber. The NZS 3603 does not include the requirement for timber member thickness. However, the required washer size is summarised in Section 2.4.1.4.

For ease of installation, Eurocode 5 (2004) requires holes to be drilled 1mm larger than the bolt diameter. On the other hand, NZS 3603 (1994) permits the holes to be drilled 10% larger than the bolt diameter. In this research, larger tolerances for drilled holes are necessary because the thermocouple wire is to be inserted parallel along the shank of bolts. However, one drawback of having larger holes for the bolts is the reduction of stiffness of the bolted joints.

Carefully spacing of bolts in a joint is essential. Spacing the bolts either too close to the edge of the member or too close together cause premature failure such as by splitting. NZS3603 (1994) and Eurocode 5 (2004) include minimum spacing and minimum edge distance required for bolt joints.

2.2.2.3 Potential Issue of Bolts in Elevated Temperature Conditions

In bolted joints, the head and the nut of the fasteners are exposed to the external environment. Depending on the architectural design, it may visually be a unique characteristic or it may be a negative aspect. However, from the fire engineering perspective, exposing heads and nuts enhances the heat transfer from the environment into the core of the connection at the initial fire developing stage. This poses an integrity problem for the joints, especially the embedding strength of timber. Therefore this is focused on in this research.

2.2.3 Embedment Strength of Timber

2.2.3.1 General

One of the most important factors that determine the load carrying capacity of a bolted connection is the embedding strength of the timber member (Timber Engineering STEP 1, 1995). At the same time, the geometry of the joint and the yield moment of the fastener also influence the load carrying capacity.

As defined in Timber Engineering STEP 1 (1995), the embedding strength is the average compressive stress at maximum load in a specimen of timber or wood based panel under the action of a stiff linear fastener with the fastener's axis perpendicular to the surface of the specimen. Embedment strength itself is a system property instead of an individual wood property. This is because embedment strength depends on:

1. The density of the timber or wood based panel members;
2. The diameter of bolt,
3. The angle between force and grain direction; and
4. The friction between fastener and timber or wood based panel members.

As discussed in the previous section, the tolerance of drilled holes in timber member reduces the load carrying capacity of the joint system. However, the friction between the bolt and the timber as well as the constraint produced by the washers under the heads and nuts increases the load carrying capacity. The effect of the increased capacity is called the 'chain effect' or 'rope effect'.

The review of the embedment testing procedures according to ISO 10984-2 (1999) standard is included in the Code Requirement category.

2.2.3.2 Embedment Testing at Elevated Temperatures

Chapuis and et al. (2005) conducted tests on the embedment resistance of timber under heated conditions. The findings from the experiments showed that embedment strength decreases initially as the temperature increases from 20°C to approximately 80°C. A local minimum occurs at 80°C with an embedment strength magnitude of 30% compared to that when the temperature is 20°C. As the temperature continues to increase, the embedment strength increases slightly up to 140°C before decreasing again to 200°C. This is due to the positive effect on the strength of wood drying. Embedment strength testing beyond 200°C was not conducted.

2.2.3.3 Embedment Strength Calculations

The equation to calculate the embedment strength, f_h is shown below:

$$f_h = \frac{F_{max}}{d\,t} \qquad \text{Equation 2-1}$$

where F_{max} = Maximum load
d = Diameter of dowels
t = Thickness of specimen

Some other relevant equations for calculating initial deformation, elastic deformation, foundation modulus and others can be found in ISO 10984-2 (1999). The Load-Deformation curve shall be corrected as shown in the same reference, if necessary.

2.2.3.4 Characteristic Embedment Strength Calculations

According to Eurocode 5 (2004), for bolts and dowels of size up to 30mm diameter, the characteristic embedding strength values for timber loaded parallel to the grain direction, $f_{h,0,k}$ in units of N/mm² is:

$$f_{h,0,k} = 0.082(1 - 0.01d)r_k \qquad \text{Equation 2-2}$$

where d = Diameter of bolts [mm]
ρ_k = Wood density [kg/m³]

The characteristic embedding strength values for timber when loaded at an angle to the grain direction, $f_{h,\alpha,k}$ in units of N/mm² is:

$$f_{h,a,k} = \frac{f_{h,0,k}}{k_{90}\sin^2 a + \cos^2 a} \qquad \text{Equation 2-3}$$

where $f_{h,0,k}$ = Characteristic embedding strength for timber loaded parallel to grain direction [N/mm²]
d = Diameter of bolts [mm]
ρ_k = Wood density [kg/m³]
k_{90} = Timber category dependent factor [-]

The k_{90} value is dependent on the timber is a softwood or a hardwood. In NZ, most of the timber used for timber construction is softwood and LVL is made of softwood, therefore k_{90} can be calculated according to Equation 2-4. The equation to calculate k_{90} for hardwood can be found in Eurocode 5 (2004).

$$k_{90} = 1.35 + 0.0015d \qquad \text{Equation 2-4}$$

As soon as the structural joint is loaded at an angle to the grain direction, the characteristic strength drops. As shown in Figure 2-1 below, the rate of decrease for the embedment strength of softwood is greater than for hardwood due to a larger k_{90} value for softwood independent of bolt diameter.

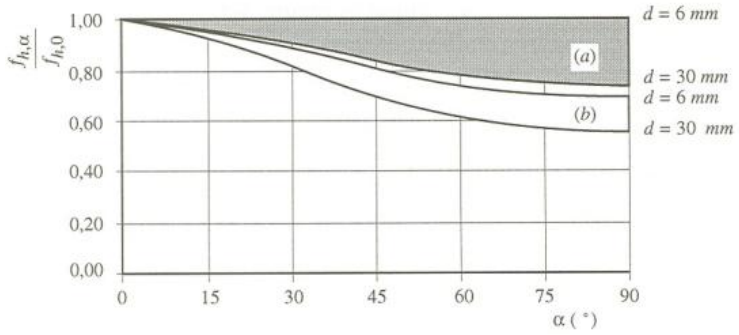

Figure 2-1: Influence of loading angle on embedding strength (a) Softwood, (b) Hardwood (Timber Engineering STEP 1, 1995).

2.2.3.5 Characteristic Embedment Strength of LVL

Scheibmair (2003) conducted detailed studies related to the embedment strength testing for Hyspan – LVL. Instead of using the F_{max} value to calculate the embedment strength of LVL (see Equation 2-1), Scheibmair used the lower fifth percentile load and the cross sectional area between the timber and dowel interface shown below.

$$f_{h,k} = \frac{P}{A} \qquad \text{Equation 2-5}$$

Where $f_{h,k}$ = Characteristic embedding strength

P = Lower fifth percentile embedment load

A = Cross-sectional area between timber and dowel = d × t where d = bolt diameter, t = timber member thickness

The characteristic embedment strength found for Hyspan – LVL when loaded parallel to grain direction was 53.8 MPa. When loading direction is perpendicular to the grain direction, the characteristic embedment strength reduced to 41.8 MPa.

2.2.4 Laminated Veneer Lumber (LVL)

Among all the material used in the research project, namely LVL, mild steel plates and bolts, the characteristics and mechanical performance of mild steel plates and bolts are well defined compared to LVL. Since LVL is made of natural material, its properties are the most variable compared to the other two materials used in the experiment (Scheibmair, 2003). By understanding characteristics of timber and the manufacturing process of LVL, the material behaviour of LVL can be obtained.

The development history of LVL is summarised in Lau (2006), Müller (2000) as well as in CWC (web page). The process of making LVL is found in Lau (2006) and Scheibmair (2003). Beside that, Nelson Pine Industries Ltd (web page) includes the process of manufacturing the LVL. The making of LVL may differ slightly from one company to another and the product produced from each different company may differ slightly as well.

2.2.4.1 Characteristics of LVL

Compared to sawn timber and glue laminated timber (glulam), the material properties of LVL are much more closely spread about their average value. This is due to the number of layers of veneers used in LVL compared to glue-laminated timber. Sawn timber always has the largest variability because the weakest point within a sawn timber, usually the largest knots, may penetrate throughout the depth of timber. For glue-laminated timber, the material characteristics are vary less than sawn timber boards for the reason that multiple studs are glued together. Therefore the weak point of glulam only penetrates through thickness of one lamination and the possibility of having multiple weak points aligned is negligible. Similarly to glulam, the weak point for LVL only penetrates through each veneer thickness. Due to the large number of

veneer layers, the weak points can be regarded as randomly distributed within the LVL. Thus, LVL can be assumed to have negligible defects. As a consequence, the material properties of LVL can be determined confidently and closer to the mean value than sawn timber and glulam as shown in Figure 2-2.

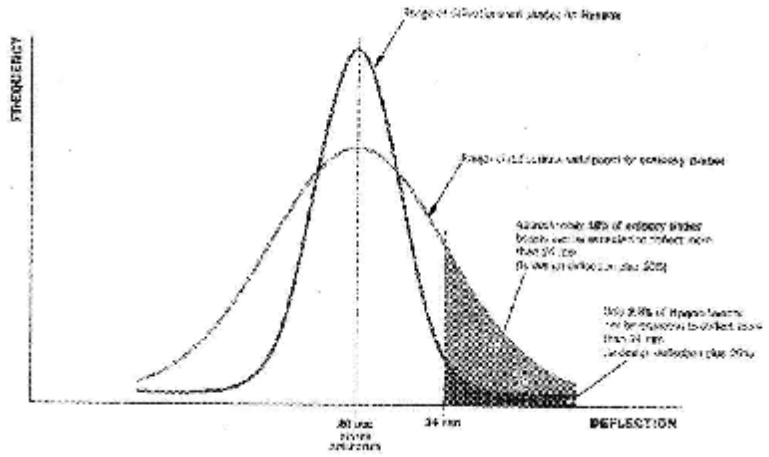

Figure 2-2: Comparison of material characteristics (CHH, 2002).

2.2.4.2 LVL Products

There are several difference ranges of LVL products available commercially. Each type of LVL product has its unique application and functions. The types of products are namely Hyspan; Hybeam; Hy90; Hychord; Truform; Edgeform and Hyplank. The functions and properties of each type of product can be found in the product information brochures of Carter Holt Harvey (CHH, 2002 – 2004). Since Hyspan is the only product used for the research, the information for Hyspan is summarised below. Most of the LVL products can be treated with chemicals (CHH, 2002a) to class H3. The treated products can withstand the weather.

2.2.4.2.1 Hyspan – Structural LVL (CHH, 2002)

The Structural LVL – Hyspan is specially fabricated for structural usage which complies with the requirement of AS/NZS 4357 (1995). It has very high structural reliability and has very consistent dimensional accuracy.

Typical usages of this type of LVL are namely rafters, floor joints, beams and lintels members in the framing of houses and similar buildings. Readily available Hyspan sizes are of thickness ranging from 36mm to 63mm and with depth from 150mm to 600mm.

The limit state properties for design with Hyspan tabulated in the technical information brochures for Hyspan published by CHH (2002) is duplicated as Table 2-1 below.

Table 2-1: Limit state properties for design with Hyspan (CHH, 2002).

Elastic Moduli		
Modulus of elasticity	E	13200 MPa
Modulus of rigidity	G	660 MPa
Characteristic Strength		
Bending	f'_b	42 MPa
Tension parallel to grain	f'_t	27 MPa
Compression parallel to grain	f'_c	34 MPa
Shear in beams	f'_s	4.5 MPa
Compression perpendicular to grain	f'_p	12 MPa
Shear at joint details	f'_{sj}	4.8 MPa
Joint Group		J4

2.2.5 Johansen's Yield Theory – European Yield Theory

2.2.5.1 General

Johansen's Yield theory had been widely used to predict the failure mode of timber connections in ambient conditions. The predictions are made based on known the timber member thickness, yield moment and diameter of fasteners used as well as the embedment strength of the timber. According to Timber Engineering STEP 1 (1995), one important assumption for the derivation of Johansen's ultimate load equations is that the fastener and the timber are assumed to perform as ideal rigid materials. This

means when load is applied to force the fastener into the timber, no movement will be detected until the load reaches the ultimate load (See Figure 2-3 (a)). When the ultimate load is reached, the embedment rate is constant. However, timber does not perform as rigid material. A realistic load-embedment curve is shown as Figure 2-3 (b). Typically, as the load increases, the rate of embedment increases. When the load reaches its ultimate value the embedment rate becomes constant.

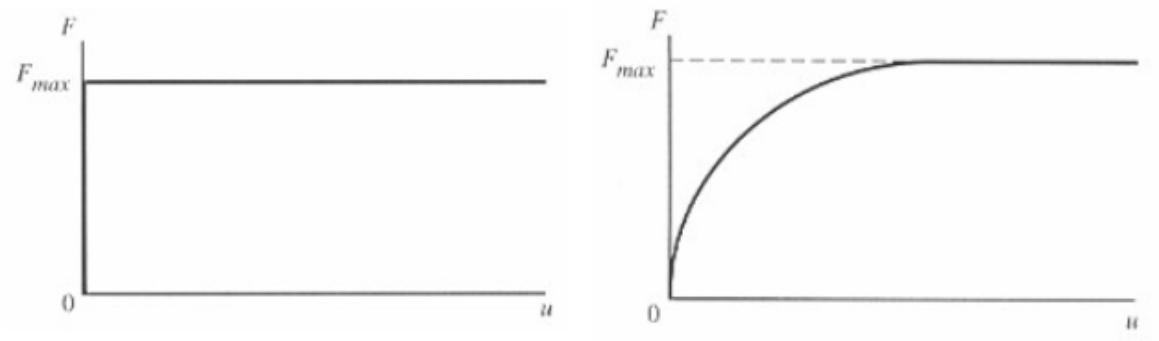

(a) Ideal **(b) Real**

Figure 2-3: Load-embedment characteristic (Timber Engineering STEP 1, 1995).

2.2.5.2 Nomenclature for Johansen's Equations

The descriptions of variables used in Johansen's Equations are listed in Table 2-2.

Table 2-2: List of variables used in Johansen's Equations

Variables	Descriptions	Units
t	Timber thickness	mm
f_h	Embedding strength	kN/mm²
$b = \frac{f_{h,2,k}}{f_{h,1,k}}$	Characteristic embedding strength ratio	[-]
d	Fastener diameter	mm
M_y	Fastener yield moment design value	kNmm
F	Resistance per shear plane per fastener	kN
$F_{ax,Rk}$	Characteristic axially withdrawal capacity of the fastener	kN
Subscript 1	Side members	[-]
Subscript 2	Centre member	[-]
Subscript k	Characteristic value	[-]
Subscript d	Design value	[-]

2.2.5.3 Johansen's Equations

Johansen's Equations can be categorised into two major categories, namely Timber-to-Timber (or Wood Products) connections and Steel-to-Timber connections. For Timber-to-Timber connections, the structural members are made of timber products only while for Steel-to-Timber connections, steel plates are used either as side members or centre member in the structural connection. Under each category, the equations are subdivided for a single shear plane and double shear plane connections. Thelandersson and Hans (2003) and Timber Engineering STEP 1 (1995) give similar Johansen's Equation whereas the Eurocode 5 (2004) gives slightly different equations. Eurocode 5 (2004) identified the importance of the rope effect contribution to the connection strength and therefore included the rope effect functions into the original Johansen's Equations. The rope effect is the term used to describe the clamping effect of fasteners into the timber connections when it bends (see Figure 2-4).

(a) Before load application **(b) After load application**

Figure 2-4: Rope effect on connection when the bolt bends.

In this research, the Johansen's Equations used are taken from Eurocode 5 (2004). The equations which are relevant to this research are included in Table 2-3 and Table 2-4 below:

Table 2-3: Johansen's Equations for double sheared timber – to – timber connections (Eurocode 5, 2004)

	Failure Mode		Equations	Reference
Timber-to-Timber (Panel-to-Timber) Connections (Double Shear)	G	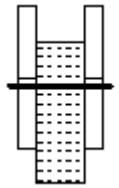	$F_{V,RK} = f_{h,1,k} t_1 d$	Equation 2-6
	H	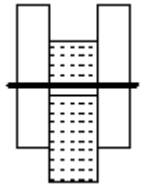	$F_{V,RK} = 0.5 f_{h,2,k} t_2 d$	Equation 2-7
	J	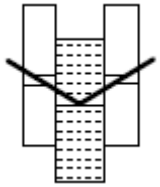	$F_{V,RK} = 1.05 \frac{f_{h,1,k} t_1 d}{2+b} \left[\sqrt{2b(1+b) + \frac{4b(2+b) M_{y,Rk}}{f_{h,1,k} d t_1^2}} - b \right] + \frac{F_{ax,Rk}}{4}$	Equation 2-8
	K	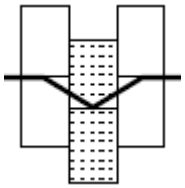	$F_{v,Rk} = 1.15 \sqrt{\frac{2b}{1+b}} \sqrt{2 M_{y,Rk} f_{h,1,k} d} + \frac{F_{ax,Rk}}{4}$	Equation 2-9

Table 2-4: Johansen's Equations for double sheared alternating timber – to – steel connections (Eurocode 5, 2004)

		Failure Mode		Equations	Reference
Steel-to-Timber Connections - Steel Plate as Centre Member (Double Shear)		F	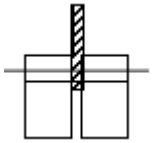	$F_{v,Rk} = f_{h,1,k} t_1 d$	Equation 2-10
		G	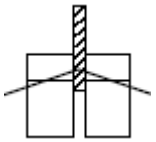	$F_{v,Rk} = f_{h,1,k} t_1 d \left[\sqrt{2 + \frac{4M_{y,Rk}}{f_{h,1,k} d t_1^2}} - 1 \right] + \frac{F_{ax,Rk}}{4}$	Equation 2-11
		H	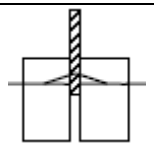	$F_{v,Rk} = 2.3\sqrt{M_{y,Rk} f_{h,1,k} d} + \frac{F_{ax,Rk}}{4}$	Equation 2-12
Steel-to-Timber Connections – Timber as Centre Member (Double Shear)	**Thin Steel**	K		$F_{v,Rk} = 1.15\sqrt{2M_{y,Rk} f_{h,2,k} d} + \frac{F_{ax,Rk}}{4}$	Equation 2-13
	Independent of steel thickness	J Or L	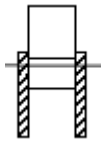	$F_{v,Rk} = 0.5 f_{h,2,k} t_2 d$	Equation 2-14
	Thick Steel	M	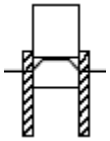	$F_{v,Rk} = 2.3\sqrt{M_{y,Rk} f_{h,2,k} d} + \frac{F_{ax,Rk}}{4}$	Equation 2-15

Equation 2-8, Equation 2-9, Equation 2-11, Equation 2-12, Equation 2-13 and Equation 2-15 have another additional term $\frac{F_{ax,Rk}}{4}$ which takes into account the rope effect. Eurocode 5-1 (2004) suggested a maximum value of 25% of the Johansen part of the equations. Therefore these equations can be simplified as shown below:

$$F_{V,RK} = 1.25\left\{1.05\frac{f_{h,1,k}t_1 d}{2+b}\left[\sqrt{2b(1+b)+\frac{4b(2+b)M_{y,Rk}}{f_{h,1,k}dt_1^2}}-b\right]\right\} \quad \text{Equation 2-8(i)}$$

$$F_{v,Rk} = 1.25\left\{1.15\sqrt{\frac{2b}{1+b}}\sqrt{2M_{y,Rk}f_{h,1,k}d}\right\} \quad \text{Equation 2-9(i)}$$

$$F_{v,Rk} = 1.25\left\{f_{h,1,k}t_1 d\left[\sqrt{2+\frac{4M_{y,Rk}}{f_{h,1,k}dt_1^2}}-1\right]\right\} \quad \text{Equation 2-11(i)}$$

$$F_{v,Rk} = 1.25\left\{2.3\sqrt{M_{y,Rk}f_{h,1,k}d}\right\} \quad \text{Equation 2-12(i)}$$

$$F_{v,Rk} = 1.25\left\{1.15\sqrt{2M_{y,Rk}f_{h,2,k}d}\right\} \quad \text{Equation 2-13(i)}$$

$$F_{v,Rk} = 1.25\left\{2.3\sqrt{M_{y,Rk}f_{h,2,k}d}\right\} \quad \text{Equation 2-15(i)}$$

According to Timber Engineering STEP 1 and Eurocode 5-1 (2004), connections that consist of steel members of thickness less than or equal to (0.5 × d) are considered as a thin steel connections. If the steel thickness is greater or equal to (1.0 × d), they are considered as a thick steel connection. For intermediate steel thicknesses, the load carrying capacity can be predicted by linear interpolation from the equation for thin and thick steel plates. In this research, the steel plate used is at the boundary condition of intermediate and thin steel plate.

2.2.6 Potential Timber Failure Mode

According to Quenneville and Mohammad (2000), there are four potential failure modes that can occur when timber is subjected to conditions in excess of the ultimate condition. They are crushing, splitting, shear plug failure and tear out as shown in Figure 2-5. Wood tension failure is also possible if the width of the timber section is small. Each failure mode will be described briefly.

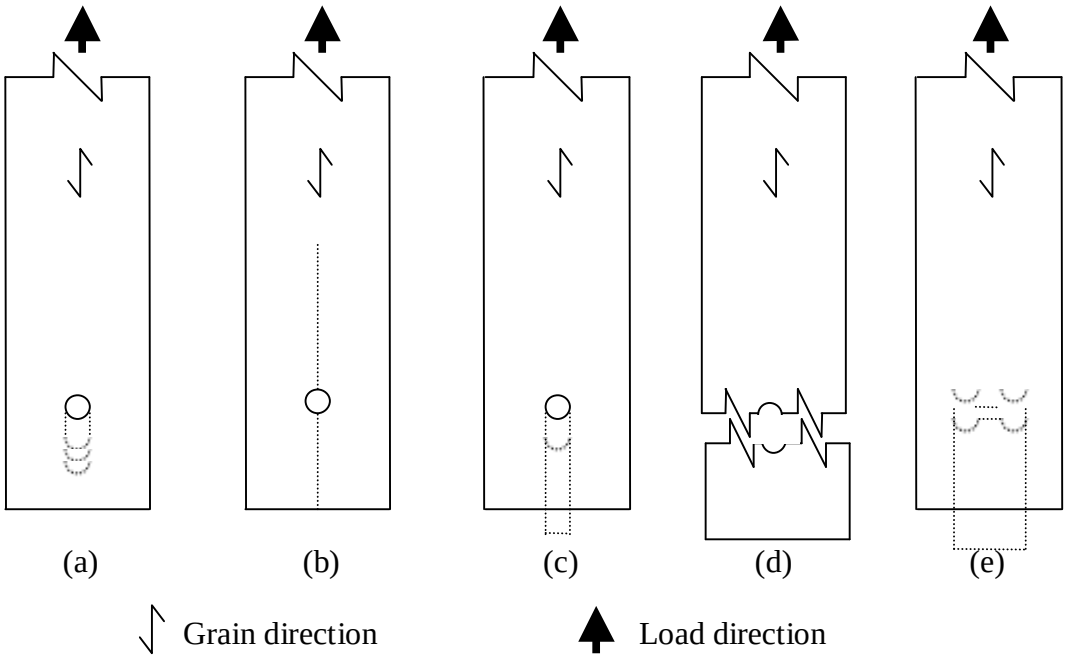

Figure 2-5: Potential Failure Mode of Timber (Quenneville and Mohammad, 2000).
(a) Crushing, (b) Splitting, (c) Shear plug, (d) Wood Tension, (e) Tear Out (for 2 bolts)

2.2.6.1 Crushing (C)

When load is applied, the fastener starts to push into the timber. Wood as a relatively soft material will absorb the force by crushing of the fibres. This failure mode can occur when load is applied either parallel or perpendicular to the grain direction and when the distance between the end of timber and the fastener is reasonable large. When the loading direction is perpendicular to the grain direction, the crushing deformation is not the same as the deformation caused by loading parallel to the grain direction. This is due to the length of wood fibres.

2.2.6.2 Splitting (S)

Splitting usually occurs along the weakest line parallel to the grain direction and is mainly caused by tension perpendicular to the grain. When the applied load reaches the critical value of wood, the wood will split along the grain direction.

2.2.6.3 Shear Plug (SP)

Shear plug failure can only occur when load applied is parallel to the grain direction. This failure mode usually occurs when the fastener is near to the end of the timber. When load is applied up to its critical point, a piece of wood (usually of width about that of the fastener diameter) is sheared off.

2.2.6.4 Wood Tension (WT)

In this failure mode the whole cross section of the timber is broken. This failure usually occurs when the width of the timber is small, and when the hole is very large.

2.2.6.5 Tear Out (TO)

Tear out failure is a combination of tearing and shearing. When load is applied, the timber in the line of the fasteners is torn apart and the timber is shorn off. This failure only occurs in multiple connector joints.

2.3 Elevated Temperature Conditions

2.3.1 Behaviour of Timber at Elevated Temperatures

2.3.1.1 General behaviour

Timber is categorised as combustible material because it burns when subjected to elevated temperature. However, the ease of ignition of timber is low compared to highly combustible materials such as gasoline. If a solid timber is to be ignited within a short to medium period without an external ignition source, the surface temperature of a solid timber needs to be well beyond 400°C (Timber Engineering STEP 1 (1995)). With the presence of an external ignition source, timber will ignite at a lower, but still considerably high temperature, of 300°C (Timber Engineering STEP 1 (1995) and Babrauskas (2003)). The density of timber plays a role on the ease of ignition of timber as well. The higher the density the longer it will take to ignite the timber (Timber Engineering STEP 1 (1995)).

For burning timber, the heat release rate (HRR) is dependent on the oxygen availability. Also, the HRR depends on the shape and size of timber, the nature of initial heating regime and the density of the timber (Timber Engineering STEP 1). Large surface to volume ratio encourages the combustion of timber. It not only increases the ease of ignition, it also stimulates faster flame spread. The relationship between wood density (oven-dry) and rate of combustion is shown in Figure 2-6.

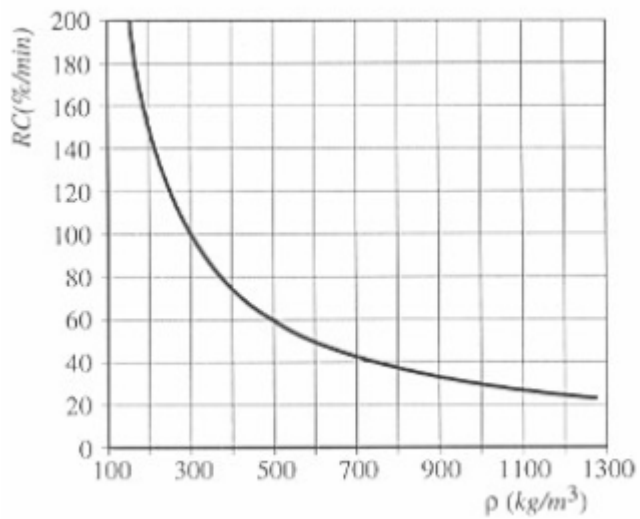

Figure 2-6: Relationship between density and rate of combustion.
(Timber Engineering STEP 1 (1995))

From Figure 2-6, it can be seen that the higher the wood density the lower the rate of combustion.

2.3.1.2 Behaviour of timber at various elevated temperatures

Under elevated temperature, wood undergoes chemical decomposition by giving off organic combustible gases, a process called pyrolysis. Once the combustion process has taken place, a layer of charcoal is formed. This layer of char acts as an insulation around the unpyrolised wood since the thermal conductivity of charcoal is only one sixth of the value for dry solid timber (Timber Engineering STEP 1).

Chapuis et al (2005) reported that, the lignin of the wood undergoes a glass transition stage when the wood temperature reaches 70°C to 80°C. According to the authors, "*Shear stress is generally not affected by fibre strength but mostly related to the*

failure of the lignin matrix". The degradation of the lignin is the main problem in timber structures at elevated temperature. It results in crushing of the timber when the structure is loaded. On the other hand, Reszka and Torero (2006) suggested the lignin matrix reached the glass transition phase at approximately 100°C.

Once the wood temperature reaches 100°C, the moisture in the wood starts to evaporate. As the moisture in the wood evaporates, the dimension of the wood shrinks. The steam generated in the wood takes the lowest resistance path, such as open pores and joints, to escape from the timber. If the surrounding temperature of the timber is beyond 100°C, the temperature of the timber will remain at 100°C until all the moisture in the timber has evaporated. This is because all the heat absorbed by the timber is used to evaporate the moisture.

According to Timber Engineering STEP 1 (1995), once the temperature in the timber reaches 150°C to 200°C, the timber undergoes the pyrolysis process. This chemically degrades the timber and gases are generated and released from the timber. Browning on the surface is clearly seen as a result of pyrolysis (See Figure 2-7). Within this range, the gases are mostly incombustible carbon dioxide, CO_2, (70%) and a small portion of combustible carbon monoxide, CO, (30%). The proportion of combustible gases increases as the temperature in the timber increases until ignition occurs.

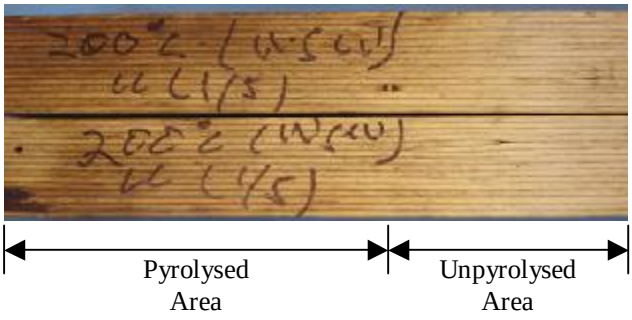

Figure 2-7: Browning of timber surface due to pyrolysis.

Once the timber ignites, the timber surface temperature increases rapidly. The burning consumes the combustible gases that were generated and released. Pyrolysis continues below the burning layer and charcoal starts to form at the burning layer. The rate of char generation increases as the temperature gets higher.

2.3.2 Fire Performance of Structural Timber Members

According to White (2002), the fire endurance of a timber member or wood assembly depends on three different items, i.e.:

1. Performance of any available protective membrane;
2. Extent of charring of the structural wood element; and
3. Load carrying capacity of the remaining uncharred portions of the structural wood element.

Buchanan (2001) published various methods to protect structural members and connections from exposure to elevated temperatures and fire. One of the methods is to protect the structural members and connections from exposure to the external environment by surrounding the members and the connections with gypsum board. Another method is for the timber members to be treated with fire-retardant chemicals before being used (Walker, 1993).

Alternative methods of fire protection for the structural connection are to embed the dowels into the structural members or by applying other timber products, such as plywood or Medium-Density-Fibreboard (MDF). Either method can prevent or delay the dowels from being exposed to elevated temperatures, thus slowing the heat transfer from the external environment into the core of the structures.

When steel plates are to be used as part of the structural connection or when nail-on plates are used in timber connections, these can pose problems to the structural stability at elevated temperature. The large surface area of highly thermal conductive steel encourages the heat to transfer externally into the core of the connections, thus accelerating the thermal degrading process of the timber members. One of the methods to protect the structure from this problem is to paint the steel plate with intumescent paint. Lau (2006) showed that by applying intumescent paint on the steel plates, it greatly increases the fire resistance of the connection. Another method which is not visually attractive, but feasible, is to introduce gypsum board or other timber products around the highly thermal conductive area.

The charring of the timber members is a very significant issue when dealing with structural fire designs. As mentioned previously, timber when exposed to heat will thermally degrade (pyrolysis) and burn away. This reduces the overall dimension of the timber. The dimensional change of the timber due to shrinkage at elevated temperature as described in Section 2.3.1.2 is relatively insignificant compared to the dimensional change caused by combustion, i.e. charring.

The char formed on the surface of the burning area has practically no load carrying capacity (Kodur & Harmathy (2002), White (2002)). Whilst the loads imposed on the member remain constant and the dimension of the members reduces due to burning, the stress on the member becomes larger and larger. The member will lose its load bearing capacity when the cross section of the non-fire damaged (residual section) of the timber member is reduced to the size where the stress applied on the section exceeds the strength of the timber member (Timber Engineering STEP 1 (1995)).

In order to guarantee the survival of a timber structure in the event of fire, the performance of the fire protection around the timber members and its connections has to be reliable. Beside this, the load carrying capacity of the residual section of timber members must be able to continue bearing the stress imposed on it. An assurance about the load carrying capacity of the residual section of the timber member is possible through the understanding of charring effect on timber. The charring effect is described in the following section.

2.3.3 Charring of Wood

2.3.3.1 General

Charring is the process of a char layer forming on the burning surface of timber member when the member was exposed to fire. At elevated temperature, the wood undergoes a pyrolysis process (thermal degradation of wood) and produce combustible gases. The combustible gas is then burned away, leaving the charred layer on the timber surface. The charring process takes place when the timber member reaches a temperature of 280°C to 300°C. Figure 2-8 obtained from White (2002) is a very good example to distinguish the char, pyrolysis and residual timber.

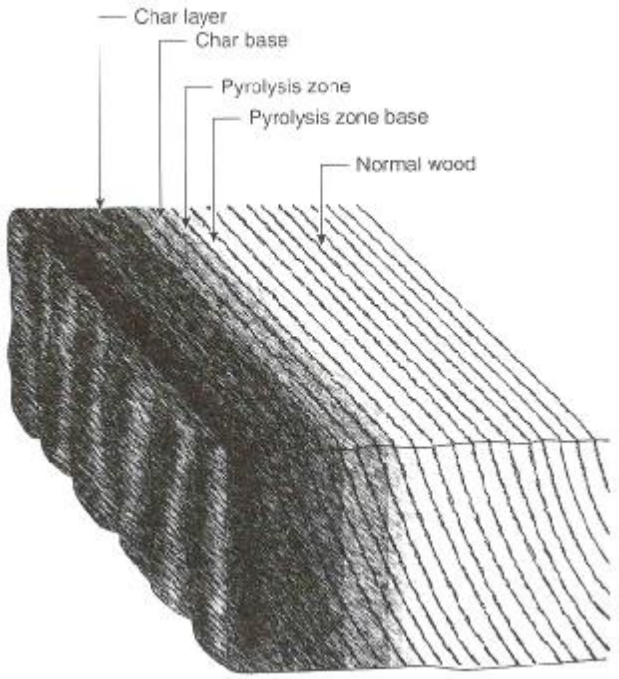

Figure 2-8: Degradation zones in a wood section (White, 2002).

2.3.3.2 Rate of Charring

The fire resistance of a timber member is mainly dependant on the member dimensions. According to Erchinger and Frangi (2005), the load applied during the fire test (30%), 15%, 7.5% of the carrying capacity at normal conditions) has no significant influence on the fire resistance of the connection. The main factor that contributes to the fire resistance of a timber member is the rate of charring, which is dependent on the fire exposure. The charring rate can generally be explained as the linear rate that wood is converted to char (Kodur & Harmathy (2002). Frangi and Fontana (2003) defined the charring rate as the ratio of the distance between the char line from the original wood surface and the fire duration time. A constant value of 0.6mm/min is usually taken as the charring rate. The assumption of a constant charring rate is only valid for ISO-fire exposure conditions. However it is a reasonable assumption provided the timber members are large. In the New Zealand code NZS 3603 (1994), a nominal rate of 0.65 mm/min is adopted. The Australian code AS1702.4:1990 published an equation to calculate the charring rate, β, shown as below:

$$b = 0.4 + \left(\frac{280}{r_k} \right)^2$$ Equation 2-16

Where β = Charring rate [mm/min]

ρ_k = Characteristic wood density [kg/m³]

One limitation of Equation 2-16 is that it is only valid for wood with a moisture content of 12%. One assumption in applying this equation is that there is a pyrolysis layer 7.5 mm thick below the char layer and this has zero load carrying capability. The Australian code is more conservative compared to the Eurocodes, which only assume a 7 mm pyrolysis layer underneath the char layer.

According to Kodur & Harmathy (2002), some primary factors that influence the charring rate are the density, the moisture content, the contraction of the wood and external heat fluxes. Figure 1-10.7 of Kodur & Harmathy (2002) showed that the higher the moisture content, the lower the charring rate. This phenomenon is expected because the moisture in the wood needs to be evaporated before pyrolysis can occur. A similar effect was observed when comparing the wood density, i.e. the higher the wood density, the slower the charring rate. At constant moisture content, the higher the wood density the lower the charring rate. This is directly related to the amount of wood fibre to be degraded.

2.3.3.3 Effect of Char on Timber

The advantage of char on the burning surface is that the char perform as an insulation layer to prevent heat to transfer into the pyrolysis layer. The thermal conductivity of charcoal is only approximately one sixth of the thermal conductivity of a pure solid (Timber Engineering STEP 1 (1995)). Nonetheless, the cracks that formed on the char layer remarkably increase the heat transfer into the pyrolysis layer (Frangi & Fontana (2003)). These cracks can be seen in
Figure 2-9 (Lau (2006)).

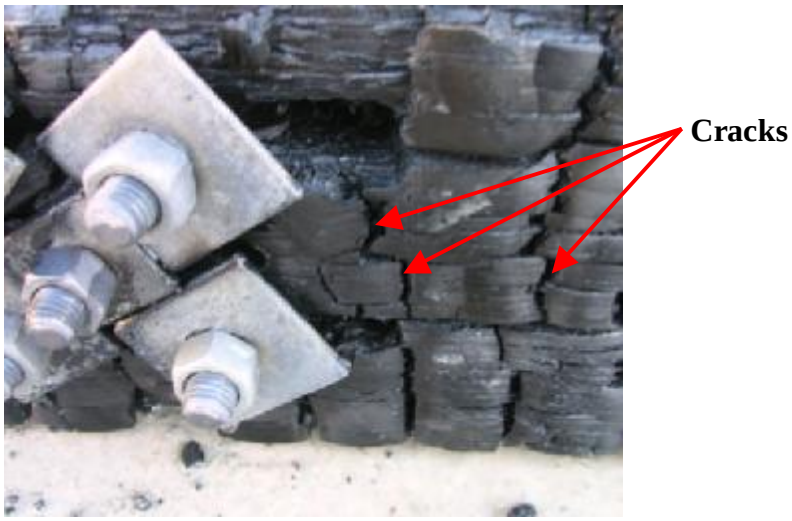

Figure 2-9: Cracks on char layer (Lau, 2006).

2.3.3.4 Charring Line

According to Buchanan (2001), for small members when exposed to fire, allowance for charring around the corners of the cross section of the members must be accommodated. The rounded corners have radius equal to the depth of charring and the cross sectional area lost due to rounding has magnitude of $0.215r^2$. The centre of gravity for the lost area is 0.223r from either side of the member side. Refer to Figure 2-10 for details.

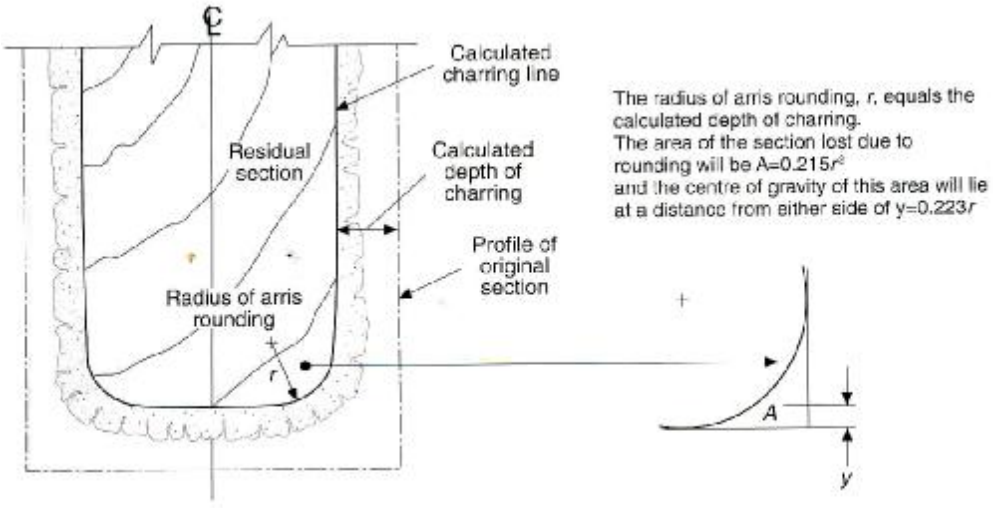

Figure 2-10: Rounded corners of member after fire exposure (Buchanan, 2001)

2.3.4 Fire Resistance Calculation Methods

There are two alternative methods, as described by Buchanan (2001).

2.3.4.1 Effective Cross Section Method (Reduced Cross Section Method)

The Effective Cross Section Method is also known as Reduced Cross Section Method. The basis to calculate the fire resistance of timber member using the effective cross section method is the residual section of timber. The effective depth of char, d_{ef} can be calculated using Equation 2-17.

$$d_{ef} = d_{char} + k_o d_o \qquad \text{Equation 2-17}$$

Where d_{char} = Charring depth [mm]

k_o = Reduction factor [-]

d_o = 7 mm (zero strength of timber below char-line)

The factor k_o is dependent on the required time of fire resistance and the surface protection. Information from Eurocode 5 (2004) includes a summary of the k_o calculation formulae and is reproduced below as Table 2-5:

Table 2-5: k_o values for Equation 2-17 (Eurocode 5 (2004)).

Unprotected Surfaces	$t_{f,req} < 20\,\text{min}$	$k_o = \frac{t_{f,req}}{20}$
	$t_{f,req} \geq 20\,\text{min}$	$k_o = 1$

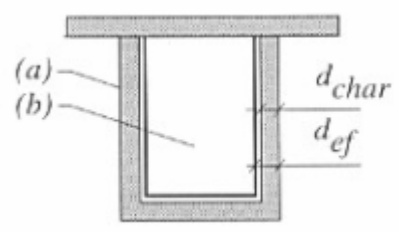

Figure 2-11: Schematic drawing of char line definition (Timber Engineering STEP 1 (1995)).

2.3.4.2 Reduced Strength and Stiffness Method

Based on tests conducted under heated conditions, the relationship between strength and stiffness of timber is approximately linear with respect to the temperature. The higher the temperature, the greater reduction the strength and the stiffness. Using this

relation, an equation for the reduction factor depending on the perimeter of the fire exposed residual cross section (P) and the area of the residual cross section (A_r) was found. This equation is included in Eurocode 5 (2004) as below:

$$k_{\mathrm{mod},f} = 1.0 - \frac{1}{200}\frac{P}{A_r} \qquad \text{Equation 2-18}$$

Where P = Residual cross section perimeter [m]

Ar = Residual cross section area [m²]

A graphical relation for this reduction factor depending on tension (t), compression (c), bending (m) and modulus of elasticity (E) is shown as Figure 2-12.

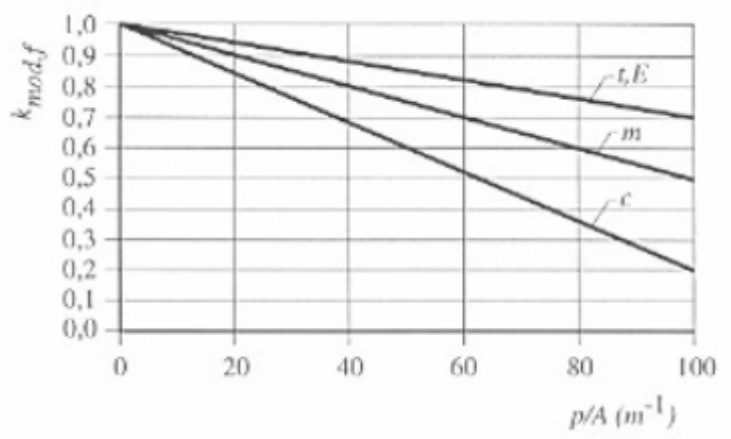

Figure 2-12: Reduction factors for tension, compression, bending and modulus of elasticity at reduced cross-section area (Timber Engineering STEP 1 (1995)).

According to König (2005), studies conducted under fire conditions showed that the influence of temperature on the strength properties of timber is greater compared to those tests conducted under heated conditions.

2.3.5 Fire Severity

2.3.5.1 Overview

Fire severity, as described in Buchanan (2001) is the measure of destructive potential of a fire. In all structural fire safety design, the concept is to have the fire resistance greater (or equal) to the fire severity, i.e. fire resistance ≥ fire severity. The fire resistance is defined as the measure of the ability of the structure to resist collapse, fire spread or other failure during exposure to a fire of specified severity.

There are three methods to define fire severity and fire resistance, namely the time, temperature and strength. They are summarised below:

Methods	Fire Resistance ≥ Fire Severity
Time	Time to failure ≥ Expected fire duration or National Code Requirement
Temperature	Structural Element (or System) failure temperature ≥ Maximum expected fire temperature
Strength	Load Capacity at elevated temperature ≥ Load Carried during fire

2.3.5.2 Standard Temperature Time Curves – ASTM E119 and ISO 834

Two of the most widely known standard temperature time curves for standard fire testings are ASTM E119 (2002) and ISO 834 (2000). Generally both the standard curves give similar trends with a rapid increase temperature during the initial 5 minutes and then maintain a lower rate of temperature increase after 5 minutes.

In the ISO 834 (2000) specification, the standard temperature-time curve follows Equation 2-19, however the standard fire based on ASTM E119 (2002) follows discrete points as shown as Table 2-6 below. Assuming the ambient temperature is 20°C, the temperature for ISO 834 standard fire at the same discrete time as for ASTM E119 is shown in Table 2-6 as well. For ease of presentation, data in Table 2-6 was plotted as Figure 2-13.

$$T = 345\log_{10}(8t+1) + T_o \qquad \text{Equation 2-19}$$

where T_o = Ambient temperature (°C)

t = Time (minutes)

Beside these most common standard time-temperature curves as discussed above, the Eurocode also provides two other alternatives design fires, namely a hydrocarbon fire curve and a external fire curves. However, these alternatives standards are not discussed here. Detailed descriptions are provided in Buchanan (2001).

Table 2-6: ASTM E119 (2002) and ISO 834 (2000) Time-Temperature curves at discrete defined time.

Time (minutes)	ASTM E119 (°C)	ISO 834 (°C)
0	20	20
5	538	576
10	704	678
30	843	842
60	927	945
120	1010	1049
240	1093	1153
480	1260	1257

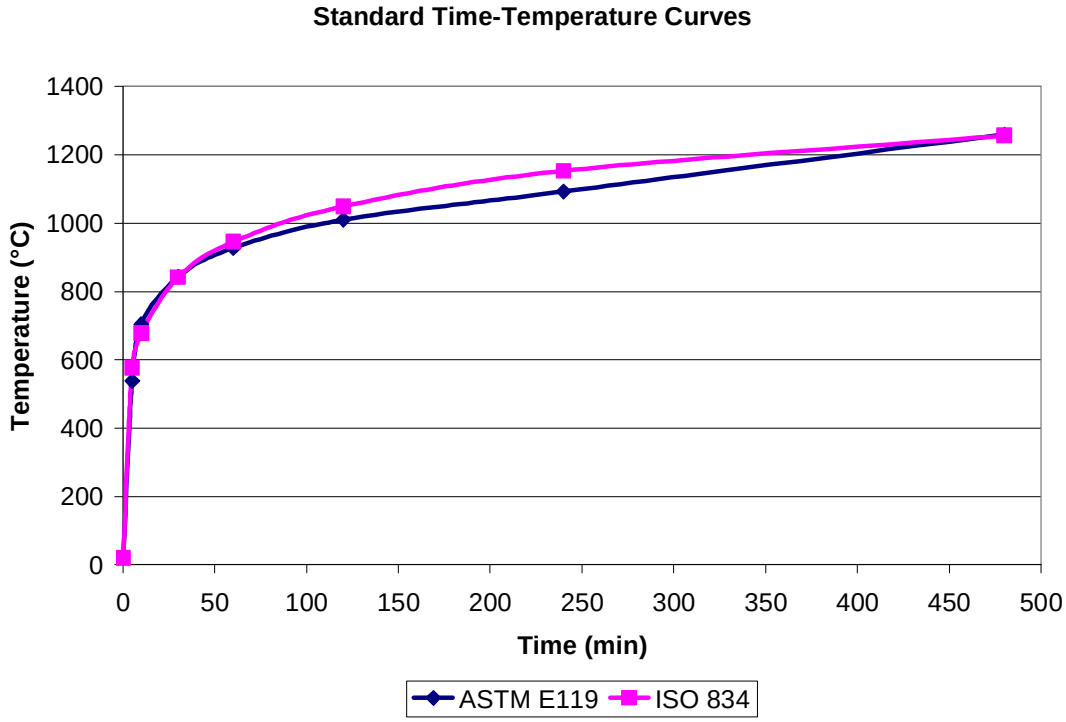

Figure 2-13: Standard Time-Temperature curves.

2.3.5.3 Equivalent Fire Severity

The fire severity posed by standard fire curves (ISO 834 (2000) and ASTM 119 (2002)) is not necessary equivalent to the real fire severity. A real fire may initially have a very sudden rise in temperature and reaching its decay phase shortly after. On the other hand, for a standard fire, the temperature initially rises rapidly (not as rapid as a real fire) for a certain period of time before continuing increasing temperature at a slower rate. This is illustrated in Figure 2-14 below.

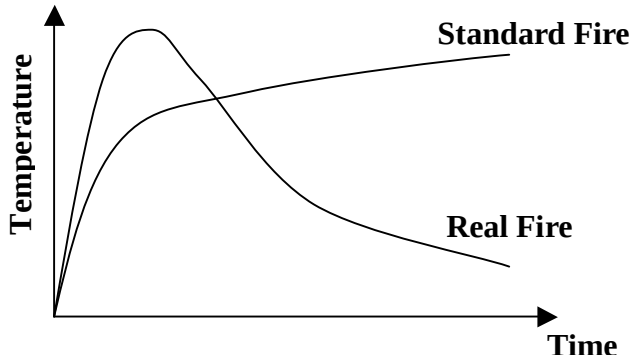

Figure 2-14: Example of a Real fire and a Standard fire.

All standard fire resistance tests are conducted using exposure to standard fire curves. In order to convert the fire resistance from standard fire testing to a realistic fire conditions or vice versa, a method of equalising fire severity is required. Buchanan (2001) published several methods to calculate the equivalent fire severity. The methods are:

1. Equal area concept,
2. Maximum temperature concept,
3. Minimum load capacity concept,
4. Time equivalent formulae – (i) CIB Formula,
   (ii) Law formula,
   (iii) Eurocode formulae.

According to Lau (2006), among all methods, Equal Area Concept and Time-Equivalent Formulae are of particular significant. Due to the lack of physical meaning of the equal area concept in assessing fire severity, Nyman (2001) proposed an expansion of the equal area concept to a radiant exposure area correlation concept. He

used the total energy impinging upon the surface of a structure to establish the severity of a fire. This new concept is expressed as the area under a plot of the emissive power of the compartment gases against time. The radiant heat flux, $\dot{Q}''$ in units of kW/m² is calculated using Equation 2-20. The emissivity of compartment gases was assumed to have value of 1.

$$\dot{Q}'' = e\ s\ T^4 \qquad \text{Equation 2-20}$$

where
ε = Emissivity of gas = 1
σ = Stefan-Boltzmann constant = 5.67×10^{-8}
T = Temperature of compartment gases (°C)

The radiant exposure area correlation can be applied to any fire exposure time-temperature profiles. The relationship between a standard fire resistance and the real fire resistance is illustrated in Figure 2-15. Standard fire resistance and real fire resistance has the same magnitude of cumulative radiant heat flux.

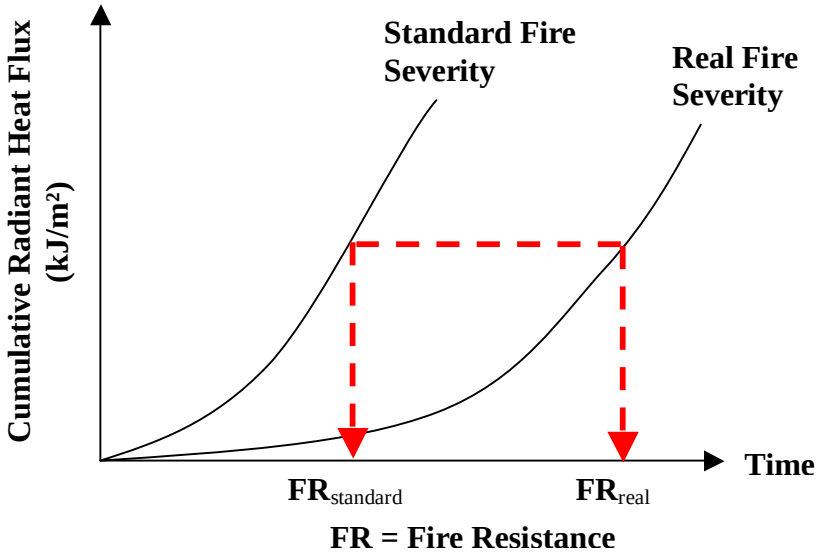

Figure 2-15: Relationship between standard fire resistance and real fire resistance.

For example, if the real fire exposure curve is known and the failure time of an assembly under the exposure of the standard ISO 834 fire is known, the failure time of that assembly in real fire exposure can be determined using the relationship between standard fire resistance and real fire resistance. In order to use equal radiant area concept, the energy characteristics for the compartment fire and the standard fire is

assumed to be identical and the proportion of convective heat transfer and radiant heat transfer from the heat source to the testing specimen are identical.

2.4 Code Requirements

2.4.1 NZS 3603 (1994) Design Code for Bolted Connections in Ambient Conditions

2.4.1.1 Overview

This section is the overview and summary of NZS 3603:1994 – New Zealand Timber Design Code. All the timber connections in the research were designed to NZS 3603 (1994). According to the CHH report (CHH, 2002), Hyspan LVL is categorised as J4 Group for design purposes due to it high tensile strength characteristic. Hyspan LVL is categorised as joint group J4 for the basic density of the LVL product is approximately 380 kg/m^3. The minimum spacing between fasteners and the formulae to calculate the design strength of timber as stated in NZS 3603 (1994) is summarised.

2.4.1.2 Minimum Spacing

Depending on the direction of load, different fastener spacings are required. A schematic drawing for a bolted connection with minimum spacing requirement obtained from NZS 3603 (1994) is shown as Figure 2-16 below.

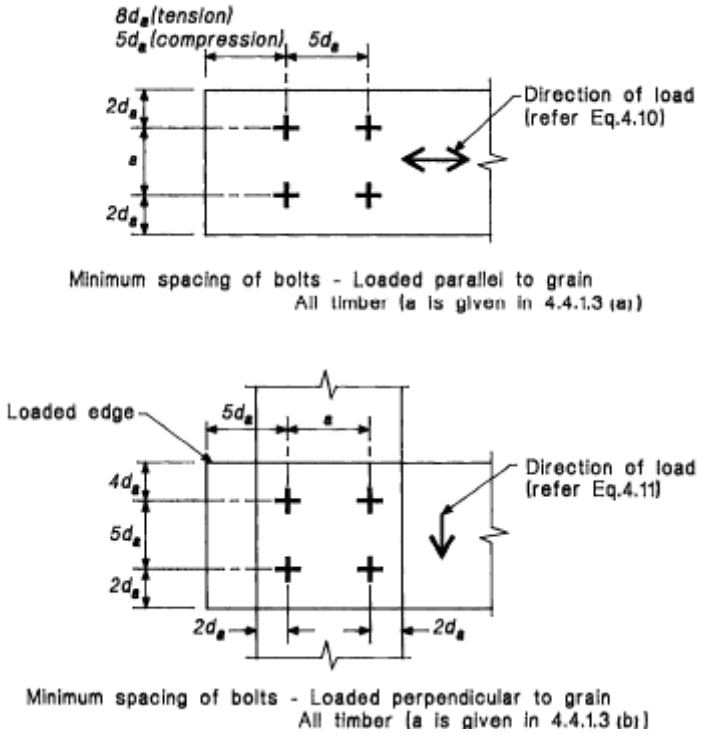

Figure 2-16: Spacing requirement for bolted connections (NZS 3603 (1994)).

In this research all the connections are loaded in tension parallel to the grain direction.

Since the force applied in all the research experiments is parallel to the grain direction, NZS 3603 (1994) Clause 4.4.1.3 suggests an equation to calculate the spacing between fasteners in a row across the grain.

$$a = d_a\left(\frac{n-4+r}{r-1}\right) \qquad \text{Equation 2-21}$$

Where a = Spacings between fasteners across grain direction

n = Total number of fasteners in connection

r = Number of rows of fasteners across the grain

da = Fastener diameter

One other critical condition to comply with NZS 3603 (1994) is that the spacing must not be less than $2.5d_a$.

2.4.1.3 Drilled Holes Dimension

NZS 3603 (1994) Clause 4.4.1.1 states that the diameter of the hole for a bolt shall be not less than the bolt diameter and shall not exceed it by more than 10%. Due to difficulties with inserting thermocouple wire along the shank of bolt for the purpose of this research, the holes are drilled 12.5% larger than the diameter of bolt.

2.4.1.4 Washer Requirement

In order for the design connections to comply with NZS 3603 (1994) Clause 4.4.1.1, all bolted joints with timber side members require a washer at each end of the bolt. Depending on the diameter of the bolt different washer size are required. A summary of bolt diameter vs. washer size is shown below:

Table 2-7: Required washer dimensions (NZS 3603 (1994)).

Bolt Diameter	Washer Dimensions	Washer Surface Area
≤ 8 mm	20mm × 20mm × 1.5mm	400mm²
≤ 12 mm	35mm × 35mm × 3mm	1225mm²
≤ 20 mm	50mm × 50mm × 4mm	2500mm²
≥ 20 mm	65mm × 65mm × 5mm	4225mm²

The washer dimensions shown in Table 2-7 are for square washers. However, a round washer is equally suitable provided the surface area is not less than the requirement of a square washer and the thickness is maintained.

2.4.1.5 Design Equations and Criteria

For laterally loaded bolted joints, the strength shall satisfy the following equation

$$S^* \leq \Phi Q_n \qquad \text{Equation 2-22}$$

Where S^* = Design load effects on joint

Φ = Strength reduction factor

Q_n = Nominal joint strength

The nominal joint strength depends on the number of fasteners, the characteristics strength of the fasteners as well as the type of connection. It can be calculated using the following equation:

$$Q_n = nKQ_{sk} \qquad \text{Equation 2-23}$$

Where Q_n = Nominal joint strength

n = Number of fasteners

Q_{skl} = System characteristic strength of fasteners (See below)

K = Modification factor = 1.5 for steel plate side member

As all the joints to be tested for this research had three members (double shear surface), the system characteristic strength of fastener, Q_{sk} is equivalent to $2Q_{kl}$. (See Table 2-8).

Table 2-8 – Characteristic strength for a single bolt in dry timber loaded parallel to the grain (Table 4.9, NZS 3603:1994)

Type of joint	Effective timber thickness (b_e)	System characteristic strength Q_{skl}
1. Two member 	Smaller of $2b_1$ and $2b_2$	Q_{kl}
2. Three member 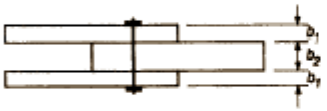	Smaller of $2b_1$ and b_2	$2Q_{kl}$
3. Multiple member 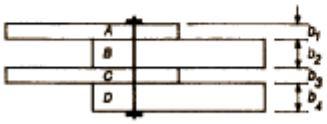	(i) Between A and B Smaller of b_1 and b_2 (ii) Between B and C Smaller of b_1 and b_2 (iii) etc.	(i) Q_{kl} (ii) Q_{kl} (iii) etc. Total characteristic load = sum of characteristic loads
4. Alternative steel and timber members	As for types 1, 2 or 3 except that b_e is based on thickness of timber members only	1.25 x value calculated for joint types 1, 2, or 3

Depending on the thickness of the timber member, the characteristics strength, Q_{kl}, for a single bolt in a two-member joint loaded parallel to grain can be determined from Table 4.10 of NZS 3603 (1994).

2.4.2 Yield Stress Reduction of Steel Bolt at Elevated Temperature Conditions

2.4.2.1 NZS 3404 (1997) Strength Reduction of steel

According to NZS 3404 (1997), the yield stress of steel starts to decrease when the temperature of the steel reaches temperature of 215°C. The reduction continues at a constant rate until 905°C. Once the steel reaches 905°C, it has lost all of its strength.

2.4.2.2 Eurocode 3 (2003): Strength Reduction of steel

The Eurocode 3 (2003) suggests a different reduction factor trend for the yield stress of steel when exposed to elevated temperature. Instead of the yield stress starting to reduce at 215°C as in NZS 3404 (1997), Eurocode 3 (2003) suggests the yield stress only starts to reduce when the steel temperature reachs 400°C. Beyond 400°C, the relationship between the reduction factor and temperature is not linear as suggested in NZS 3404 (1997).

A schematic drawing of the reduction factor from NZS 3404 (1997) and Eurocode 3 (2003) is shown in Figure 2-17.

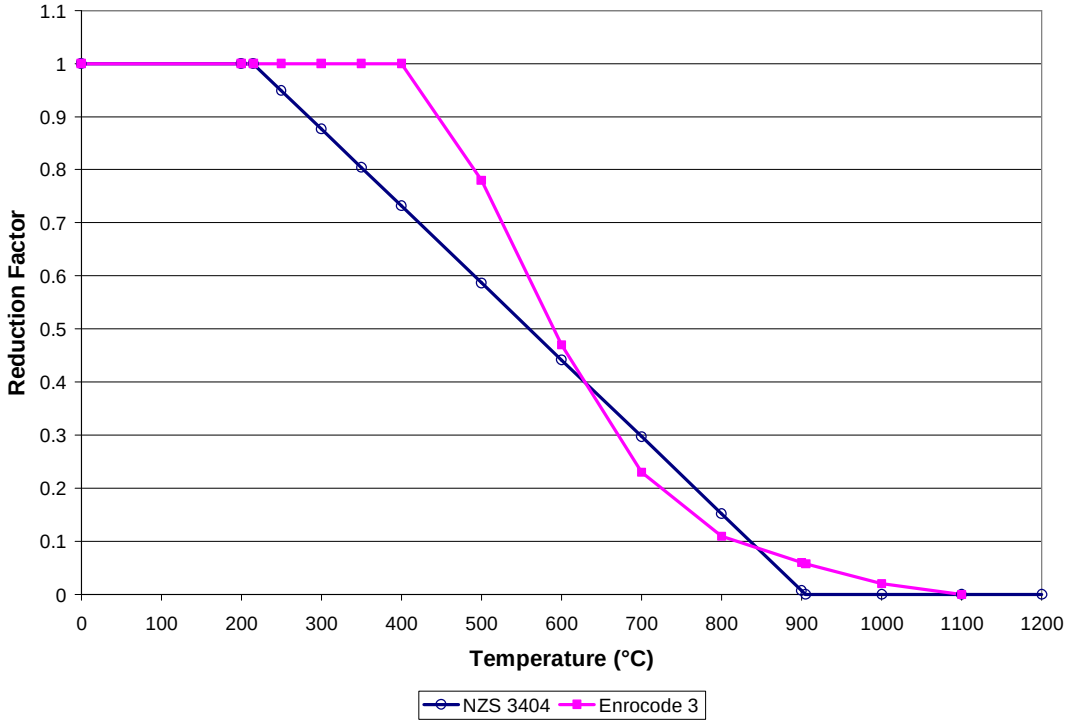

Figure 2-17: Comparison of yield stress reduction factor between NZS 3404 (1997) and Eurocode 3 (2003).

2.4.3 Yield Moment of Bolts

2.4.3.1 ISO 10984: 1999- Timber structures — Dowel-type fasteners — Part 1: Determination of yield moment.

International Standard Organisation (ISO) has published a standard for testing the yield moment of dowel type fasteners, i.e. ISO 10984 Part 1 (1999). According to ISO 10984 (1999), the load applied onto the fastener is via two point loading. Figure 2-18 below shows a schematic drawing of the loading on a fastener during bending tests.

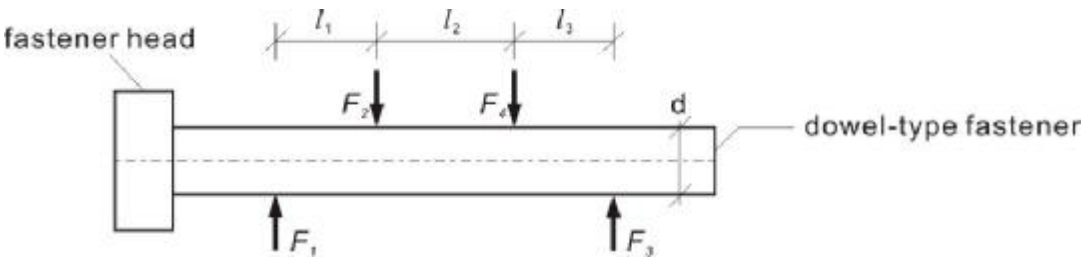

Figure 2-18: Loading on dowels in ISO yield moment testing (ISO 10984, 1999).

In order to comply with ISO 10984 (1999), the distance l_1 and l_3 must be at least 2d and the distance l_2 must be greater than d and smaller than 3d, where d represents the diameter of the fastener.

Since only bolts are use in this research, other dowel type fasteners are not considered here. For a bolt, it must be bent to a degree equivalent of (110/d) at a rate such that the angle is reach within (10±5)s. To measure the yield moment, M_y, it shall be taken as the greater value of ($F_1 \times l_1$) and ($F_3 \times l_3$).

2.4.3.2 prEN409 - Timber Structures – Test methods – Determination of the yield moment of dowel type fasteners – Nails, Bolts and Dowels

The testing method for nails, prEN409 "Timber Structures – Test methods – Determination of the yield moment of dowel type fasteners – Nails", is also applicable to bolts and dowels (Timber Engineering STEP 1 (1995)). The characteristic yield moment value can be calculated as:

$$M_{y,k} = 0.8 f_{u,k} \frac{d^3}{6}$$ Equation 2-24

where $M_{y,k}$ = Characteristic yield moment
$f_{u,k}$ = Tensile strength of the fastener
d = Diameter of bolt

Typical yield stress, f_y, and tensile strength, $f_{u,k}$, used in the European countries are summarised in Table 2-9. In this research, all the bolts used for testing are grade 4.8.

Table 2-9: Yield stress, fy, and tensile strength, fu,k, for ordinary bolts. (Timber Engineering STEP 1 (1995))

Bolt Grade	4.6	4.8	5.6	5.8	6.8
f_y (MPa)	240	320	300	400	480
$f_{u,k}$ (MPa)	400	400	500	500	600

There is also an alternative method to measure the yield moment of dowel type fasteners recognised by ISO. However, this will not be discussed in this report.

2.4.4 Embedment strength testing procedures according to ISO 10984-2(1999)

2.4.4.1 Overview

In this research, only LVL is used. Therefore only the testing method for laminated wood product with a single grain direction will be reviewed. For LVL, the force applied can either be compression or in tension when testing parallel to grain and can be compression when testing perpendicular to grain.

2.4.4.2 Testing Requirements

One important requirement for conducting a standard embedment test is to ensure the fastener used is not subjected to bending during the test and is perpendicular to the surface of the wood sample. The direction of force applied during a standard embedment test depends on the type of timber.

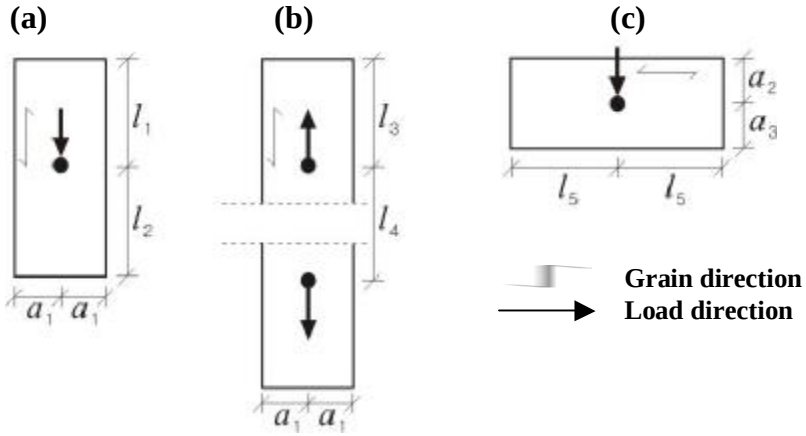

(a) Compression parallel to grain
(b) Tension parallel to grain
(c) Compression perpendicular to grain

Figure 2-19: Schematic drawing of correct loading direction for embedment tests of LVL (ISO 10984:2 (1999)).

2.4.4.3 Testing Sample Dimensions and Preparations

The dimension of testing wood sample as shown in Figure 2-19 above depends on the fastener size and is summarised in Table 2-10. One other requirement is to condition the wood sample in a controlled environment before the test commences. The samples

are to be left in environment of humidity of (65±5%) and temperature of (20±2°C) until the mass of the samples remains constant for at least 6 hours.

2.4.4.4 Requirement of Testing Equipment

A schematic drawing of embedment test as in ISO 10984 Part 2 is shown as Figure 2-20. The steel apparatus which holds the fastener in position should not be in contact with the testing sample.

It is crucial the fastener used for the ISO embedment testing should be identical to the fastener size used in practice. Beside, an estimation of the maximum load that the testing specimen can bear must be known so that the loading procedure required by ISO standard can be followed. The load procedures can be found from ISO 10984: Part 2 (1999).

The test will only cease when either the maximum load is reached or a displacement of 5mm was observed.

Table 2-10: Size of wood testing sample (ISO 10984: Part 2 (1999)).

Measurement	Bolts or dowels	Test piece material
a_1	3d	Timber or wood based sheet products
l_1	7d	
l_2	7d	
l_3	7d	
l_4	30d	
a_1	5d	Timber or layered wood products with one grain direction
a_2	5d	
l_5	20d	

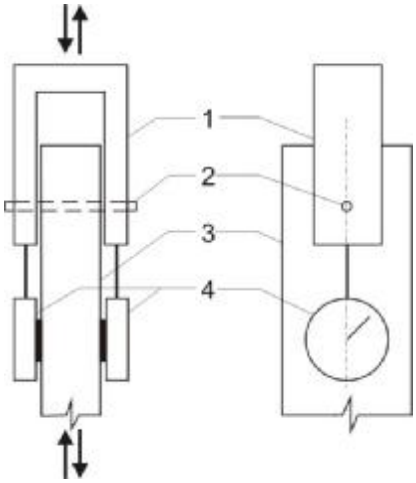

1. Steel apparatus
2. Fastener
3. Test piece
4. Displacement gauge attached to the test piece

Figure 2-20: Typical embedment test arrangement (ISO 10984: Part 2 (1999)).

3 Description of Testing Equipment

3.1 Measuring Devices

The measurements that were taken during each experiment runs were:

1. Temperature,
2. Load, and
3. Displacement of timber members when load was applied.

A Universal Data Logger (UDL) was used to process and record all the required data for this research. All the processed data was output in Microsoft Excel format for ease of analysis.

The temperatures at various specimen locations were recorded using K-type thermocouples whereas the tensile load applied to the specimen was measured using a load cell. A potentiometer measures the displacement of the specimen continuously throughout the experiment duration.

1. Thermocouple

In all the research experiments conducted, K-type thermocouples were used. K – type thermocouples are made by welding Chromium (Cr) and Aluminium (Al) metal together. The welded bead is the sensing part of thermocouple. The working temperature range of this type of thermocouple is between -270°C to 1372°C, which is ideal for this research.

Due to the high cost of thermocouple wire, extension grade K-type wire was used to transfer the readings from the thermocouple wire to the equipment which records the information. The extension grade wires typically have a lower ambient temperature limit compared to the thermocouple wire, so it cannot be exposed to high temperatures.

2. Load Cell

Before the load cell was put in service, it was calibrated to a working range of 0kN to 100kN. Once the calibration was done, it did not need to be repeated after every experiment.

3. Potentiometer

The potentiometer used had a working range up to displacement of 40mm. Each time before commencing an experiment, the potentiometer reading was set to zero. Data was collected through wiring the load cell to the data recording equipment.

3.2 Furnace

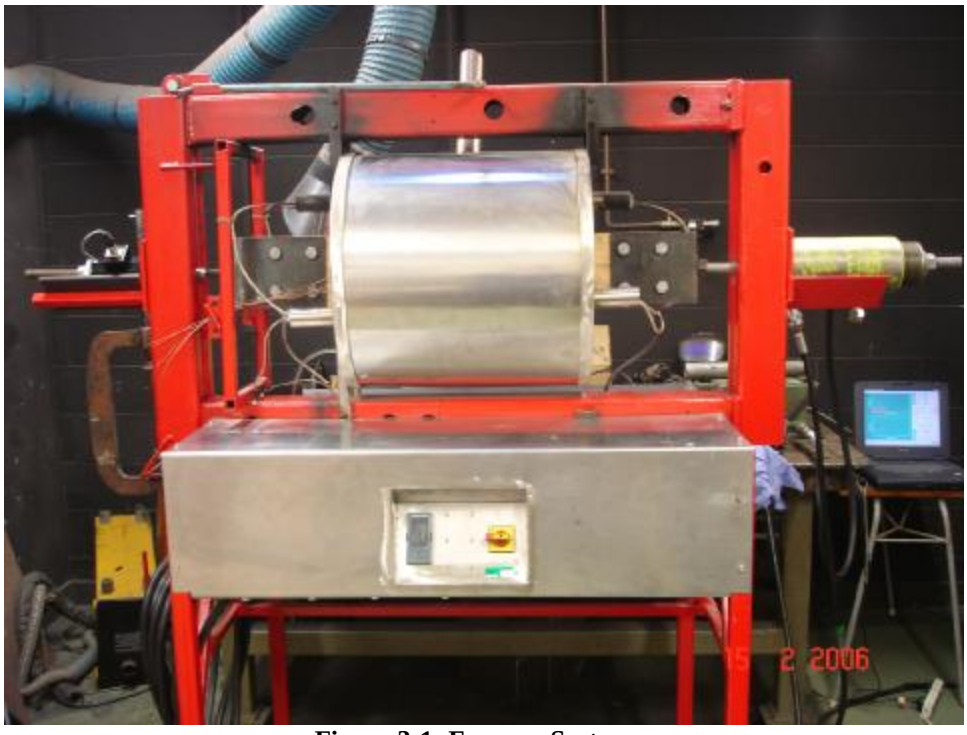

Figure 3-1: Furnace System.

The furnace system used for this research project is powered by electricity. There are a total of three spiral heating coils installed in the 0.5m long furnace cylinder (see Figure 3-1). The temperature of each heating coil was measured using a thermocouple which was connected to the temperature control system. The temperature control

system was monitored electronically using a feedback loop method from the average temperature measured from the three coils.

At the furnace cylinder ends are two square openings of dimensions of 0.18m×0.18m. This is to allow the testing specimen to slide through the furnace and extend outside the furnace. Before the specimen can be placed in the furnace, the load cell seat must be lifted to allow the specimen to slide into the furnace.

3.3 Temperature-Time Curve from furnace

Due to limitations of the furnace, the maximum testing temperature that could be used was 750°C. A comparison between a typical Temperature-Time curve obtained from the furnace heating elements and the Standard Temperature-Time curve is shown as Figure 3-2.

From Figure 3-2, it can be seen that the temperature in the furnace takes a longer time to reach the desired temperature set by the ISO 834 (2000). The reason for the difference between the furnace and the standard Temperature-Time curve is the different heating method. The heating curve of the ISO 834 can be achieved by using a gas burner whereas the heating in the available furnace is by electricity.

After 6 minutes from switching on the power for the furnace, the temperature in the furnace become higher than the standard ISO 834 curve. Not until approximately 15 minutes from turning on the furnace did the standard and the furnace Temperature-Time curve coincide.

Due to the difference in the Temperature-Time curve that was achieved in the furnace, some correlation has to be introduced to relate the temperature to the ISO 834 curve.

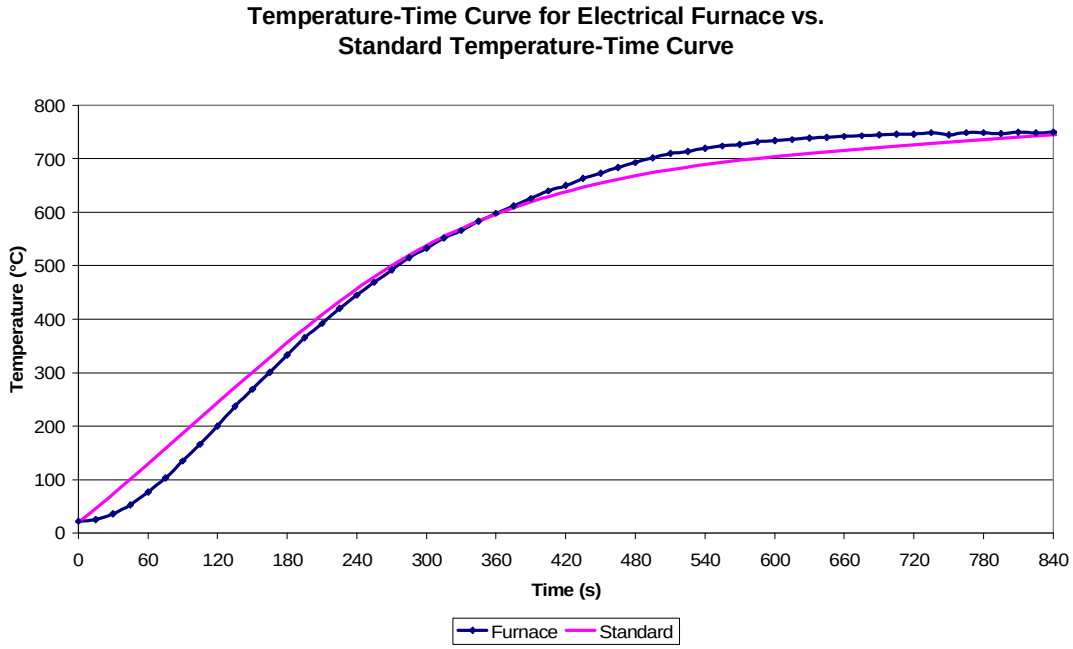

Figure 3-2 Comparison between Standard and furnace Temperature-Time curves.

4 Design of Connections

4.1 Outline

In this research, three different types of connections, namely the WWW connection, the WSW connection and the SWS connection were used. Two sets of connections, one which used only one fastener in the connection and the other which used multi-fasteners in the connection, were tested under different conditions. This chapter discusses the arrangement of the different types of testing specimens in detail. A tabulated summary of all the experiments conducted is also included. Since some connections have only one fastener while the others have multiple fasteners, the testing load for these different connections were also determined.

4.2 Specimen Layout Description

4.2.1 Overview

A total of three different types of specimen were used for experimental testing. They were namely:

1. Wood-Wood-Wood specimen (WWW),
2. Steel-Wood-Steel specimen (SWS), and
3. Wood-Steel-Wood specimen (WSW).

The descriptions of these specimens are given in the following sections.

The experiments can generally be categorised into three different types, which are:

1. Ambient Tests,
2. Heated Tests, and
3. Fire Tests.

For the Ambient Tests, the specimens were tested at room temperatures, whereas for the Heated Tests the specimens were heated at the desired furnace temperature for a period of 2 hours before testing. The standby time of 2 hours allowed heat to penetrate into the specimens. In the Fire Tests, the specimens were exposed to temperatures

which followed the furnace's Temperature-Time Curve as shown in Chapter 3. With the results obtained from the Fire Tests, it gives a quantitative measurement of embedment strength of timber exposed to fire and it also shows the consequences for timber structures exposed to standard fire conditions. The procedures to carry out the tests are explained in the Chapter 5.

At least one of each type of connection was tested to the categories discussed above. Table 4-1 below lists all the tests that were conducted in this research project. All the experiments conducted for Ambient Tests and Heated Tests are one-bolt connection specimens. A total of two experiments for each type of connection were to be conducted for the Fire Tests, one of a one-bolt connection and one of a multi-bolt connection.

The position of the bolt for each type of single bolted connection specimen was defined at the centre point of all bolts as designed by Lau (2006) and is described in Section 4.6. Full design of the connection for this research is included in Section 4.7.

Table 4-1: List of experiments conducted.

Category	Furnace Temperature Set-point	Specimens		
		WWW	WSW	SWS
Ambient	≈ 15°C	●	●	●
Heated	80°C	●	●	●
	100°C	●	●	●
	120°C	●	●	●
	150°C	●	●	●
	200°C	●	●	●
	250°C	●	●	●
Fire	1 bolt	●	●	●
	4 bolts		●	●
	5 bolts	●		

4.2.2 Materials Used

The required materials to assemble the test specimens are as below:

Table 4-2: Required materials to assemble testing specimens.

Materials	Dimensions
LVL	45mm × 150mm
	63mm × 150mm
Steel Plate	6mm × 130mm
Bolts (1)	Ø12mm × 100mm; Ø12mm × 120mm; Ø12mm × 180mm
Bolts (2)	Ø16mm × 100mm; Ø16mm × 120mm
Washers	3mm x 40mm × 40mm × Ø12mm
MDF Board	6mm × 150mm

4.3 Load combinations for Ambient Conditions

There are only three different load combinations for the ultimate limit state that need to be considered for structural design at ambient conditions for light timber frame structures because earthquake load and wind load are not critical. These equations are summarised as Equation 4-1, Equation 4-2 and Equation 4-3 below. Loads that are important for timber structures are namely gravity load, live load and snow load.

1.	1.4 G	Equation 4-1
2.	1.2 G + 1.6 Q	Equation 4-2
3.	1.2 G + 1.2 S	Equation 4-3

where G = Gravity load
Q = Live load
S = Snow load

Since the study is particularly for the bottom chord of a roof or floor truss, load combinations of G, Q and S loads for roof and floor trusses need to be investigated. The loads at normal conditions for roof and floor trusses are summarised below.

Table 4-3: Summary of loads for normal ambient conditions.

Load	Roof (kPa)	Floor (kPa)
G	0.2	0.5
Q	0	2.5
S	0.5	0

The loads calculated from Equation 4-1, Equation 4-2 and Equation 4-3 using the published load combination values for each type of load from Table 4-3 are summarised below.

Table 4-4: Summarised loads results for roof and floor structures at ambient conditions.

	Load Combination Equations for Ambient Conditions	Roof (kPa)	Floor (kPa)
Equation 4-1	1.4 G	0.28	0.70
Equation 4-2	1.2 G + 1.6 Q	0.24	4.60
Equation 4-3	1.2 G + 1.2 S	0.84	0.60

The maximum load combination for a tensile member in the bottom chord of a roof and floor truss are 0.84 and 4.6 kPa respectively.

4.4 Structural Design for Fire Conditions

The principles when designing timber structures for fire conditions is very similar to the design principles for timber structures at normal ambient conditions. However there are some differences between the designs for each condition. Buchanan (2001) outlines the main differences of the fire conditions design compared to ambient conditions design. The differences are summarised below:

1. The applied loads are less,
2. Internal forces may be induced by thermal expansion,
3. Strengths of materials may be reduced by elevated temperatures,
4. Cross-sectional areas may be reduced by charring,

5. A smaller safety factor can be used, because of the low likelihood of the event of fire,
6. Deflections are not important (unless they affect strength), and
7. Different failure mechanisms need to be considered.

Under constant load, the stress in timber increases steadily as the surfaces of the timber burns to char. The unburnt residual timber section can be assumed to only suffer minimal loss of strength due to elevated temperatures. Therefore, the failure mode of timber connections is due to the stress in the member exceeding the material strength.

4.5 Load combinations for Fire Conditions

According to NZS 4203 Clause 2.4.3.4, the structural members which may be exposed to elevated temperatures shall be designed for a combined load of gravity load and live load. Snow load is not of particular interest. The load combinations to be considered for fire conditions from SNZ 1992 are:

1. G Equation 4-4
2. G + 0.4 Q Equation 4-5

The loads calculated from Equation 4-4 and Equation 4-5 by using the published load combination values for each type of load from Table 4-3 are summarised below.

Table 4-5: Summarised loads results for roof and floor structures at fire conditions.

	Load Combination Equations for Fire Conditions	Roof (kPa)	Floor (kPa)
Equation 4-4	G	0.2	0.5
Equation 4-5	G + 0.4 Q	0.2	1.5

The maximum load combination for a tensile member in the bottom chord of a roof and floor truss for fire conditions is 0.2 and 1.5 kPa respectively.

By taking the ratio between the maximum load combination for a tensile member for fire condition and for ambient condition, the load factor can be found, i.e.:

$$\text{Load Factor} = \frac{\text{Load Combination}_{\text{max, fire}}}{\text{Load Combination}_{\text{max, ambient}}} \qquad \text{Equation 4-6}$$

The use of the load factor is to calculate the expected loads on the structure during a fire compared to the loads that would cause collapse at ambient temperatures.

The calculated load factor for roof and floor are tabulated below:

Table 4-6: Load factor for roof and floor structures.

	Roof	**Floor**
Load Factor	$\frac{\text{Load Combination}_{\text{max, fire}}}{\text{Load Combination}_{\text{max, ambient}}} = \frac{0.2}{0.84} = 0.24$	$\frac{\text{Load Combination}_{\text{max, fire}}}{\text{Load Combination}_{\text{max, ambient}}} = \frac{1.5}{4.6} = 0.33$

From the calculation, a roof structure at fire conditions can only bear 24% of the applied load at ambient conditions before failure occurs whereas a floor structure at fire conditions can only bear 33% of the applied load at ambient conditions before failure.

By using the load factor, the relative fire resistance for a particular structure can be concluded. The lower the load factor, the higher the fire resistance. This is because a lower load factor means that it has a larger load bearing capacity before failure occurs.

The expected forces for the connections under fire condition can be obtained by multiplying the load factor by the designed forces for the connections under ambient conditions, i.e.

$$S^*_{\text{fire}} = \text{Load Factor} \times S^*_{\text{ambient}} \qquad \text{Equation 4-7}$$

Obtained from Lau (2006), the connections are being designed for a tensile force of 70kN under normal ambient conditions. Therefore the tensile force for the connections under fire conditions is:

	Roof	Floor
$S^*_{Ambient}$	70 kN	70 kN
Load Factor (LF)	0.24	0.33
S^*_{Fire}	$S^*_{Fire} = LF \times S^*_{Ambient}$ $S^*_{Fire} = 0.24 \times 70\,kN$ $S^*_{Fire} = 16.8\,kN$	$S^*_{Fire} = LF \times S^*_{Ambient}$ $S^*_{Fire} = 0.33 \times 70\,kN$ $S^*_{Fire} = 23.1\,kN$

The tensile force in fire, S^*_{fire}, would be 16.8 kN for a roof member and 23.1 kN for a floor member.

4.6 Single Bolted Connection

4.6.1 WWW Specimens

As the name suggests, the WWW specimen consisted only of timber members. The parts and dimensions required to build a WWW specimens are shown as Table 4-7 below and the isometric view of the whole WWW specimen assembly is presented as Figure 4-1.

Table 4-7: Parts and dimensions for WWW specimens.

Items	Qty	Dimensions	Usage
M12 Bolts and Nuts	2	Φ12×180mm	Connections
Washers	4	40mm×40mm×3mm×Φ12	
150mm×45mm LVL	2	150mm×45mm×530mm	Side joining members
150mm×63mm LVL	2	150mm×63mm×450mm	Centre joining members

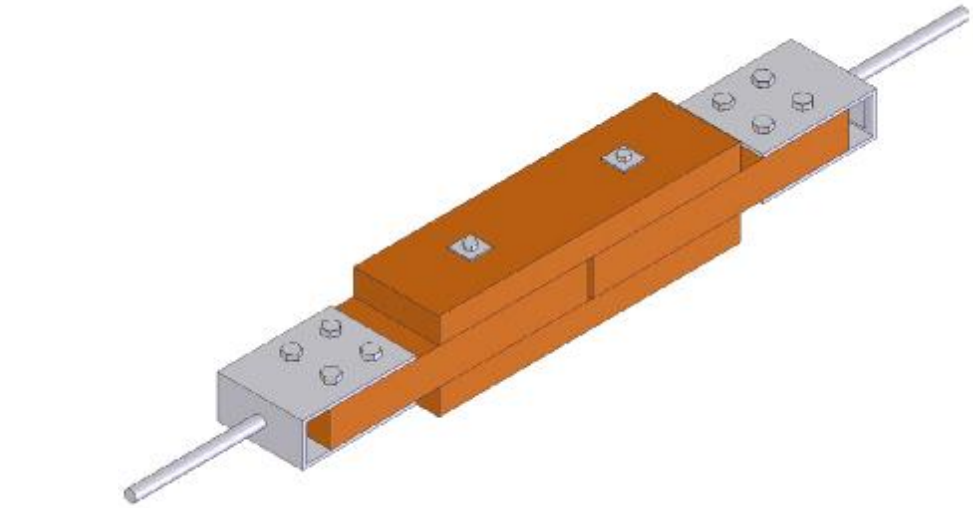

(a) Isometric View of WWW Specimen

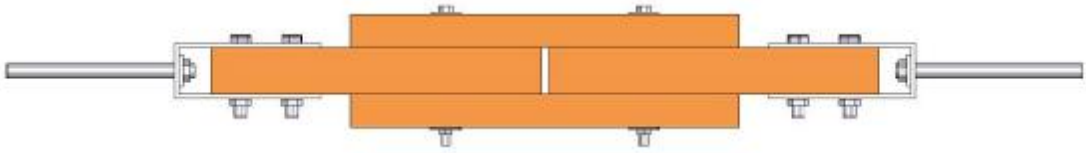

(b) Side View of WWW Specimen

(c) Top View of WWW Specimen

Figure 4-1: Schematic drawing of WWW specimen assembly.

In the experiment, a total of eight M16 bolts were used to bolt the specimen onto metal brackets which hold the specimen in place in the furnace as shown in Figure 4-1. These bolts were used for connecting the WWW specimen to the metal brackets in the experiment because this can ensure that failure will occur at the tested connections that uses smaller bolts, i.e. M12 bolts.

The location of M12 bolts in the timber members are shown as Figure 4-2 below. The calculated load based on NZS 3603 will be determined in Section 4.6.4.

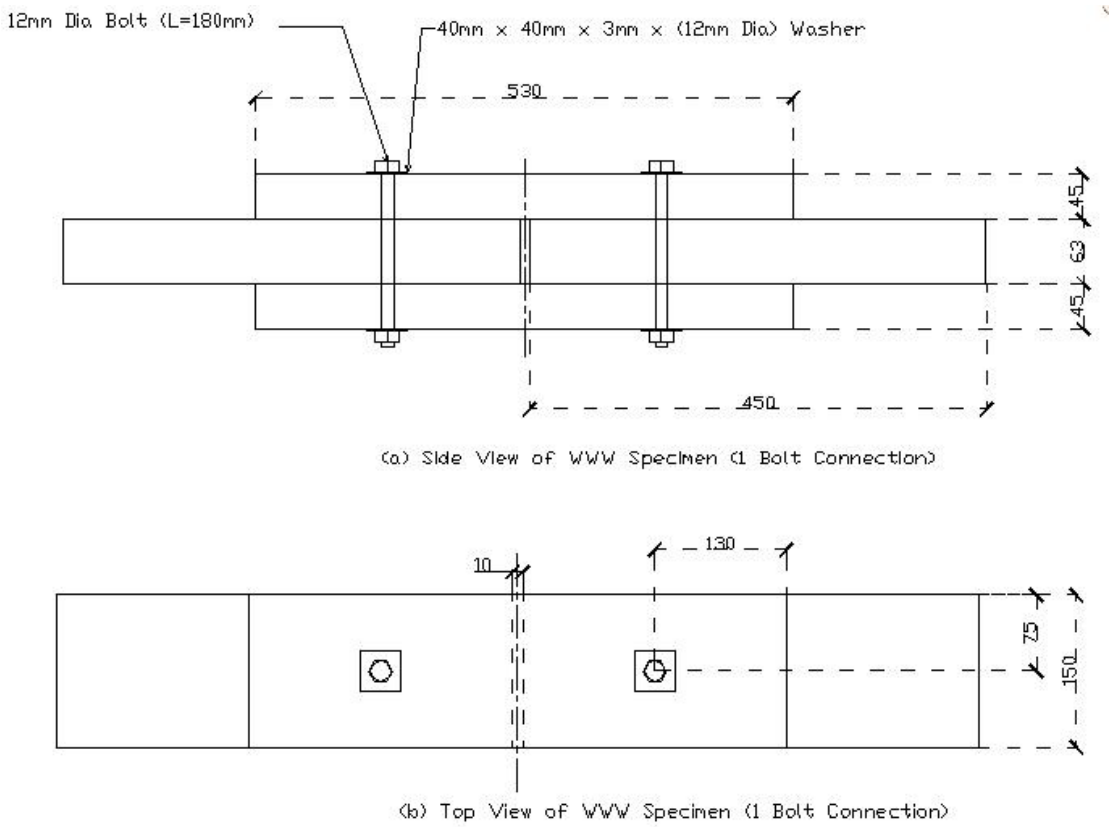

Figure 4-2: Location of M12 dowels on WWW specimens.

Thermocouples were inserted into the specimens at various locations. They are as follows:

1. In between the washer and bolt head;
2. In between the side and the main members;
3. Along the bolt shank at the mid-depth of the side member;
4. Along the bolt shank at the mid-depth of the main member;
5. The mid-depth of the side member; and
6. The mid-depth of the centre member.

Two sets of temperature measurement were taken at each location. For ease of visualisation, the locations are marked with crosses in Figure 4-3 below.

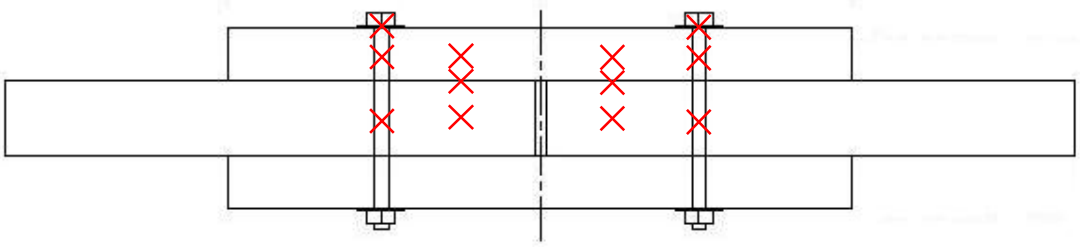

Figure 4-3: Location of temperature measurement for WWW Connection.

Beside these locations where temperature readings were taken, thermocouples were also used to measure:

1. The furnace air temperature;
2. The average furnace element temperature; and
3. The air temperature at furnace exhaust.

During the experiment, the movement of the timber members was measured by fixing potentiometers on one of the main members. The specimens were subjected to load 2 hours after the pre-test heating stage. A load cell and a jack-system were used to apply and monitor the load applied to the members. The potentiometer was calibrated before the furnace was turned on.

4.6.2 WSW Specimens

For the WSW type of specimens, a 130mm × 6mm galvanised steel plate is sandwiched between the timber side members. A total of four timber side members are required in this kind of specimen. The details of parts and dimensions required to build a WSW specimens are shown as Table 4-8 below and the isometric view of the whole WSW specimen assembly is presented as Figure 4-4.

Table 4-8: Parts and dimensions for WSW specimens.

Items	Qty	Dimensions	Usage
M12 Bolts and Nuts	2	Φ12×120mm	
Washers	4	40mm×40mm×3mm×Φ12	
150mm×45mm LVL	4	150mm×45mm×450mm	Side joining members
130mm×6mm Steel Plate	1	130mm×6mm×275mm	Centre joining member
150mm×6mm MDF Board	2	150mm×6mm×312mm	Filling between side members

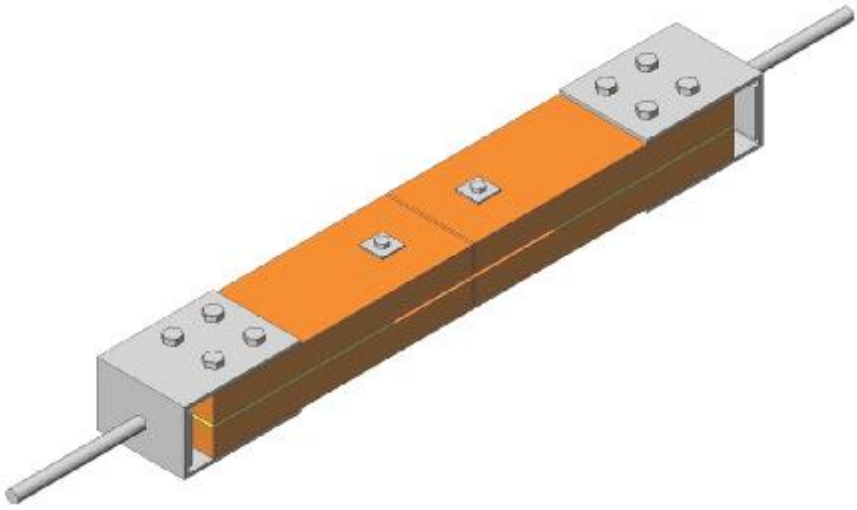

(a) Isometric View of WSW Specimen

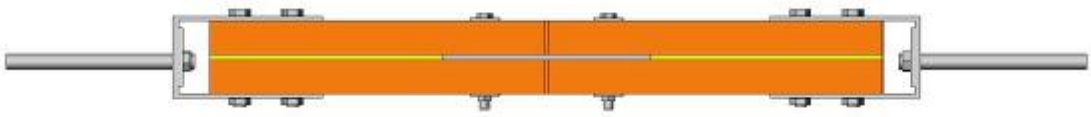

(b) Side View of WSW Specimen

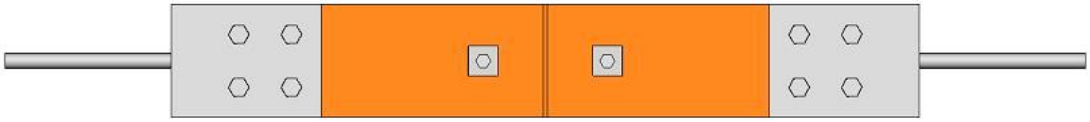

(c) Top View of WSW Specimen

Figure 4-4: Schematic drawing of WSW specimen assembly.

In a similar fashion to the WWW specimen, eight M16 bolts were used to bolt the specimen to the steel brackets which hold the specimen in place in the furnace. For the WSW connections, MDF boards of dimension 150mm × 6mm × 312mm were sandwiched between the timber side members. One of the reasons for inserting these

boards is to stabilise the whole specimen while fixing the specimen to the brackets. Besides, it also prevents the hot air flowing through the void between the side members.

The positions where the M12 bolts were located in the WSW specimens are shown as Figure 4-5 below. The load capacity for one-bolt WSW connection was calculated as shown in Section 4.6.4.

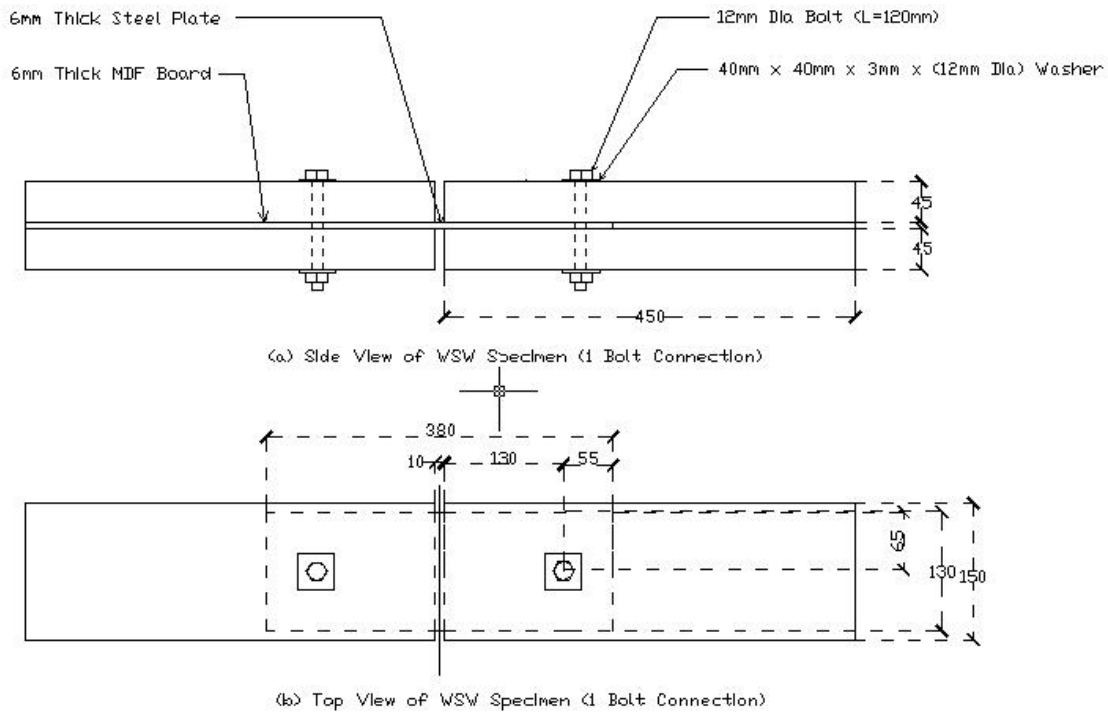

Figure 4-5: Location of M12 and M16 dowels on WSW specimens.

Temperatures at several locations on the specimen were also measured throughout the duration of the experiment. They were:

1. In between the washer and the bolt head;
2. In between the side and the main members;
3. Along the bolt shank at the mid-depth of the side member;
4. Along the bolt shank at the mid-depth of the main member; and
5. The mid-depth of the side member.

Two sets of temperature measurement were taken at each location. For ease of visualisation, the locations are marked with crosses in Figure 4-6.

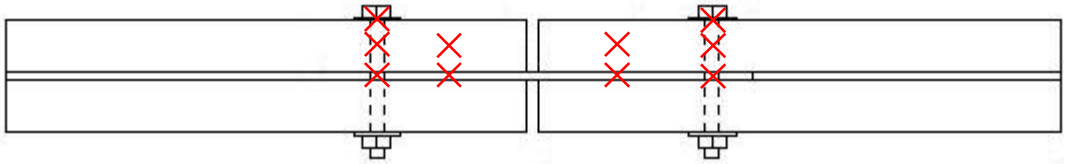

Figure 4-6: Thermocouple locations in WSW connection.

Other temperature readings and the potentiometer readings which were also recorded during each experiment are identical to the WWW connections.

4.6.3 SWS Specimens

In contrast to the WSW specimens as described in Section 4.6.2, the timber member is sandwiched in between the steel plate side joining members for the SWS specimen. The parts and dimensions of the SWS specimens are tabulated as Table 4-9. An isometric view of the SWS specimen is also included as Figure 4-7. No washer was required for the SWS connection because the bolt heads and nuts are not contacting with timber.

Table 4-9: Parts and dimensions for SWS specimens.

Items	Qty	Dimensions	Usage
M12 Bolts and Nuts	2	Φ12×100mm	
150mm×63mm LVL	2	150mm×63mm×450mm	Centre joining members
130mm×6mm Steel Plate	2	130mm×6mm×380mm	Side joining members

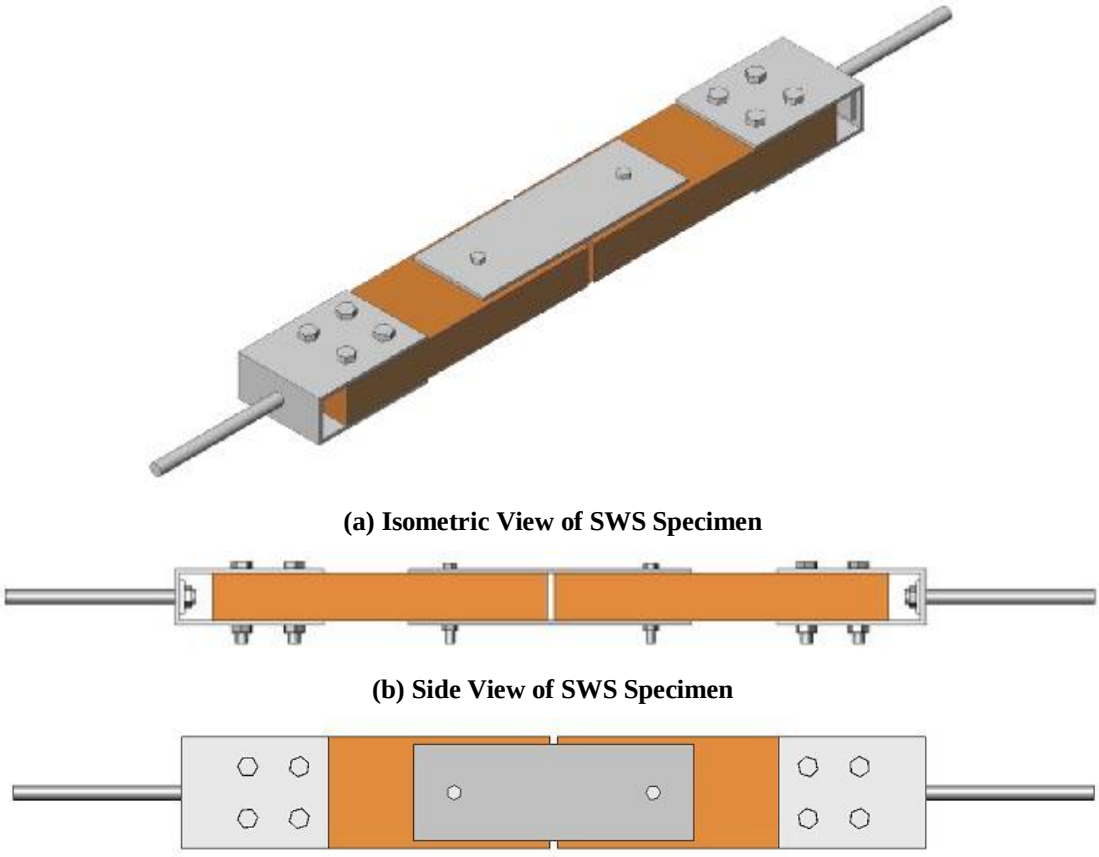

(a) Isometric View of SWS Specimen

(b) Side View of SWS Specimen

(c) Top View of SWS Specimen

Figure 4-7: Schematic diagram of isometric view of SWS specimen assembly.

Among all the three types of specimen, the SWS specimen is the smallest in size due to its thinner side members. The positions where the M12 bolts are to be located in the SWS specimens are shown in Figure 4-8.

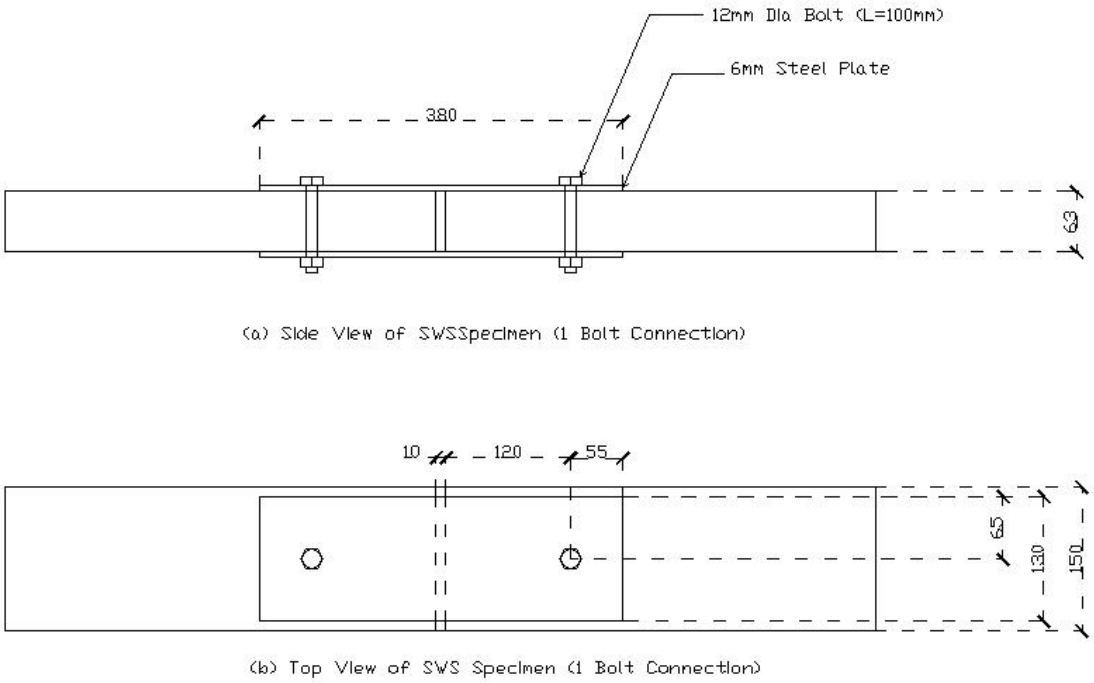

Figure 4-8: Location of M12 and M16 dowels on WSW specimens.

The load capacity for one-bolt SWS connection was calculated and shown in the Section 4.6.4.Temperatures at various locations in the specimen are also measured throughout the duration of the experiment. They are as follow:

1. In between the side member and the bolt head;
2. In between the side member and the main member;
3. Along the bolt shaft at the mid-depth of the side member;
4. Along the bolt shaft at the mid-depth of the main member; and
5. The mid-depth of the main member.

Two sets of temperature measurement were taken at each location. For ease of visualisation, the locations are marked with crosses in Figure 4-6 below.

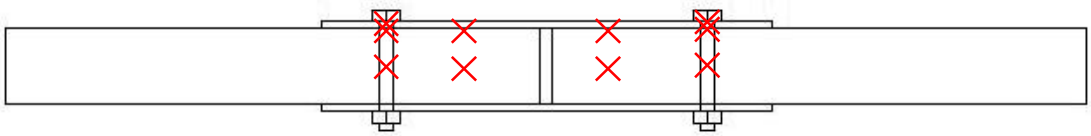

Figure 4-9: Thermocouple locations in SWS connection.

Other temperature readings and potentiometer readings which were also recorded during each experiment are identical to the WWW specimens.

4.6.4 Load Capacity of singly-bolted connections

In the following sections, the load carrying capacity for each type of connection was calculated based on the characteristic strength of a M12 bolt and the timber member thickness according to NZS 3603 (1994).

4.6.4.1 WWW Specimen

As described above, the WWW connections are made of 45mm thick side timber members and 63mm thick centre timber members. The side members are bolted to the centre members using M12 bolts.

The strength of a laterally loaded bolted connection must satisfy the strength limit state as follows:

$$N^* \leq \Phi Q_n \qquad \text{Equation 4-8}$$

where ΦQ_n = Design Strength

N^* = Design load effects on joint produced by strength limit state loads

Φ = Strength Reduction Factor

The nominal joint strength for a three member connection is given as:

$$Q_n = 2Q_k \qquad \text{Equation 4-9}$$

where Q_k = Characteristic strength as given in NZS3603 Table 4.10

From NZS 3603 Table 4.10, the characteristic strength, Q_k, for a single 12mm bolt in a two member joint of dry 63mm timber loaded parallel to grain direction is 10.5kN. Since there is no timber thickness of 63mm included in NZS 3603 Table 4.10, the value for a timber of thickness 65mm was chosen.

Therefore the nominal joint strength is:

$$Q_n = 2 \times 10.5 \text{ kN} = 21 \text{ kN}$$

This means joint with one bolt has a strength of 21 kN, and could carry a design load, N*, of ($Ø \times Q_n$) = 14.7 kN.

Based on the load factor calculated in Section 4.4, the load carrying capacity for a single bolted WWW connection in fire is:

	Roof	**Floor**
Load Factor	0.24	0.33
Load Capacity, $S^*_{Fire, 1 Bolt}$	= 14.7 × 0.24 = 3.3 kN	= 14.7 × 0.33 = 4.9 kN

4.6.4.2 SWS Connection

The SWS connections are similar to the WWW connections. Instead of 45mm thick timber side members for the WWW connections, the side members are 6mm thick steel plate. The main member is 63mm thick.

The strength of a laterally loaded bolted connection must satisfy Equation 4-8 and the nominal joint strength for a three steel and timber alternating member connection is given as:

$$Q_n = 1.5 \times 2 \times Q_k = 3Q_k \qquad \text{Equation 4-10}$$

Similar to the WWW connection, Q_k is equal to 10.5 kN. Thus, the nominal joint strength, Q_n, is:

$$Q_n = 3 \times 10.5 \text{ kN} = 31.5 \text{ kN}$$

This means that a joint with only one bolt has a strength of 31.5 kN, and could carry a design load, N*, of ($Ø \times Q_n$) = 22.1 kN.

Based on the load factor calculated previously, the load carrying capacity for a single bolted SWS connection in fire is:

	Roof	Floor
Load Factor	0.24	0.33
Load Capacity, $S^*_{Fire, 1\ Bolt}$	= 22.05 × 0.24 = 5.3 kN	= 22.05 × 0.33 = 7.3 kN

The stress introduced to the steel plate in a SWS connection when load is applied must be checked so that the tensile stress is greater or equal to the design tensile load on the steel plate, i.e. $S^* \leq \Phi \times R_n$.

Similarly R_n can be calculated by cross-sectional area of steel plate in units of mm^2 multiplied by the characteristic tensile strength of steel plate in units of MPa, i.e.: $R_n = f_t \times A$. Hence, the designed tensile force can be calculated using the following equation:

$$S^* \leq \Phi \times f_t \times A \qquad \text{Equation 4-11}$$

The characteristic tensile yield strength of mild steel plate is 275 MPa. The strength reduction factor for steel plate is taken as 0.9. In the SWS connection, the side member steel plate has cross-sectional dimensions of 130mm × 6mm.

Substituting the known variables into the right hand side of Equation 4-11 to calculate the designed tensile strength of steel plate for SWS connections:

Design tensile strength $= \Phi \times f_t \times A$
$= 0.9 \times 275\ MPa \times (130mm \times 6mm)$
$= 193\ kN$

Since there are two steel plates as side members for SWS connections, the total design tensile strength of the steel plate for the SWS connection is: 2 × 193 kN = 386 kN.

The load to be applied in the single-bolt SWS connection is 7.3 kN and the calculated design tensile strength on steel plates for SWS connection is 386 kN. Hence the steel plate will not fail under the design tensile strength for the whole specimen.

4.6.4.3 WSW Connection

Instead of steel plate side members as for the SWS connection, a single steel plate is sandwiched between the timber side members. The side members are made of 45mm thick LVL.

The strength of a laterally loaded bolted connection must satisfy Equation 4-8 and the nominal joint strength, Q_n, for a three (timber and steel) alternating member connection is obtained from Equation 4-10. From NZS 3603 Table 4.10, the characteristic strength for a single 12mm bolt in a two member joint of dry 45mm timber loaded parallel to grain direction is 9.83kN.

Therefore the Q_n is 29.5 kN. This means joint with only one bolt provide a strength of 29.5 kN, and can carry a design load, N*, of ($Ø \times Q_k$) = 20.6 kN.

Based on the load factor calculated previously, the load carrying capacity for a single bolted SWS connection in fire is:

	Roof	**Floor**
Load Factor	0.24	0.33
Load Capacity, $S^*_{Fire, 1 Bolt}$	= 20.64 × 0.24 = 5.0 kN	= 20.64 × 0.33 = 6.8 kN

The stress introduced to the steel plate in a WSW connection when load is applied must be checked so that the tensile stress is greater or equal to the design tensile load on the steel plate, i.e. $S^* \leq \Phi \times R_n$.

The load to be applied in the single-bolt WSW connection is 6.8 kN and the calculated design tensile strength on a singly 6mm thick steel plates is 193 kN. This means that the steel plate would not fail under the design tensile strength for the whole specimen.

4.6.4.4 Summary

In summary, the load that is to be carried by each type of connection during the fire test is:

WWW	4.85 kN
SWS	7.28 kN
WSW	6.81 kN

4.7 Description of Multi-bolted Connection Test Specimen

4.7.1 Design Assumptions

The design of the timber connections for this research project was based on the tensile member in the bottom chord of a roof and floor trusses. Three different types of joint will be studied, namely a Wood-Wood-Wood connection (WWW), a Wood-Steel-Wood connection (WSW) and a Steel-Wood-Steel connection (SWS). The number of metallic fasteners required according to NZS 3603 for each type of joint will also be determined.

Two assumptions that were made in the design process were:

1. The size of the timber structural members are pre-defined, and
2. The load carrying of the timber connection is 30% of the axial strength of the member.

In order to correlate the results obtained from the timber embedding strength tests using one bolt to those for real timber connections in fire conditions, tests of multi-bolted specimens exposed to fire are required. It is always better to keep most of the variables constant. In this situation, the timber member dimensions of a specimen are kept constant while the number of metallic connectors varies (Refer to Section 4.6 for detailed dimensions of each type of specimen).

4.7.2 Design Strength of Connection

It is important that in every connection the expected load is less than the expected strength, i.e. $S^* \leq \Phi R_n$, where Φ = strength reduction factor. The strength reduction factor, Φ, published in NZS 3603 Clause 2.5 for LVL is 0.9. Hence,

$$S^* \leq 0.9 \times R_n \qquad \text{Equation 4-12}$$

The expected strength, R_n, of the member is calculated from $f_t A$, i.e

$$R_n = f_t A \qquad \text{Equation 4-13}$$

where f_t = character tensile strength of LVL (MPa)

A = cross sectional area of LVL (mm^2)

For WWW and SWS connections, the main member is LVL of cross-sectional area, A, is (150 mm × 63 mm) = 9450 mm^2. According to Carter Holt Harvey Technical Information (CHH, 2001), Hyspan has a characteristic tensile strength parallel to grain, f_t, of 27 MPa.

Therefore, the expected strength, R_n, is equal to 255 kN and the expected load of the connection, S*, is thus ≤ 230 kN. With an assumption that the load to be resisted equals 30% of the expected load, the design load is 70 kN.

4.7.3 Timber Connection Design for Ambient Condition

As published in the Carter Holt Harvey Technical Information for Hyspan (CHH, 2001), Hyspan LVL is categorised as J4 group due to its high tensile strength. Therefore in this research, all the timber connection design is based on data for the J4 group.

4.7.3.1 Bolted WWW Connections

As shown in Section 4.6.1 , the WWW connections have timber side members as well as timber main members at the connection. The side members are 45mm thick and the main member is 63mm thick.

In a similar manner to the singly-bolted WWW connection, the strength of a laterally loaded multi-bolted connection must satisfy Equation 4-8 and the nominal joint strength for a three member joint must satisfy Equation 4-9. The characteristic strength for a single 12mm bolt in a two member joint in dry 63mm timber loaded parallel to grain direction is 10.5kN.

Hence, the nominal joint strength, Q_n, is 21 kN. This means a joint with only a single bolt on one side of the connection can only provide strength of 21 kN.

As calculated in Section 4.7.2, the carrying load of a multi-bolted connection is 70 kN and according to NZS 3603, the strength reduction factor, Φ, for a bolted connection is 0.7. Therefore, the total number of bolts required on one side of the joint is:

$$\text{Number of bolts} = N^* / (\Phi \times Q_n)$$
$$= 5$$

4.7.3.2 Bolted SWS Connections

For this type of arrangement, the side members are 6mm thick steel plate instead of 45mm thick LVL. The main member is 63mm thick (see Section 4.6.2). Similar to the singly-bolted SWS connection, the strength of a laterally loaded bolted connection must satisfy Equation 4-8 and the nominal joint strength, Q_n, for a three steel and timber alternating member connection must satisfy Equation 4-10.

Knowing the characteristic strength for a single 12mm bolt in a two member joint in dry 63mm timber loaded parallel to grain direction is 10.5kN. Thus, Q_n is 31.5 kN. This means a joint with only one bolt on each side of the connection can only provide strength of 31.5 kN.

As calculated in Section 4.7.2, N* = 70 kN and the strength reduction factor, Φ, for a bolted connection is 0.7. Therefore, the total number of bolts required on one side of the joint is:

$$\text{Number of bolts} = N^* / (\Phi \times Q_n)$$
$$= 4$$

The stress introduced to the steel plate in SWS connection when load is applied must be checked so that the tensile stress is greater or equal to the design tensile load on the steel plate. Calculated in Section 4.6.4.2, the total designed tensile strength for a SWS connection is 386 kN.

Since the design carrying load capacity of 70 kN for the multi-bolted SWS connection is lower than the total tensile strength of the steel plates for SWS connection, this concluded that the steel plate would not fail under the design tensile strength for the whole specimen.

4.7.3.3 Bolted WSW Connections

For this type of arrangement, the side members are 45mm thick steel plates and the main member is 6mm thick steel plate (see Section 4.6.2). The strength of a laterally loaded bolted connection must satisfy Equation 4-8 and the nominal joint strength, Q_n, must satisfy Equation 4-10. The characteristic strength, Q_k, for a single 12mm bolt in a two member joint in dry 63mm timber loaded parallel to grain direction is 9.83kN.

Substituting the known variables into Equation 4-10 shows that Q_n equals 29.5 kN. This means a joint with only one bolt on each side of the connection can only provide strength of 29.5 kN.

As calculated in Section 4.7.2, N* equals 70 kN. From NZS 3603 Clause 2.5, the strength reduction factor, Φ, for a bolted connection is 0.7. Therefore, the total number of bolts required on one side of the joint is:

$$\text{Number of bolts} = N^* / (\Phi \times Q_n)$$
$$= 4$$

The design tensile strength of steel for a WSW connection is 193 kN (see Section 4.6.4.3), which is lower than the design carrying load for a multi-bolted WSW connection of 70 kN. This concludes that the steel plate would not fail under the design tensile strength.

4.7.4 Location of Bolts in Connections

4.7.4.1 WWW Bolted Connections

Based on the assumptions given in Section 4.7.1, the calculated design strength of the connection is 70kN (see Section 4.7.2). In order to achieve the design strength, 5 bolts are required for the WWW connection (See Section 4.7.3.1).

All the connections are to be tested under tension. Therefore the requirement of NZS 3603 (1994) for bolted timber connections tested under tension are summarised in Table 4-10.

Table 4-10: Requirement summary for bolted connections according to NZS 3603 (1994).

Specific	Requirement	
End distance	$8\times d_a$	96 mm
Edge distance	$2\times d_a$	24 mm
Fastener row distance	$5\times d_a$	60 mm
Fastener Spacing (across grain)	$2.5\times d_a$	30 mm

For WWW connections with a total of 5 bolts, a value of 2 is chosen to be the number of bolts across the grain. Therefore, the width of the LVL member is divided into 3 equal sections, each section with width of (150mm / 3) = 50mm.

The design specifications of the WWW connections are summarised in Table 4-11. All the design achieved the requirement of NZS 3603 (1994).

Table 4-11: Summary of designed bolts location for WWW connections.

	Required	Design	Remarks
From Member Edge	24mm	50mm	Achieved
Spacing between bolts across grain	30mm	50mm	Achieved
Distance from Member End	96mm	100mm	Achieved
Distance between rows of bolts	60mm	60mm	Achieved

The location of the bolts in a WWW Connection is shown below as Figure 4-10.

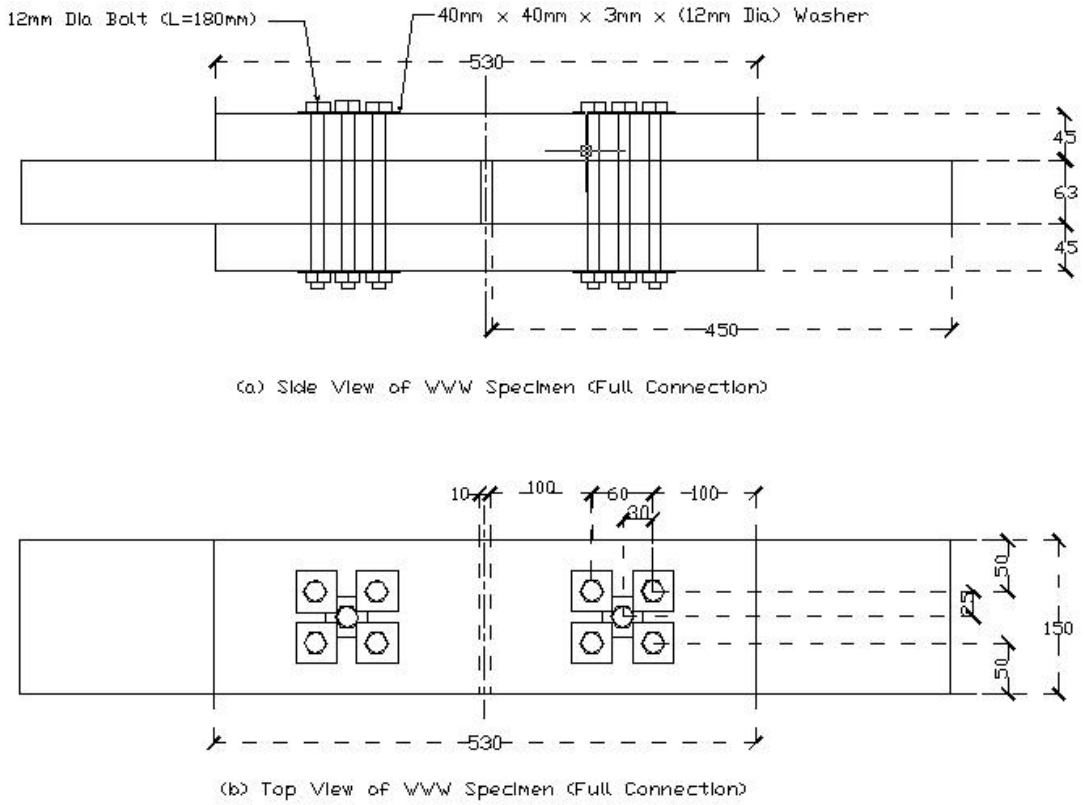

Figure 4-10: Location of bolts in WWW Connections.

4.7.4.2 SWS Bolted Connections

To achieve the calculated design strength of 70kN (See Section 4.7.2) for the SWS Connection based on the assumptions given in Section 4.7.1, a total of 4 bolts are required (See Section 4.7.3.2).

The characteristic tensile strength of Hyspan (27 MPa) is lower than the characteristic tensile strength of steel plate (275 MPa). This means that the LVL is weaker compared to steel plate. Hence, the location and spacing for SWS connection is based on the LVL instead of steel plate.

The requirements for the SWS connections are identical to the WWW connections. Therefore the information in Table 4-10 applies to the SWS connections. For SWS connections with a total of 4 bolts, a value of 2 is chosen to be the number of bolts

across the grain. Therefore, the width of the LVL member is divided into 3 equal sections, each section with width of 50mm.

The design specifications of the SWS connections are summarised in Table 4-12. All the design achieved the requirement of NZS 3603 (1994).

Table 4-12: Summary of designed bolts location for SWS connections.

	Required	Design	Remarks
From Member Edge	24mm	50mm	Achieved
Spacing between bolts across grain	30mm	50mm	Achieved
Distance from Member End	96mm	100mm	Achieved
Distance between rows of bolts	60mm	60mm	Achieved

The location of the bolts in a SWS Connection is shown below as Figure 4-11.

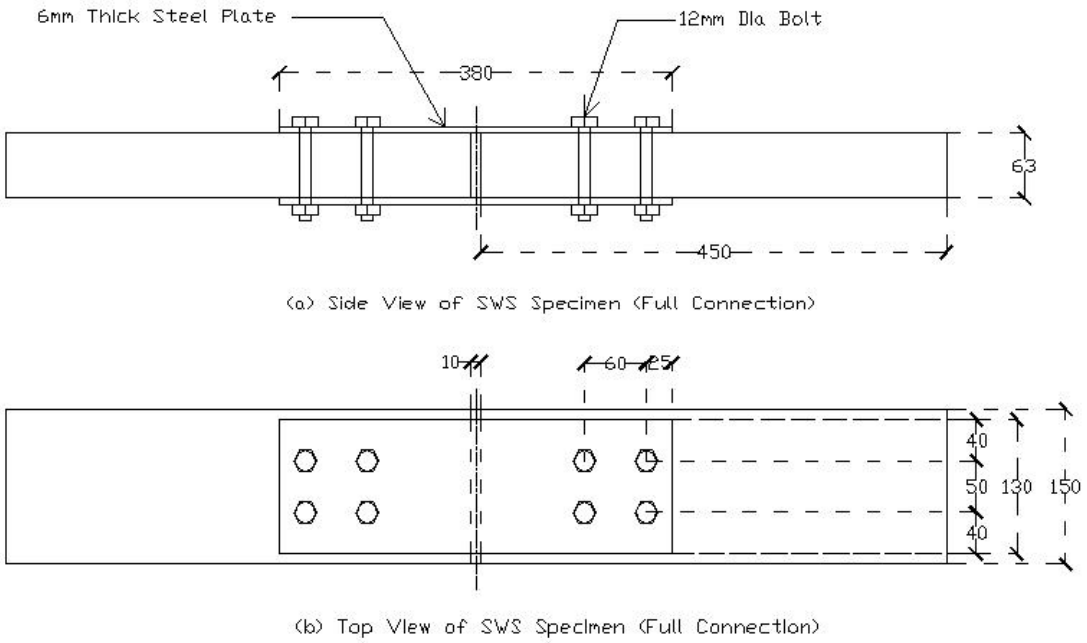

Figure 4-11: Location of bolts in SWS Connections.

4.7.4.3 WSW Bolted Connections

To achieve the calculated design strength of 70kN (See Section 4.7.2) for the WSW Connection based on the assumptions given in Section 4.7.1, a total of 4 bolts are

required (See Section 4.7.3.3). Similar to the SWS connection, the LVL is weaker compared to steel plate. Hence, the location and spacing for WSW connection is based on the LVL instead of steel plate.

The bolts spacing requirements for WSW connections are similar to the WWW connections and is summarised in Table 4-10. For WSW connections with a total of 4 bolts, a value of 2 is chosen to be the number of bolts across the grain. Therefore, the width of the LVL member is divided into 3 equal sections, each section with width of 50mm

The design specifications of the SWS connections are summarised in Table 4-13. All the design achieved the requirement of NZS 3603 (1994).

Table 4-13: Summary of designed bolts location for WSW connections.

	Required	**Design**	**Remarks**
From Member Edge	24mm	50mm	Achieved
Spacing between bolts across grain	30mm	50mm	Achieved
Distance from Member End	96mm	100mm	Achieved
Distance between rows of bolts	60mm	60mm	Achieved

The location of the bolts in a WSW Connection is shown below as Figure 4-12.

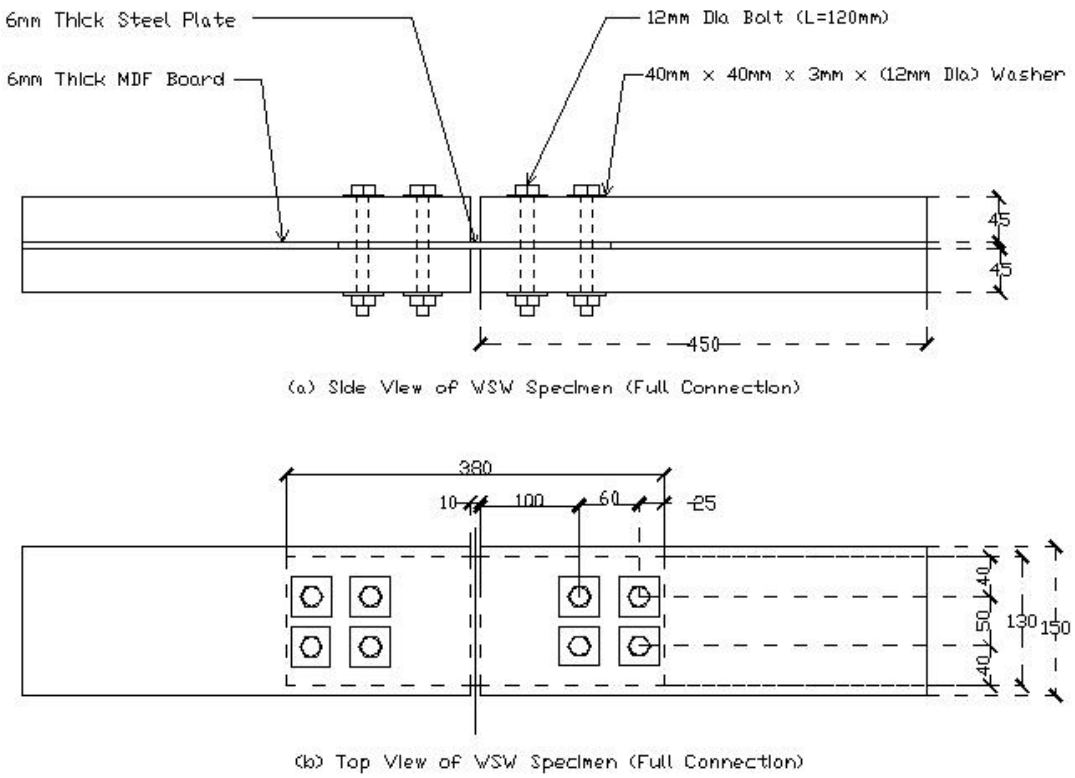

Figure 4-12: Location of bolts in WSW Connections.

5 Description of Testing Procedures, Results Analysis

5.1 Experimental Procedures

5.1.1 Ambient Tests

Specimens with only one bolt were subjected to Ambient Tests, in order to measure the embedding strength of the member. For these tests, the specimens were not heated. However, the tests were conducted using the loading frame that forms part of the furnace system. This is because all the equipment required to conduct the test was already set up and installed on the furnace system. Additionally, this ensures that identical steps were taken for all tests. The procedures to conduct an ambient test are below:

1. Place the specimen in furnace.
2. Connect the load system, thermocouples and potentiometer to the computer system.
3. Apply load until a displacement of 0.5 mm was recorded.
4. Release the load.
5. Re-apply the load until failure.

The term “Failure” in this research is defined as occurring when the timber member undergoes tension failure, the wood splits, the bolt breaks, or when the displacement reaches the limits of the equipment. The potential failure modes are discussed in more detail in Section 2.2.6.

5.1.2 Heated Tests

Specimens with only one bolt were also subjected to Heated Tests. The procedures to conduct a heated test are similar to the ambient test, with an additional heating procedure. The specimen was heated for a defined period before testing. The detailed procedures are given below:

1. Place the specimen in furnace.
2. Connect the load system, thermocouples and potentiometer to the computer system.

3. Switch on the furnace to the desired temperature settings.
4. Heat the specimen at desired temperature settings for 2 hours.
5. Apply the load until a displacement of 0.5 mm was observed.
6. Release the load.
7. Re-apply the load until failure.

The definition of "Failure" is the same as for the Ambient Tests.

5.1.3 Fire Tests

Two different specimens for each type of connection, namely a one-bolted connection and a multi-bolted connection were subjected to Fire Tests. The one-bolted connection was to compare the results obtained from the constant temperature tests with the real fire tests. The study of multi-bolted connection is to compare the findings from a single bolted connection with a multi-bolt joint. The procedures to conduct the single and multiple bolt connections are identical and are described below:

1. Place the specimen in furnace.
2. Connect the load system, thermocouples and potentiometer to the computer system.
3. Apply the pre-calculated load for 20 minutes.
4. Switch on the furnace to the maximum temperature setting of 750°C.
5. Apply load if necessary to maintain the load carried by load specimen until failure.

The definition of "Failure" is the same as for the Ambient Tests.

5.1.4 Bolt Yield Moment Tests

Bending tests of bolts at ambient temperature were conducted. Based on the yield moment obtained at ambient temperature and applying the reduction factor included in NZS 3404, the bending moment of bolt at various temperature ranges can be calculated.

Besides testing the yield moment of bolt at ambient conditions, another 4 tests were conducted using heated bolts.

The procedures to conduct bending tests are as below:

1. Two thermocouple wires, with thermocouple beads contacting the surface of bolt, were attached to each bolt using hose clamps.
2. Heat the bolt in furnace at a temperature of 250°C for 6 hours.
3. Remove the heated bolt from furnace and wrap in thermal blanket prior to testing (to reduce heat loss).
4. Place the heated bolt shank on supports 100mm apart in the Instron testing machine and connect the thermocouples to the computer.
5. Locate the seat so that load is at the centre of the 100mm span.
6. Allow the temperature of the bolt to settle to the desired temperature before testing.
7. Start loading the bolt at the speed of 1mm/min, at the same time record the load applied, displacement of the bolt and temperatures of the bolt.
8. Stop the experiment after 10 minutes.

5.2 Results Analysis

5.2.1 Experimental Embedment Strength

The arrangement of the SWS connection was the most identical to the testing apparatus as required by ISO 10984-2 (see Section 2.4.4). The differences between the standard embedment strength tests and the singly-bolted SWS connections used in this research are:

	Singly-bolted SWS connection	**Standard Embedment Test**
1.	Steel members tightly bolted to timber member.	No contact between steel members and test specimen.
2.	Two fasteners were used in each test.	Only one fastener used in test.

The standard embedment test ceased when the displacement of fastener into the timber reached 5mm or when the predicted maximum load is reached. Since in the singly-bolted SWS connections used two fasteners in each tests, it was assumed that the testing ceased when a total displacement of 10mm occurred. This assumption simply assumed that each fastener displaced 5mm.

The load experienced by the singly-bolted connection tested under constant temperature was used to calculate the embedment strength of LVL using the Johansen's Equations. Other information required to calculate the LVL embedment strength are the bending moment of bolt, the timber thickness, the experimental failure mode, and the temperature of the bolt. With all the information, knowing the failure mode, the known variables can be substituted into the correct Johansen's equations.

5.2.2 Bolt Bending Test

The standard fastener yield moment is to be tested using the two point loading method (ISO 10984:1 (1999)). However, the fastener yield moment tested for this research is via a single point loading. The support span, l, on the fastener is 100mm and the supporting points are avoided from the threads (see Figure 5-1).

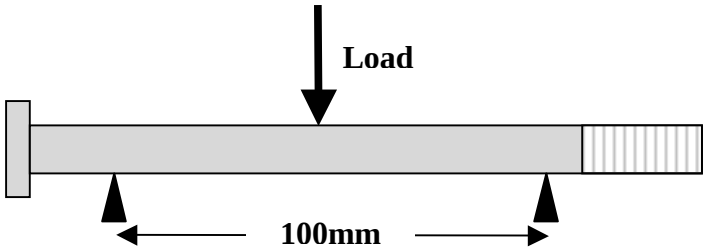

Figure 5-1: Schematic drawings of yield moment test.

To simplify the calculation process, the yield moment was calculated using the yield load, P_{yield}, from the experimental load-displacement curve. The P_{yield} is the point of which the extrapolated initial and final tangent of the load-displacement curve met. (see Figure 5-2). The yield moment, M_y, was calculated using Equation 5-1:

$$M_y = \frac{P_{yield} \times l}{4} \qquad \text{Equation 5-1}$$

where P_{yield} = Yield Strength

l = Support span

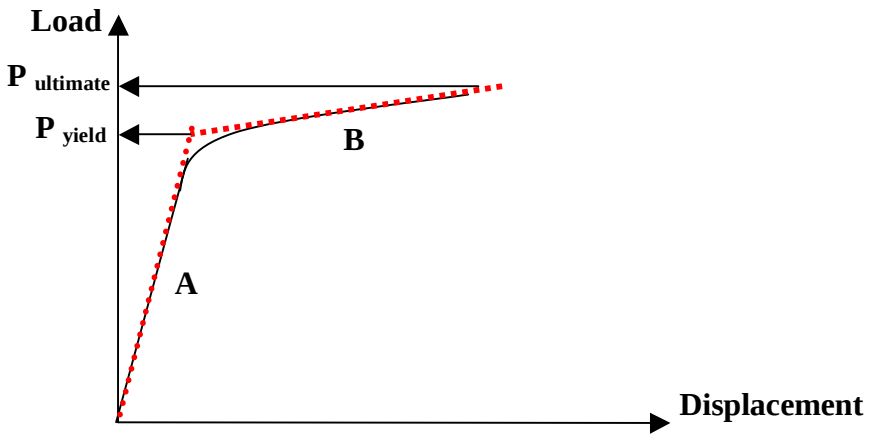

Figure 5-2: Illustration of P_{yield} value on Load-Displacement curve.

5.2.3 Bolt Yield Moment at elevated temperature

The strength of steel degraded as the steel was exposed to higher temperature. The NZS 3404 (1997) and Eurocode 3 (2003) suggested slightly different reduction factors (see Section 2.4.2). In this research, the NZS 3404 (1997) was adopted to calculate the strength reduction for the bolt and hence the yield moment.

6 Experimental Results

6.1 Overview

The results shown in this section include all the results and analysis of the three different types of connection, namely the WWW connections, the SWS connections and the WSW connections tested. The embedment strength of LVL was calculated using the Johansen's Equations based on the load of the SWS Heated Tests. This experimental embedment strength value is then used to predict the failure load and the failure mode of the WWW and WSW connections using the same equations. This also acts as a counter check of the experimental embedment strength. Finally, the experimental embedment strength is also used to predict the failure mode and failure for all types of connection tested under fire conditions.

6.2 Ambient Tests Result

The load-displacement plot at the start of each test was very variable and unpredictable. For this reason, the data for the start of each test has not been shown. The modified Load – Displacement curves, which ignored the slips at the start of testing, of singly-bolted WWW, WSW and SWS connection tested under ambient conditions, are shown as Figure 6-1. The actual Load vs. Displacement curves are included in Appendix A.

From Figure 6-1, the SWS connection is the stiffest and the WWW was least stiff among all three types of connection. The WSW connection and the SWS connection had almost the same ultimate strength (50 kN), larger than the WWW connection (35.4 kN).

The maximum load and displacement experienced by the connection at maximum applied load at ambient condition for each joint was tabulated as in Table 6-1.

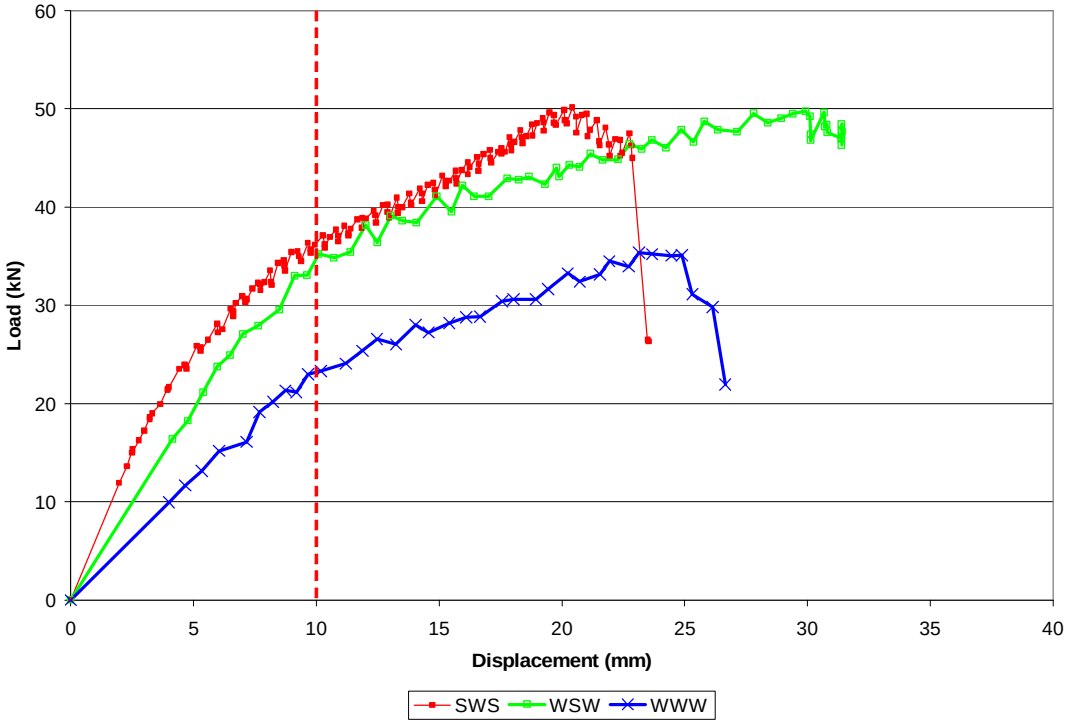

Figure 6-1: Load-Slip curves for singly-bolted WWW, WSW and SWS connection tested at ambient conditions.

Table 6-1: Summary of maximum load and displacement at maximum load for each connection type tested at ambient conditions.

Type of Connection	Maximum Load (kN)	Displacement at Maximum Load (mm)	Failure Mode*
WWW	35.4	25.5	C, S
SWS	50.1	24.5	C, S
WSW	49.7	35.0	C
*** Refer to Section 2.2.6.**			

Figure 6-1 and Table 6-1 show that at ambient conditions, the WWW and the SWS connections failed at approximately 25mm of displacement when the timber member split. On the other hand, the WSW connection reached the maximum displacement and yet no split occurred.

Figure 6-2 shows the deformation of the fasteners tested under ambient conditions. For all ambient tests, plastic deformation occurred on the shank of bolts at half the

depth of the whole connection. The counter-effect of load from the steel plate member to the fastener was obvious (see Figure 6-2(b) and (c)). Figure 6-2(d) and (i) schematically shows the crushing on the connection after the test.

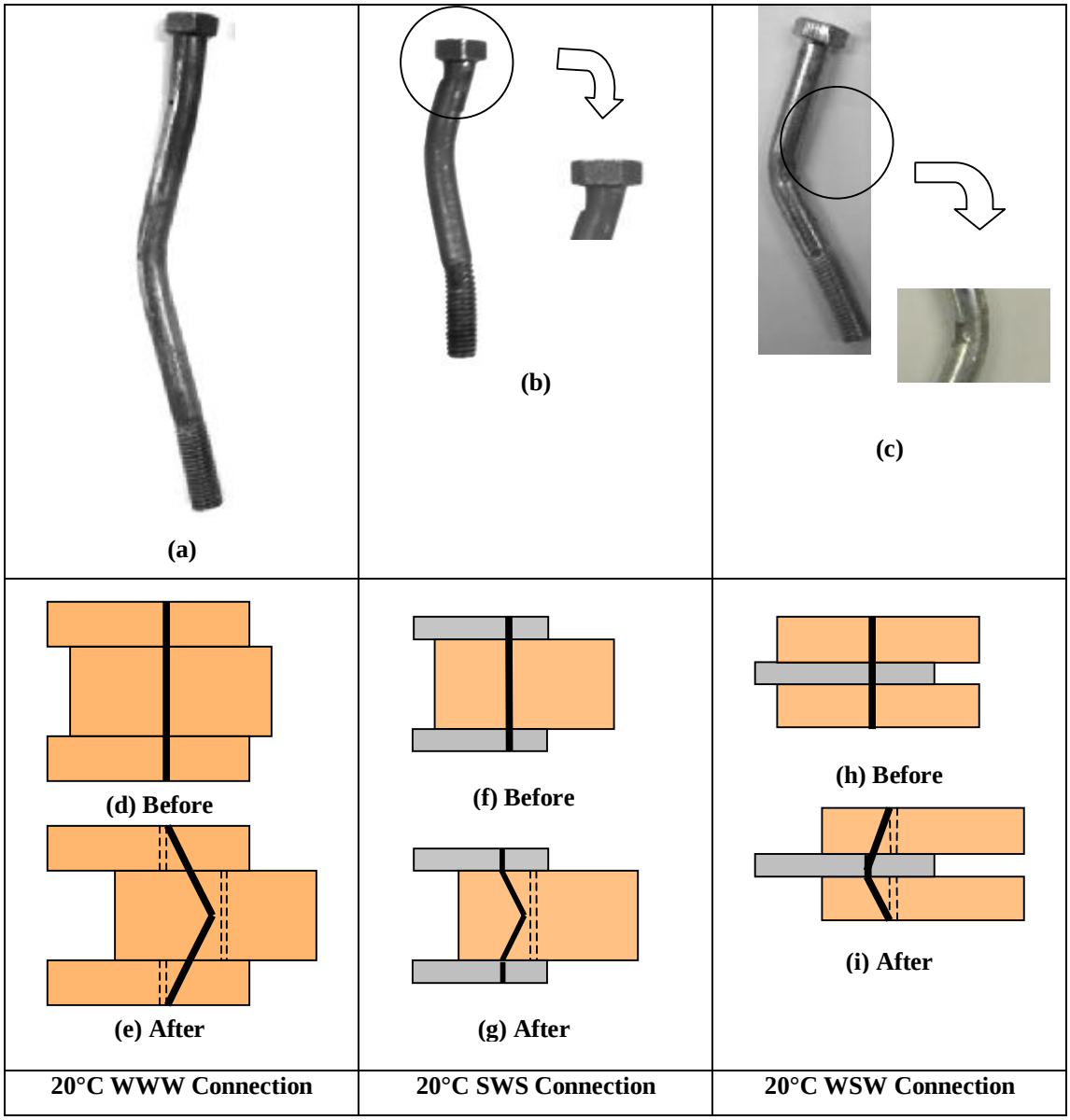

Figure 6-2: Deformed fasteners at ambient conditions for WWW, SWS and WSW connections.

6.3 Heated Test Results

Figure 6-3, Figure 6-4 and Figure 6-5 show the Load-Slip curves for all the singly – bolted WWW, WSW and SWS connections tested under ambient and constant temperature tests. These graphs are the modified Load – Displacement curves, which

ignored the slips at the start of testing. The 20°C curves shown in Figure 6-3, Figure 6-4 and Figure 6-5 were the same as in Figure 6-1.

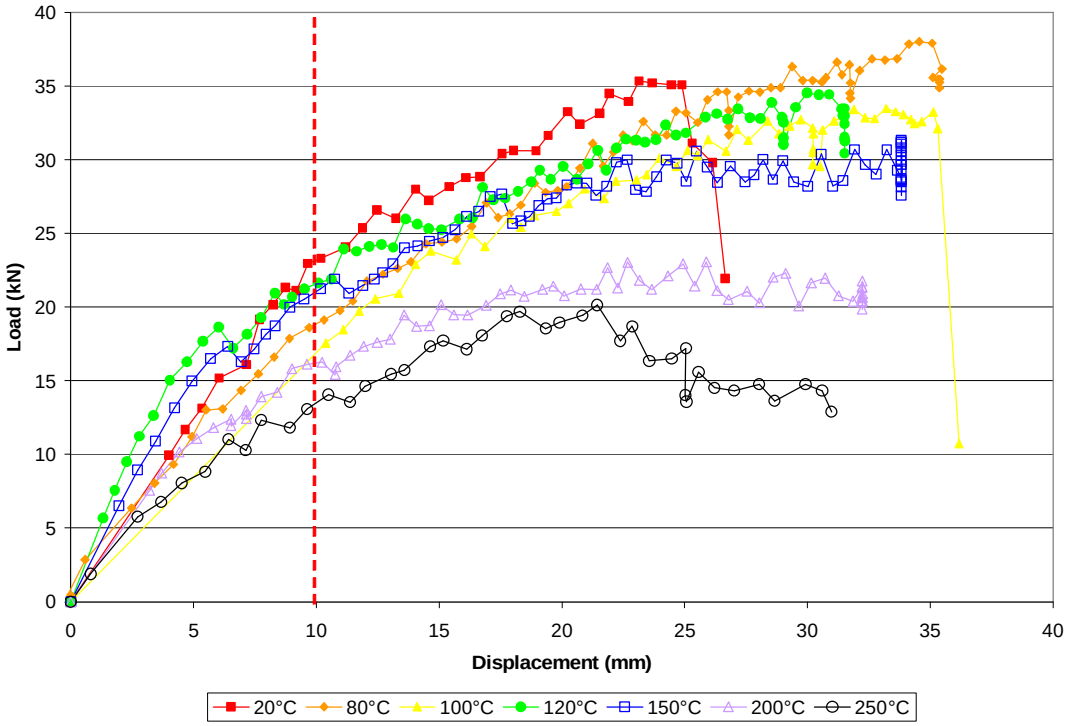

Figure 6-3: Load-Slip curves for WWW Connections at various heating temperatures.

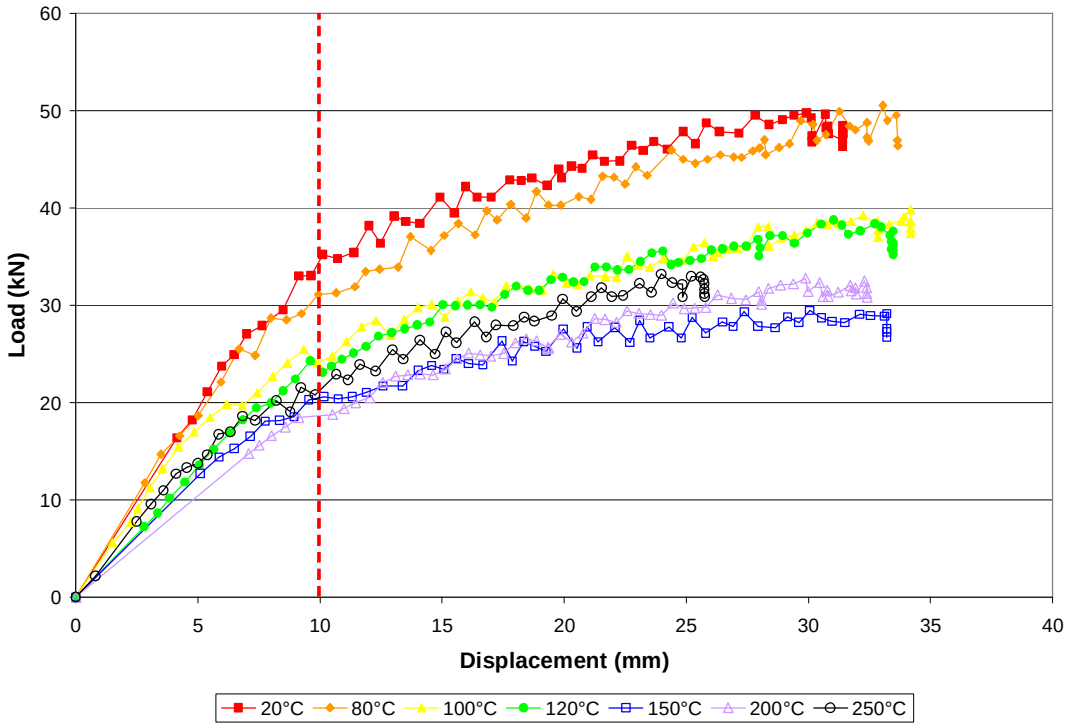

Figure 6-4: Load-Slip curves for WSW Connections at various heating temperatures.

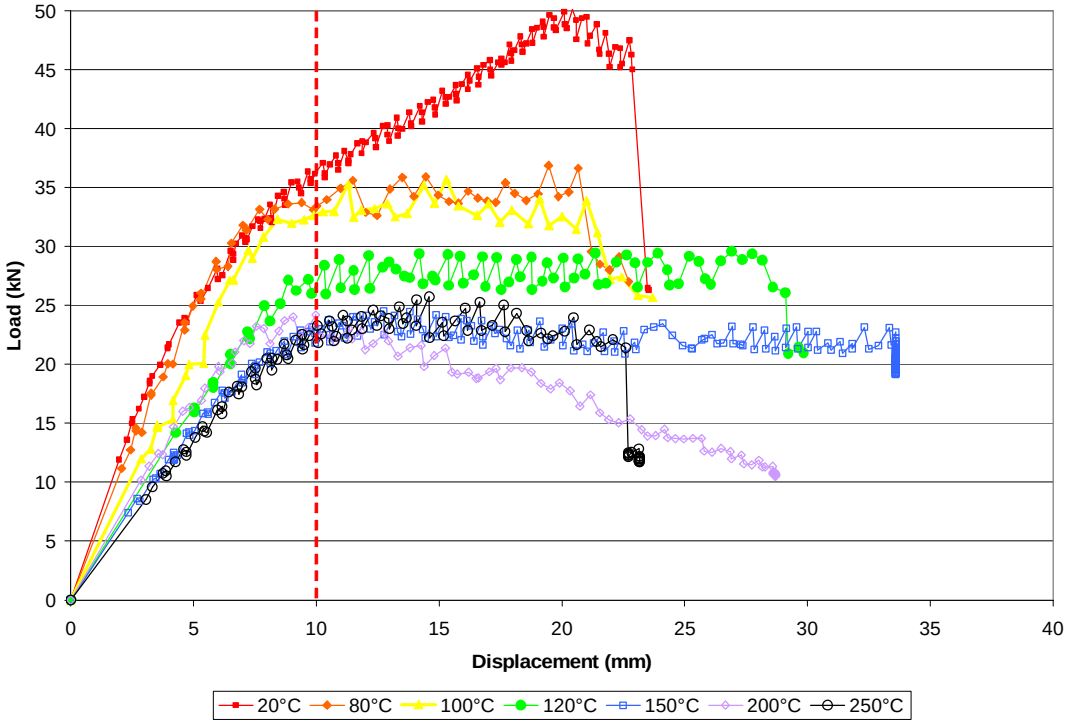

Figure 6-5: Load-Slip curves for SWS Connections at various heating temperatures

All the three graphs (Figure 6-3, Figure 6-4 and Figure 6-5) show a similar trend, i.e. reduction in stiffness and ultimate strength for higher values of the constant temperature.

For WWW and WSW connections, the Load-Slip curves initially had a very steep gradient. After reaching displacement of 7mm, the gradient reduced slightly. Throughout the testing duration, the Load-Slip curve had no sign of reaching a plateau.

However, for SWS connection tested at ambient condition, the curve had similar characteristic to the WWW and WSW connection. For connections that were exposed to higher temperature, all the Load-Slip curves reached a plateau.

The maximum load capacity, the load experienced at displacement of 10mm and the various temperatures after two hours of heating phase within all types of connection

tested at constant temperature were summarised in Table 6-2, Table 6-3 and Table 6-4 below.

Table 6-2: Experimental results for WWW Connection exposed to constant temperature.

WWW								
Environment Desired Temperature		**20°C**	**80°C**	**100°C**	**120°C**	**150°C**	**200°C**	**250°C**
Maximum Load (kN)		35.6	38.0	32.8	34.5	31.3	23.1	20.1
Load at Displacement of 10mm (kN)		23.2	18.8	16.9	21.6	21.0	16.2	13.5
Temperature at start of Test								
Centre of Side Member (°C)		21	32	46	42	77	87	101
Shear Interface (°C)		21	39	40	38	54	86	94
Centre of Main Member (°C)		21	36	43	54	56	74	91
Bolt	Bolt Head (°C)	21	42	59	66	87	118	146
	Mid-Side Member (°C)	21	48	59	58	80	115	145
	Mid-Centre Member (°C)	21	42	59	48	73	94	115
Furnace Air Temperature (°C)		21	74	100	116	149	214	293
Furnace Exhaust Temperature (°C)		21	56	77	79	144	119	254
Failure Mode*		**C**	**C**	**C**	**C**	**C**	**C**	**C**
*** Refer to Section 2.2.6.**								

Table 6-3: Experimental results for WSW Connection exposed to constant temperature.

WSW								
Environment Desired Temperature		**20°C**	**80°C**	**100°C**	**120°C**	**150°C**	**200°C**	**250°C**
Maximum Load (kN)		35.6	38.0	32.8	34.5	31.3	23.1	20.1
Load at Displacement of 10mm (kN)		23.2	18.8	16.9	21.6	21.0	16.2	13.5
Temperature at start of Test								
Centre of Side Member (°C)		13	44	56	66	85	101	115
Shear Interface (°C)		13	39	52	66	82	102	119
Bolt	Bolt Head (°C)	13	50	62	73	99	128	164
	Mid-Side Member (°C)	13	49	61	70	102	124	152
	Mid-Centre Member (°C)	13	43	51	66	80	104	128
Furnace Air Temperature (°C)		13	69	86	104	140	169	247
Furnace Exhaust Temperature (°C)		13	48	71	86	102	133	168
Failure Mode*		**C**	**C, S**	**C**	**C**	**C**	**C**	**C**
*** Refer for Section 2.2.6**								

Table 6-4: Experimental results for SWS Connection exposed to constant temperature.

SWS							
Environment Desired Temperature		**20°C**	**80°C**	**100°C**	**120°C**	**150°C**	**200°C**	**250°C**
Maximum Load (kN)		50.1	36.9	35.7	29.6	24.5	24.4	26.1
Load at Displacement of 10mm (kN)		36.3	33.3	32.7	26.9	22.0	22.6	23.2
Temperature at start of Test								
Shear Interface (°C)		18	61	76	89	116	155	204
Centre of Main Member (°C)		18	54	64	88	97	113	184
Bolt	Bolt Head (°C)	18	59	74	91	113	151	202
	Mid-Side Member (°C)	18	59	73	90	114	147	200
	Mid-Centre Member (°C)	18	60	74	90	113	138	184
Furnace Air Temperature (°C)		18	76	94	120	142	194	251
Furnace Exhaust Temperature (°C)		18	74	79	99	109	111	160
Failure Mode*		**C,S**	**C,S**	**C,S**	**C,S**	**C**	**C,S**	**C,S**
*** Refer for Section 2.2.6**								

Figure 6-6 shows that the damage severity on the bolt changed as the tested condition changed. As the temperature was higher, the damage on bolt was less significant compare to those tested close to ambient conditions.

	Heated Test: 80°C	Heated Test: 250°C
WWW		
WSW	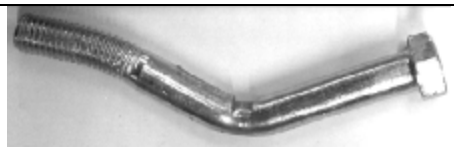	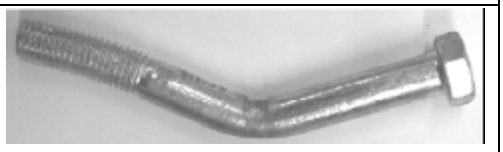
SWS	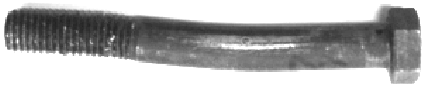	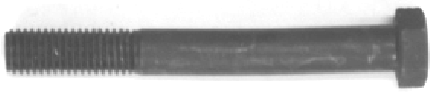

Figure 6-6: Comparison of bolt damage tested under different conditions.

6.4 Fire Tests

This section reports the results of singly-bolted connections as well as multi-bolted connections tested under fire conditions.

6.4.1 Experimental Fire Resistance vs. Standard Fire Resistance

For the Fire Tests, the time to char was assumed to be the time when excessive smoke came from the furnace. This measured time was not accurate because the design and the material used to construct of the furnace prevented observation of the process of heating the connection. Time to ignition was taken when flames were observed through the gaps between the specimen and the furnace opening. The connection was considered to have failed when it lost its ability to carry the required load.

The timelines for all specimens tested under realistic fire conditions are shown as Table 6-5. The results showed that the time to char for all experiments were similar. However, the WWW connection was the quickest to ignite because the specimen occupied the largest volume within the furnace compartment. The SWS connection, which has the smallest surface are of timber among all three types of connection, took the longest time for the specimen to ignite. The SWS specimen reached failure within the shortest period whereas the WWW specimen withstands the elevated conditions for the longest duration.

Table 6-5: Summary of timeline for real fire tests.

Type of Connection	Number of Bolts	Design Load (kN)	Average Applied Load (kN)	Time to Char (min)	Time to Ignition (min)	Time to Failure (min)
WWW	1	4.9	4.9	3.8	4.5	24.0
	5	23.1	23.0	4.0	5.0	23.2
			Average	**3.9**	**4.7**	**23.6**
WSW	1	6.8	6.8	4.2	5.9	20.0
	4	23.1	23.3	3.9	5.0	17.5
			Average	**4.00**	**5.4**	**18.8**
SWS	1	7.3	6.3	4.6	6.2	12.2
	4	23.1	22.7	3.9	6.2	13.6
			Average	**4.3**	**6.2**	**12.9**

Figure 6-7, Figure 6-8 and Figure 6-9 show the cumulative energy within the testing furnace throughout the duration of testing for all types of connection tested in fire conditions. The cumulative energy for an ISO 834 fire curve is also plotted.

As mentioned in Section 3.3, the furnace fire curve was different to the ISO 834 fire curve. The furnace fire curve slightly depends on the heating specimen. However, in order to report the fire resistance of each tested connection relative to the standard fire, the equal energy method was used. The time for the standard cumulative energy

to reached the cumulative energy when a connection fail is the standard failure time, i.e. the standard fire resistance of that connection.

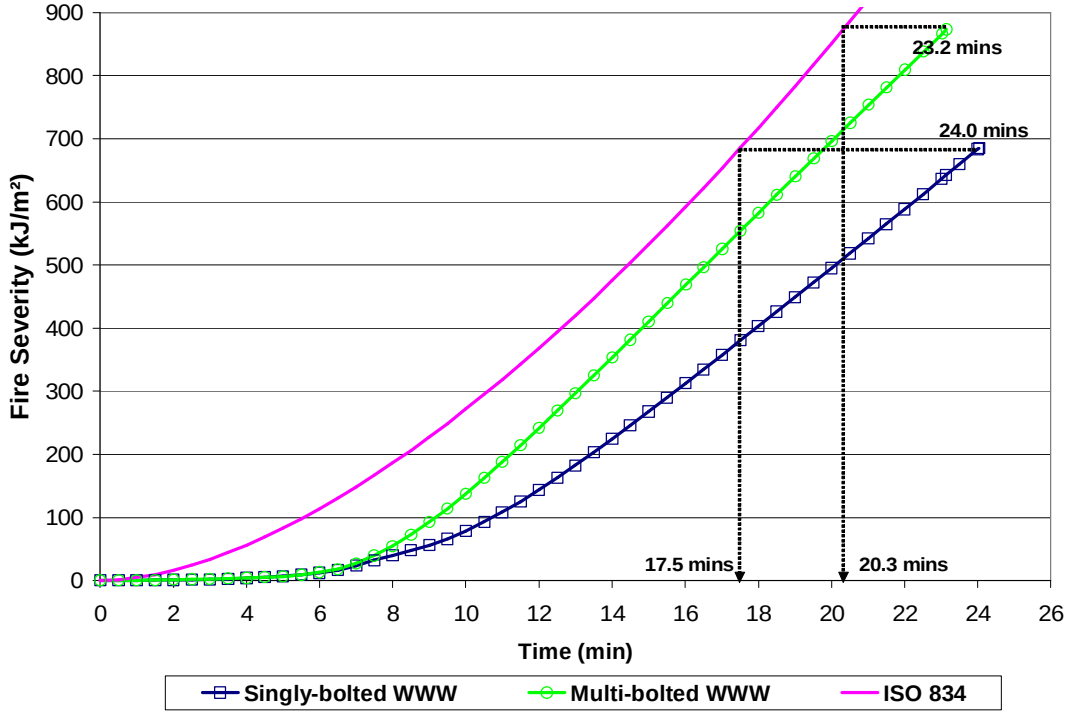

Figure 6-7: Fire resistance for WWW connections.

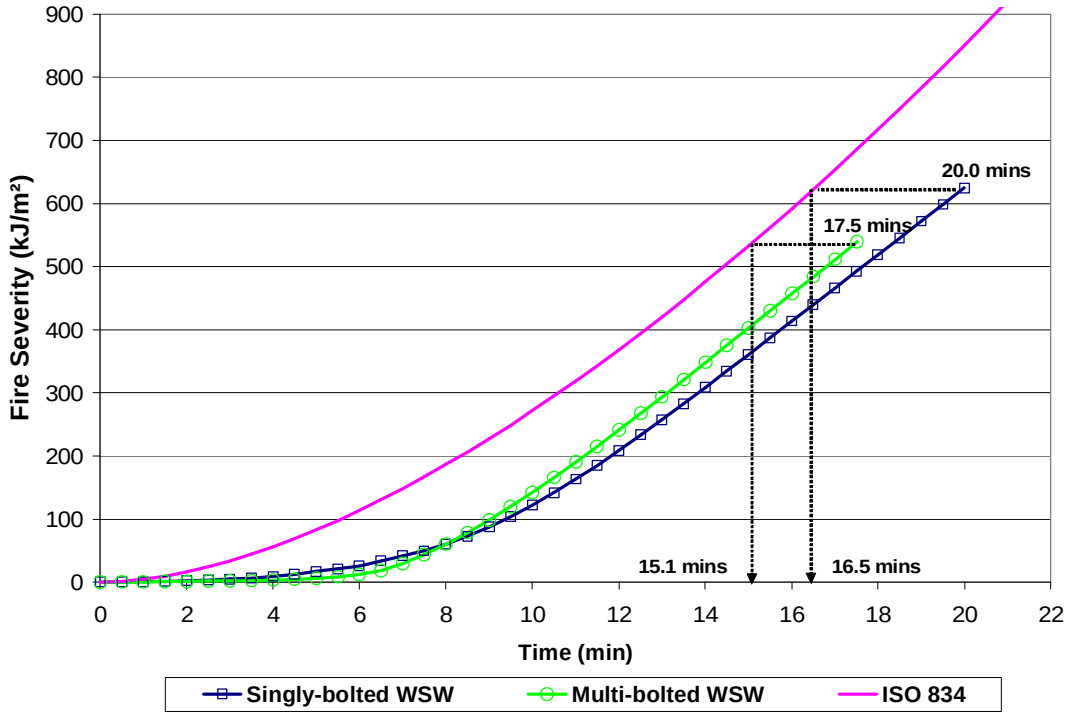

Figure 6-8: Fire resistance for WSW connections.

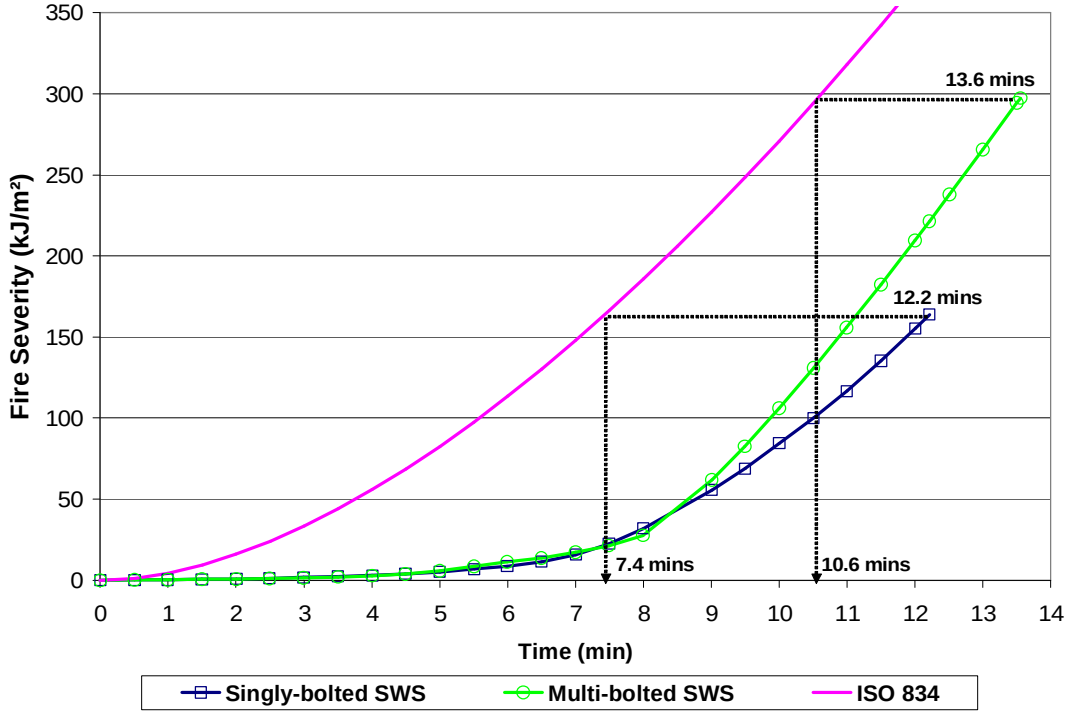

Figure 6-9: Fire resistance for SWS connections.

The experimental fire resistance and the standard fire resistance for all connections tested under fire conditions was summarised in Table 6-6. It showed that the WWW connections could resist fire for a longer period of time compare to other connections. The SWS connection performed the worst among all types of connections.

Table 6-6: Summary of fire resistance.

		Experimental Fire Resistance (min)	**Standard Fire Resistance** (min)
WWW	**1 Bolt**	24.0	17.5
	5 Bolts	23.2	20.3
WSW	**1 Bolt**	20.0	16.5
	4 Bolts	17.5	15.1
SWS	**1 Bolt**	12.2	7.4
	4 Bolts	13.6	10.6

The relationship between the applied load on connections and the displacement with respect to time under the influence of applied load for different types of connections

tested under fire conditions are shown as Figure 6-10, Figure 6-11 and Figure 6-12 below:

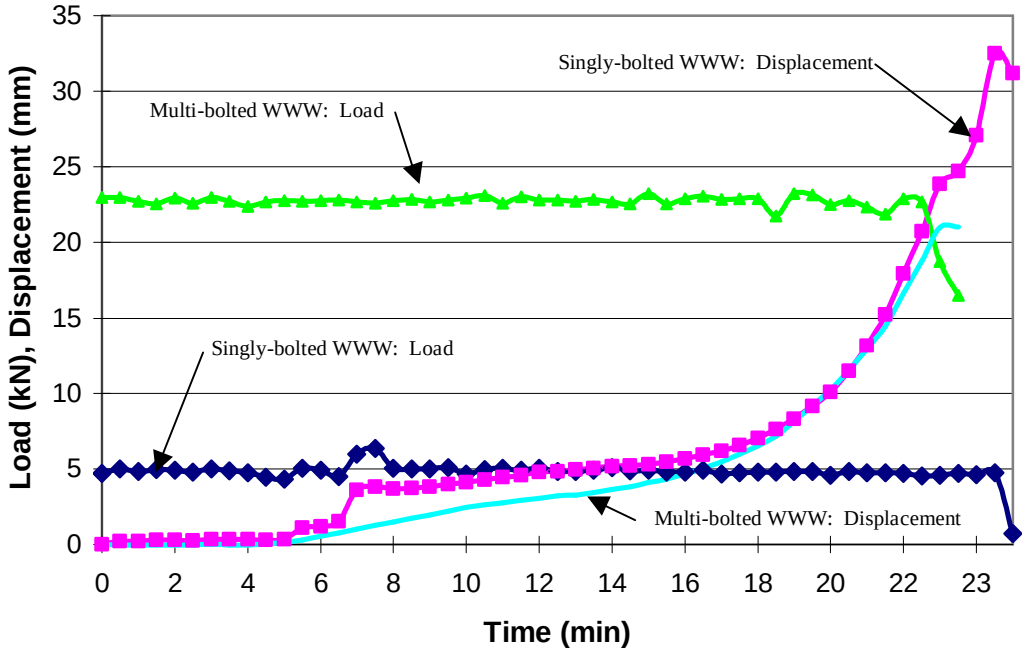

Figure 6-10: Load and Displacement relation for WWW connections fire tests.

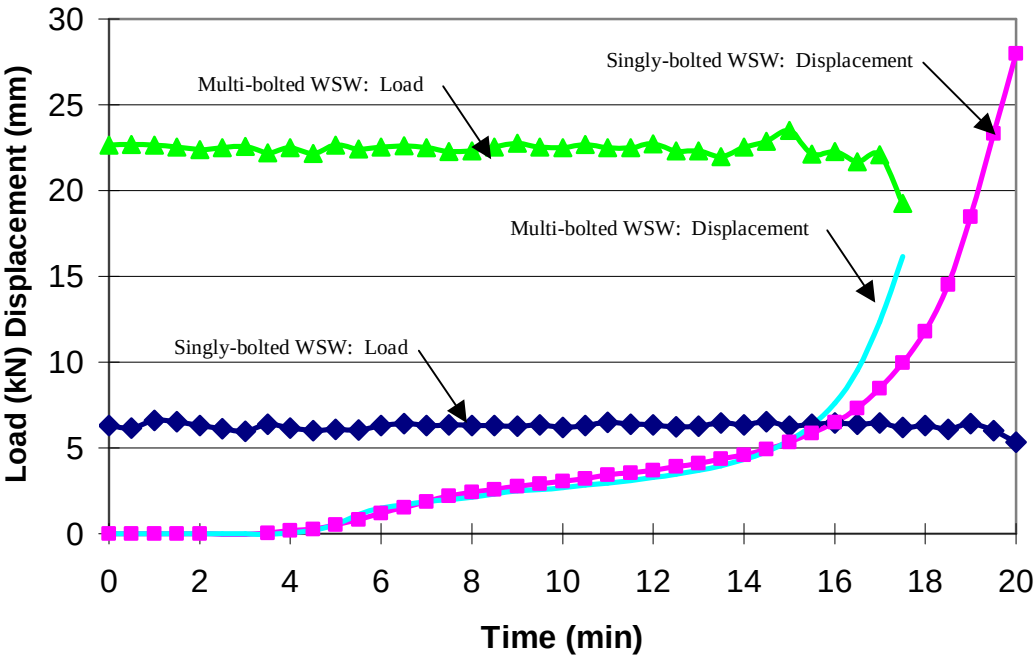

Figure 6-11: Load and Displacement relation for WSW connections fire tests.

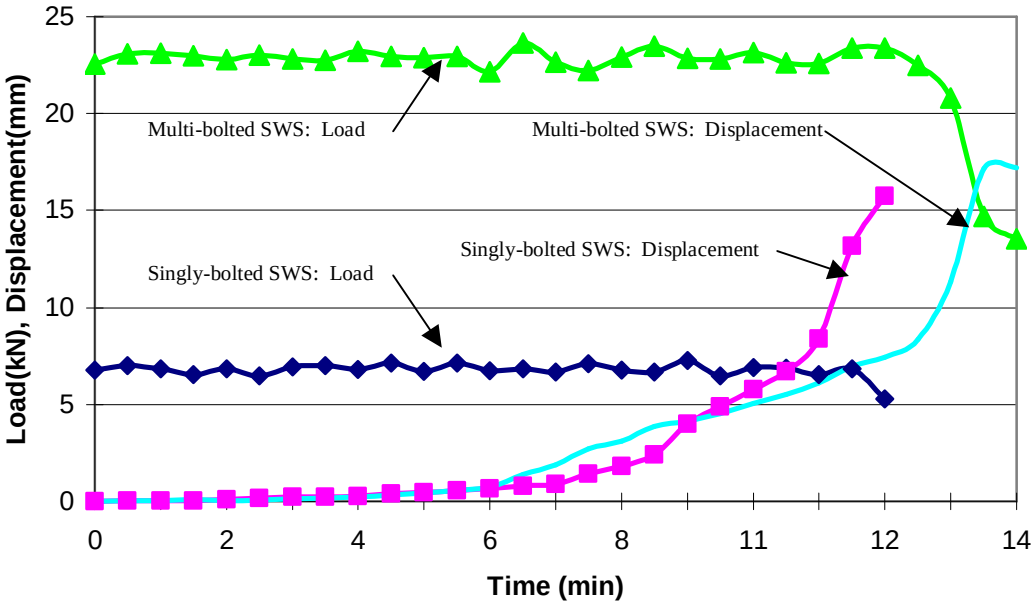

Figure 6-12: Load and Displacement relation for SWS connections fire tests.

6.4.2 Failure Mode for Fire Tested Connections

As observed after the fire tests, all connections tested (regardless of type) showed an identical failure mode, i.e. crushing as described in Figure 2-5 above.

For WWW connections tested in fire conditions, independent of the number of bolts, the both side members showed timber charring and crushing around the hot bolts and elongation of the bolt hole in the direction of the applied load. However, the dimensions of the drilled holes in the centre timber member remained unchanged.

The timber members within the SWS and WSW connections after exposure to high temperature fire tests were observed to have crushing failure similar to the side members of the WWW connections, i.e. elongation of the bolt hole in the direction of the applied load.

6.4.3 Charring Rate

The charring rate of LVL obtained experimentally is summarised in Table 6-7. The average charring depth of LVL for the SWS connections was smaller compared to the WWW and the WSW connections. Therefore the results for SWS connections were not included in the charring rate calculation. The reason for such smaller charring depth is because the steel plate members prevented the sides of the LVL from burning.

Table 6-7: Summary of charring rate for fire tests.

Type of Connection	Number of Bolts	[1]Average Char Depth (mm)	[2]Charring Rate (mm/min)	[3]Charring Rate (mm/min)
WWW	1	16.2	0.83	0.67
	5	16.8	0.92	0.72
WSW	1	15.8	1.12	0.79
	4	14.9	1.19	0.85
SWS	1	3.1	0.52	0.25
	4	3.4	0.46	0.25
[4]Mean Charring Rate			**0.84**	**0.76**
[4]Maximum Charring Rate			**1.19**	**0.85**
[4]Minimum Charring Rate			**0.83**	**0.67**
[4]Standard Deviation			**0.30**	**0.08**

[1] See Appendix B
[2] Charring Duration = Time to Failure – Time pyrolysis starts
[3] Charring Duration = Time to Failure
[4] Results excluded the data for SWS connections.

The average charring rate of 0.76 mm/mm was obtained by assuming the charring effect started as soon as the timber was exposed to elevated temperature from ambient conditions. This value was slightly higher than the values published by Lau (2006) and Lane (2004) which were 0.67 mm/min and 0.72 mm/min respectively. This calculation was performed solely to compare the value with other published values.

However, the charring rate calculated based on the duration between the time to pyrolysis starts and the time to failure, gave 3.16 mm/min. This calculation was performed because char was found in the singly-bolted specimens tested at constant temperature of 250°C. This calculation method is important because it gives a higher charring rate and can be correlated to the fact that wood only starts to char at temperature beyond 280°C.

6.5 Bending Tests

The results for the bending tests of the M12 bolts conducted using the Instron Machine are shown as Figure 6-13 below. The bolts showed elastic behaviour up to load of 4kN after which the bolt behaved inelastically as more of the bolt cross section yielded under the increasing load. By extrapolating the initial and final tangents of the load-displacement plot, a normal yield load of 6.6kN can be derived for the bolts.

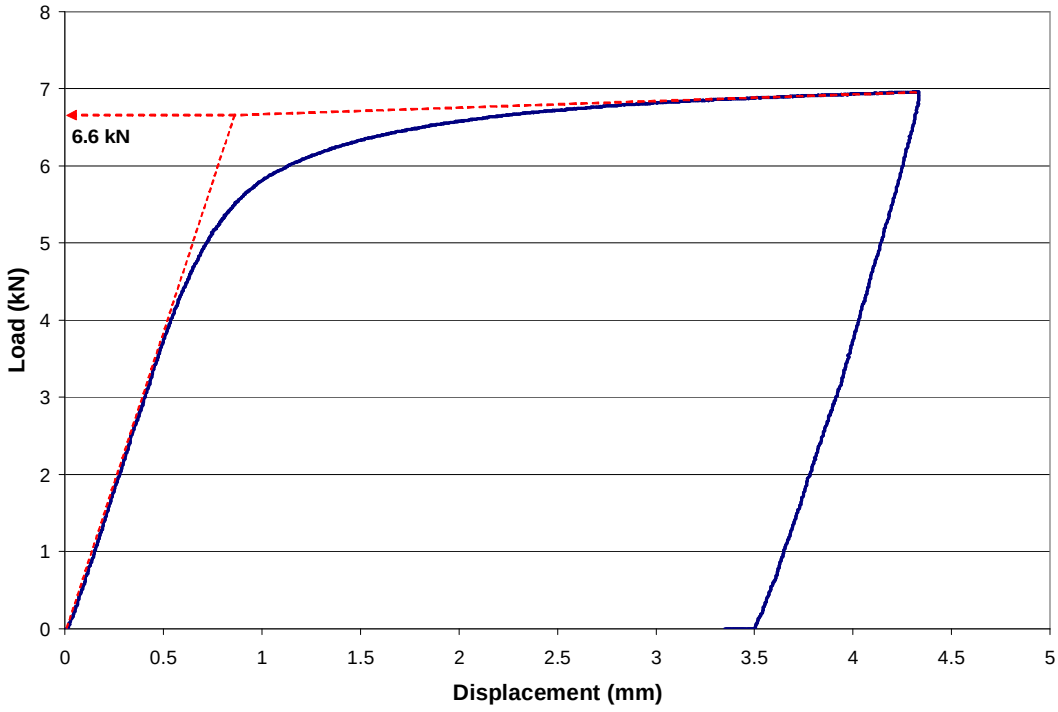

Figure 6-13: Load-Displacement Curves for M12 Bolts at ambient temperature.

According to Equation 5-1, the yield moment of the bolt is:

$$M_y = \frac{P \times l}{4} = \frac{6.6 \times 100}{4} = 165 kNmm$$

Appendix C shows the Load-Displacement curves for a series of bolts tested under different elevated temperatures. All the tests showed similar bending characteristics regardless of temperature. The reason is because the testing temperature region was below 200°C. NZS 3404 states that even though the modulus of elasticity for steel may reduce as soon as the temperature is higher than ambient, the strength of the bolt would not be reduced until the temperature exceeded 215°C.

6.6 Embedment Strength of LVL

6.6.1 Overview

Using the collected data from the Ambient and the Heated Tests, all the variables in Johansen's Equations were known except for embedment strength. Rearranging the relevant Johansen's Equations in terms of embedment strength and substituting all the other known variables, the experimental embedment strength for LVL can be calculated.

In this research, the experimental embedment strength was calculated based on the results obtained for the SWS connection because the arrangement of the SWS connection is similar to the ISO embedment strength testing requirement.

6.6.2 Experimental Embedment Strength

The load when the displacement reached 10mm for each SWS connection tested under constant temperature was used to calculate the embedment strength of LVL. The 10mm displacement was adopted on the assumption that each bolt in the connection heated under constant temperature displaced evenly when load was introduced, i.e. 5mm displacement from each bolt. The 5mm displacement was the end of the embedment strength ISO requirement.

Shown in Figure 6-14 is the calculated embedment strength using Johansen's Equations for SWS connections exposed to various temperatures. The embedment strength decreases up to bolt temperature of 120°C. However at temperatures higher than 120°C the strength increased. The test results clearly showed that as the wood started to dry due to high ambient temperature, the embedment strength of the timber increases accordingly.

The dashed line represents a modified LVL strength relative to bolt temperature whereby a linear approximation is used up to a temperature of 120°C. A constant value is assumed for all higher temperature. This modified LVL strength was then used in Johansen's Equations to compare the prediction failure load of the WWW and WSW connection tests under constant temperature conditions.

This embedment relationship is the also used to predict the failure load and failure mode for all types of connections tested in fire conditions.

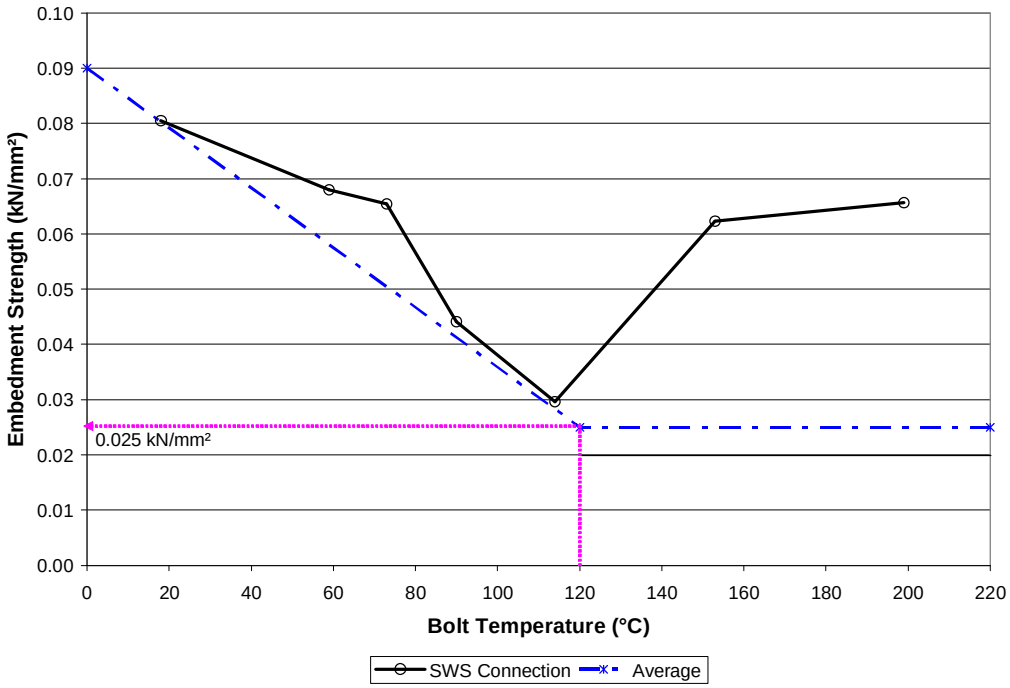

Figure 6-14: Experimental and modified embedment strength for LVL.

For timber exposed to fire conditions, unlike the timber tested under constant temperatures condition, the timber cross-section is subjected to a significant time dependent temperature and moisture gradient. The unburned residual cross-section of

the timber member is not subject to drying whereas the surface of the timber may completely lose its moisture. Therefore it is important to study the relationship between different of moisture content level across the timber cross-section with respect to timber strength.

In this research study, the embedment strength of the timber is calculated using the bolt temperature. In fact, the embedment strength of the timber is not governed by the bolt temperature but the timber temperature close to the bolt. It would be interesting to study the temperature differences between the bolt and the timber adjacent to the bolt under fire conditions using computer simulations.

6.6.3 Predicted failure load for the WWW and the WSW connections

Using the experimental embedment strength calculated from the SWS connection, the predicted failure load for each type of WWW and WSW failure mode was plotted in Figure 6-15 and Figure 6-16 respectively.

The prediction of the WWW connections using Johansen's Equations shows that up to a bolt temperature of 60°C, Failure Mode K is the most probable failure mode. Beyond a bolt temperature of 60°C, the most probable failure mode is Failure Mode H. The experimental observed failure mode showed that Failure Mode K occurred from 20°C up to bolt temperature of 150°C. This partially agreed with the predicted failure mode. At higher temperatures, Failure Mode J occurred instead of Failure Mode H. It over predicted the failure load up to 60°C and under predicted at bolt temperatures higher than 60°C. This shows that the predictions at higher temperature were conservative.

For WSW connections, the predictions show that up to bolt temperature of 150°C, Failure Mode G is the most probably failure mode. The experimental observed failure mode agreed with the predicted failure mode. The predicted failure load was also conservative because the failure load for Failure Mode G using Johansen's Equation is always lower than the actual experimental load.

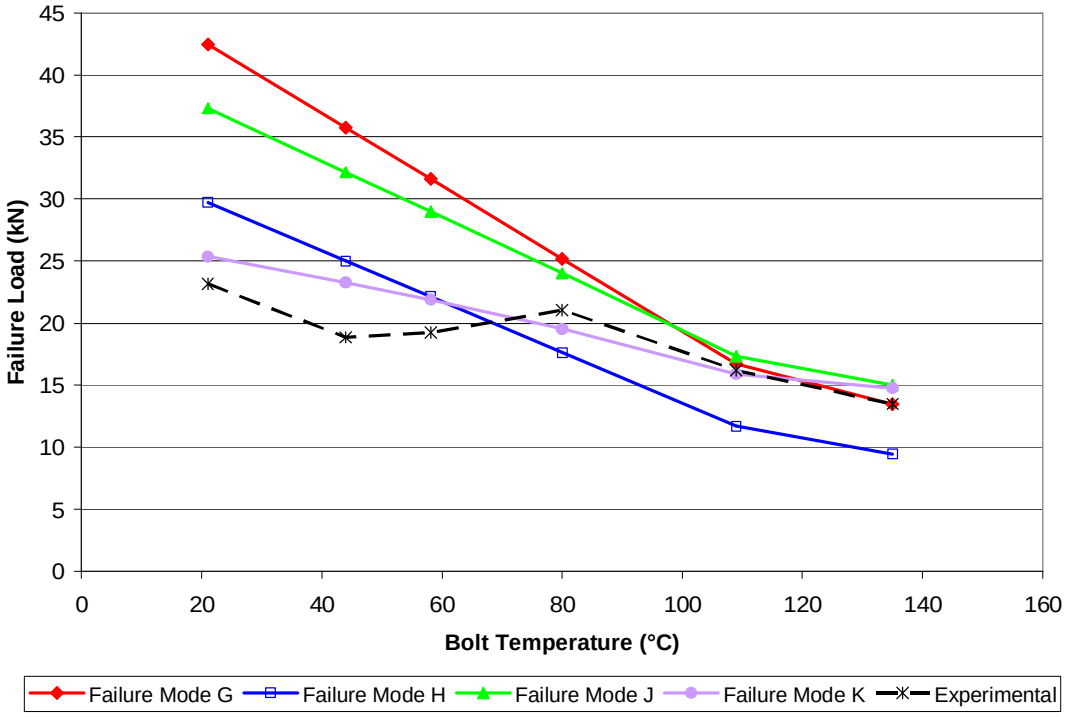

Figure 6-15: Predicted failure mode and experimental failure load for singly-bolted WWW connections tested at constant temperature.

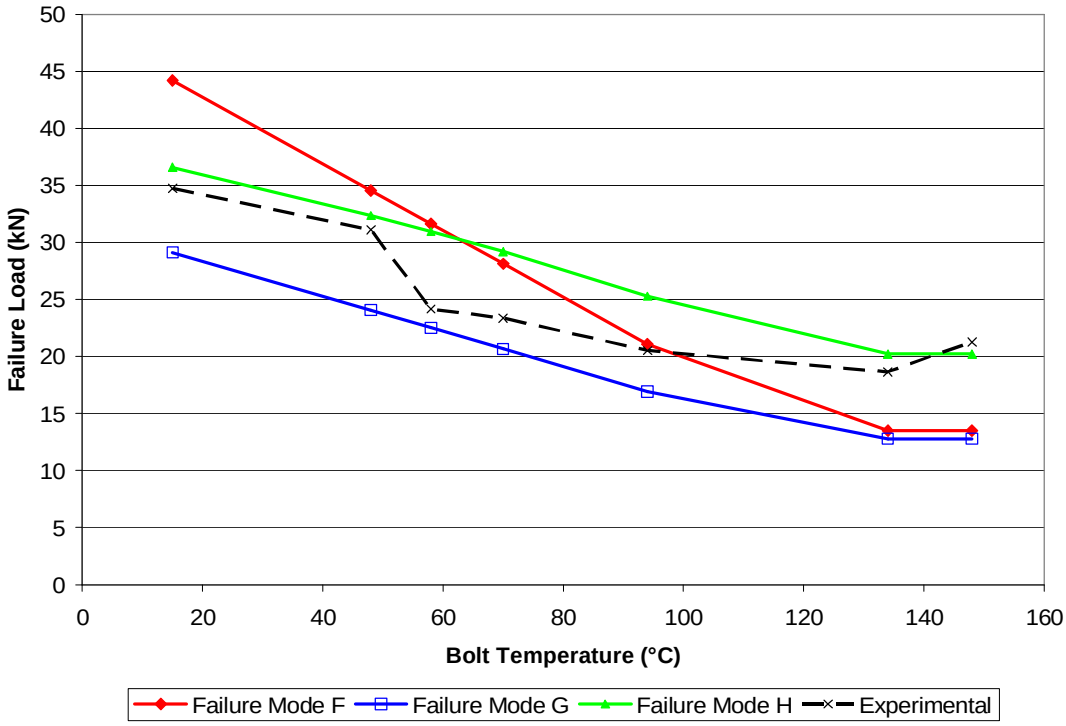

Figure 6-16: Predicted failure mode and experimental failure load for singly-bolted WSW connections tested at constant temperature.

6.7 Failure Prediction for fire tested connections

6.7.1 Overview

This section summarises the predictions of failure mode and failure load for connections tested under fire conditions. The prediction of fire tests were conducted using two methods, namely a Standard Model and a Modified Model. The standard method ignored the char rounding effect at the edges of the drilled holes which allow the bolts to pass through. Therefore, the width of the member in contact with the fastener is the residue thickness, $t_{contact}$, of timber member, i.e.:

$$t_{contact} = t - (n \times D \times q) \qquad \text{Equation 6-1}$$

where
- t = timber thickness (mm)
- n = Number of charring surfaces (-)
  (for SWS, n = 2, otherwise n = 1)
- D = Experimental charring Rate (mm/min)
- Θ = Charring duration (min)

However, the Modified Model recognized the char rounding effect at the edges of the holes and assumed the rounding had a radius equal to the char depth. Therefore, the cross section width of timber in contact with the fastener is:

$$t_{contact} = t - (2n \times D \times q) \qquad \text{Equation 6-2}$$

where
- t = Timber thickness (mm)
- n = Number of charring surfaces (-)
  (for SWS, n = 2, otherwise n = 1)
- D = Experimental charring Rate (mm/min)
- Θ = Charring duration (min)

Prediction for the SWS connection uses n = 2 as two surfaces of the timber members were burning. One the other hand, only one side of the side member was burning for the WWW and WSW connections, therefore n = 1 for the WWW and the WSW connections.

Figure 6-17 shows the difference between the Standard Model and the Modified Model.

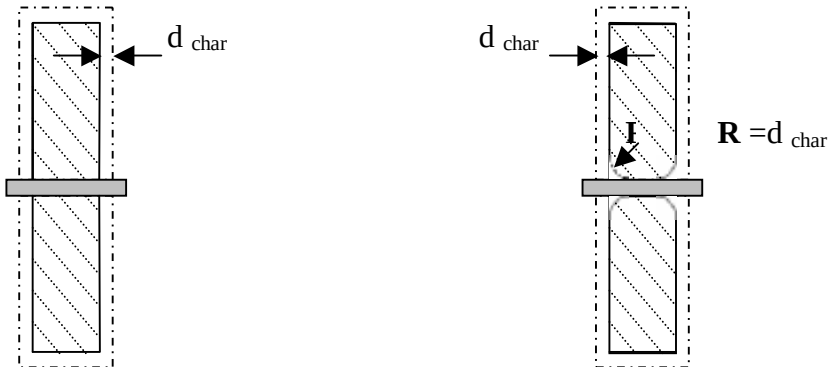

(a) Standard Model **(b) Modified Model**

Figure 6-17: Schematic drawings of Standard Model and Modified Model.

The embedment strength of LVL used in Johansen's Equation to predict the failure was taken from Figure 6-14. The experimental failure loads for multi-bolted connections were factorised to give a load per bolt since Johansen's Equations only gives prediction to failure load in units of per bolt.

6.7.2 Standard Model

This section summarised the prediction results for all fire tested connections using the standard model.

6.7.2.1 WWW Connections

From Figure 6-18 and Figure 6-19, the most probable final failure mode is Failure mode K. The tests showed that the final failure mode for the singly bolted WWW connections as well as the multiple bolted WWW connections were Mode G. The difference between the experimental applied load and the lowest predicted load is summarised in Table 6-8. For both singly and multi bolted connections, Johansen's Equations did not give a conservative prediction. It over predicted the connection failure load.

Table 6-8: Results summary for the WWW connection calculated using the standard model.

	Predicted Failure Load	Experimental Failure Load	Difference
	kN	**kN**	**kN (%)**
Singly-bolted WWW	8.9	4.6	-4.3 (-94%)
Multi-bolted WWW	8.5	*3.8	-4.8 (-126%)
*** Based on load per bolt.**			

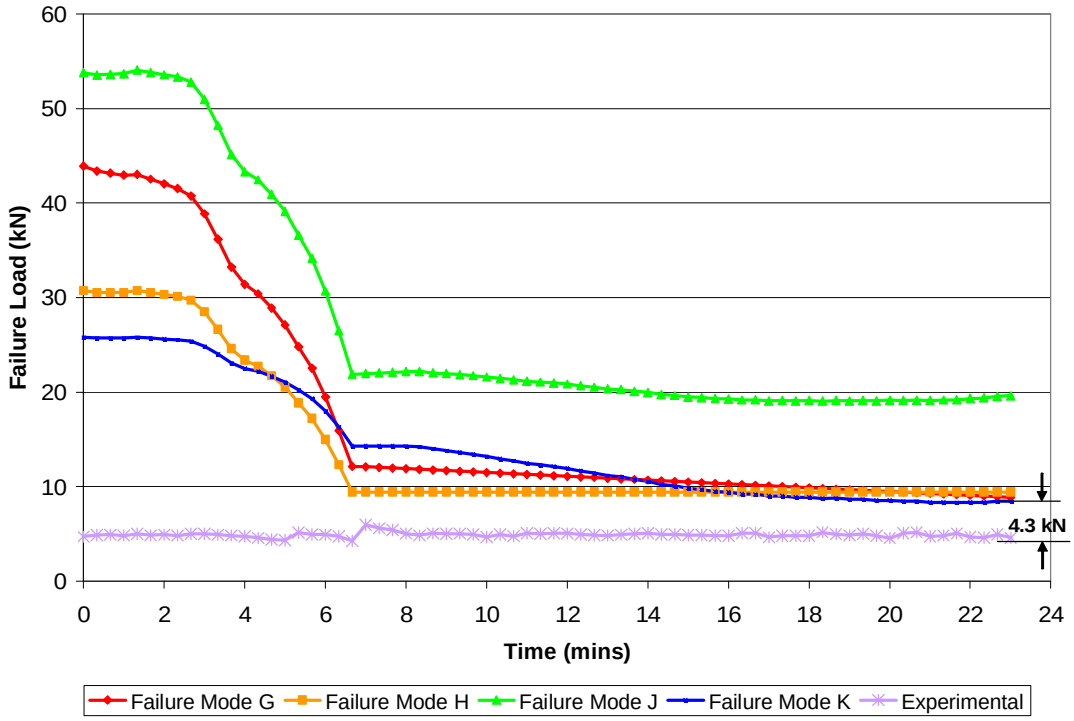

Figure 6-18: Predicted load and failure mode for a fire exposed WWW singly – bolted connection using the standard model.

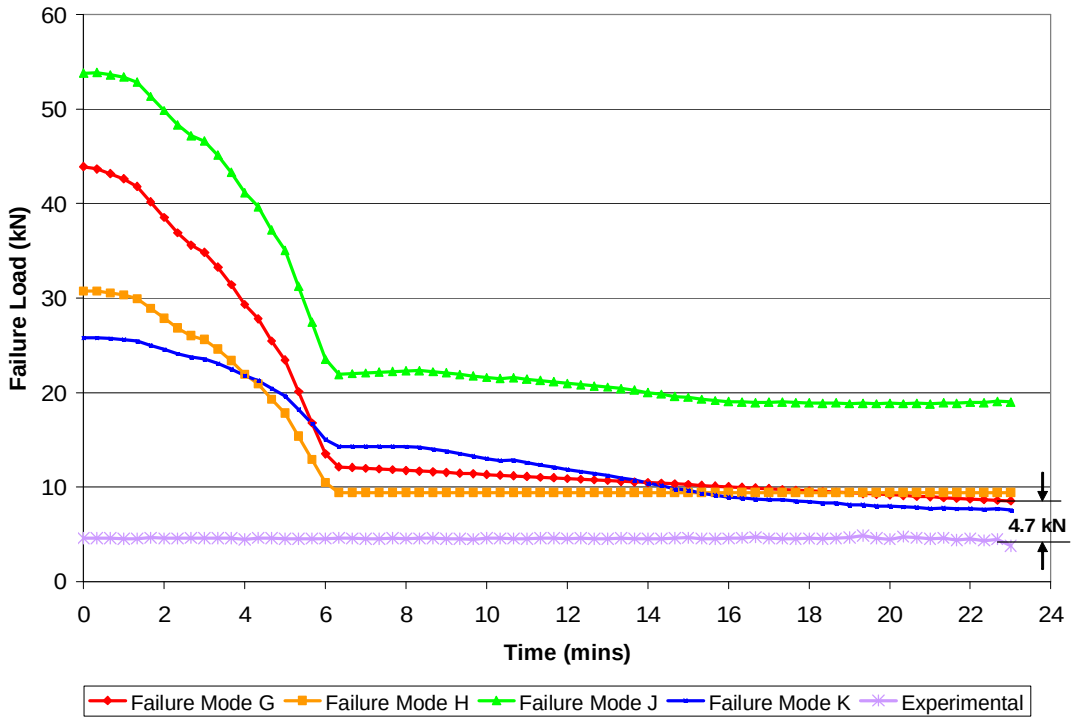

Figure 6-19: Predicted load and failure mode for a fire exposed WWW multi – bolted connection using the standard model.

6.7.2.2 WSW Connections

Based on Johansen's Equations, Failure Mode G was predicted to be the most probable failure mode (see

Figure 6-20 and Figure 6-21). However, the tests showed that Failure Mode F occurred instead of Mode G. The difference between the predicted load for Failure Mode F and Failure Mode G is minor.

The difference between the experimental applied load and the lowest predicted load for singly-bolted and multi-bolted WSW connections are summarised in Table 6-9. The Johansen's Equations did not give a conservative prediction, i.e. it over predicts the strength of the connections.

Table 6-9: Results summary for the WSW connection calculated using the standard model.

	Predicted Failure Load	Experimental Failure Load	Difference
	kN	kN	kN (%)
Singly-bolted WSW	8.76	5.33	-3.4 (-64%)
Multi-bolted WSW	9.08	*5.43	-3.7 (-67%)
*** Based on load per bolt.**			

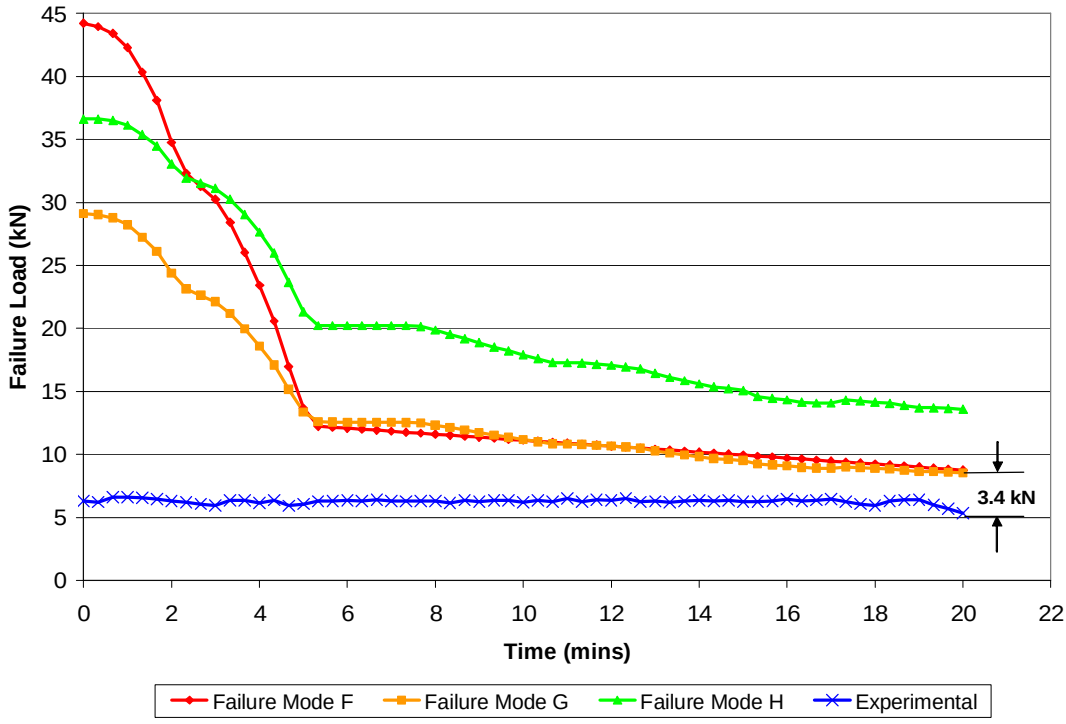

Figure 6-20: Predicted load and failure mode for a fire exposed WSW singly – bolted connection using the standard model.

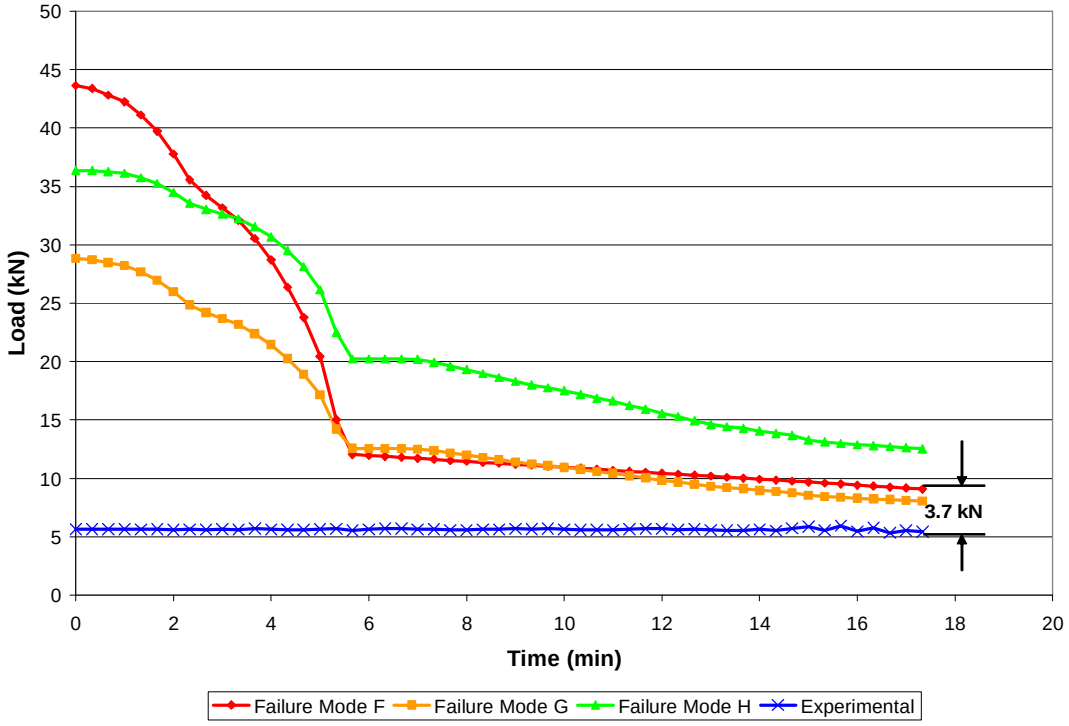

Figure 6-21: Predicted load and failure mode for a fire exposed WSW multi – bolted connection using the standard model.

6.7.2.3 SWS Connections

The calculated most probable failure mode for the SWS connection was Mode J or Mode L, depending on the thickness of the steel member (see Figure 6-22 and Figure 6-23). The predicted failure mode agreed with the experimental failure mode. However, the predicted load was slightly higher than the experimental failure mode. These predictions were not conservative.

The difference between the experimental applied load and the lowest predicted load for singly-bolted and multi-bolted SWS connections are summarised in Table 6-10.

Table 6-10: Results summary for the SWS connection calculated using the standard model.

	Predicted Failure Load	Experimental Failure Load	Difference
	kN	kN	kN (%)
Singly-bolted SWS	8.6	6.8	-1.7 (-25%)
Multi-bolted SWS	8.5	*5.1	-3.3 (-65%)
*** Based on load per bolt.**			

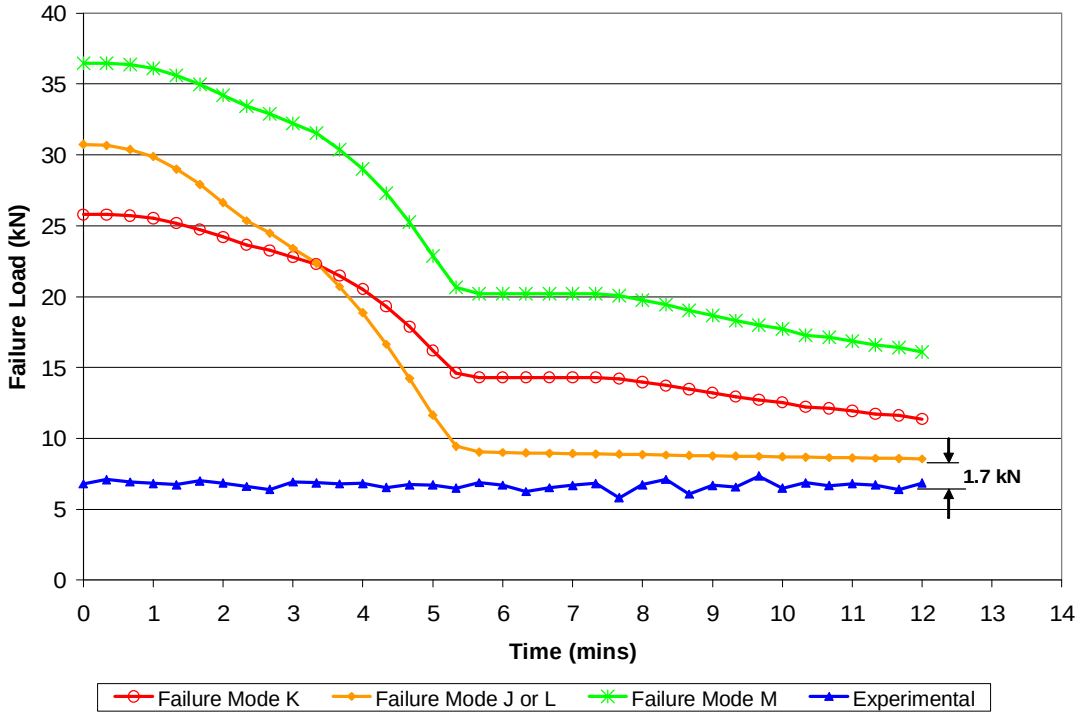

Figure 6-22: Predicted load and failure mode for a fire exposed SWS singly – bolted connection using the standard model.

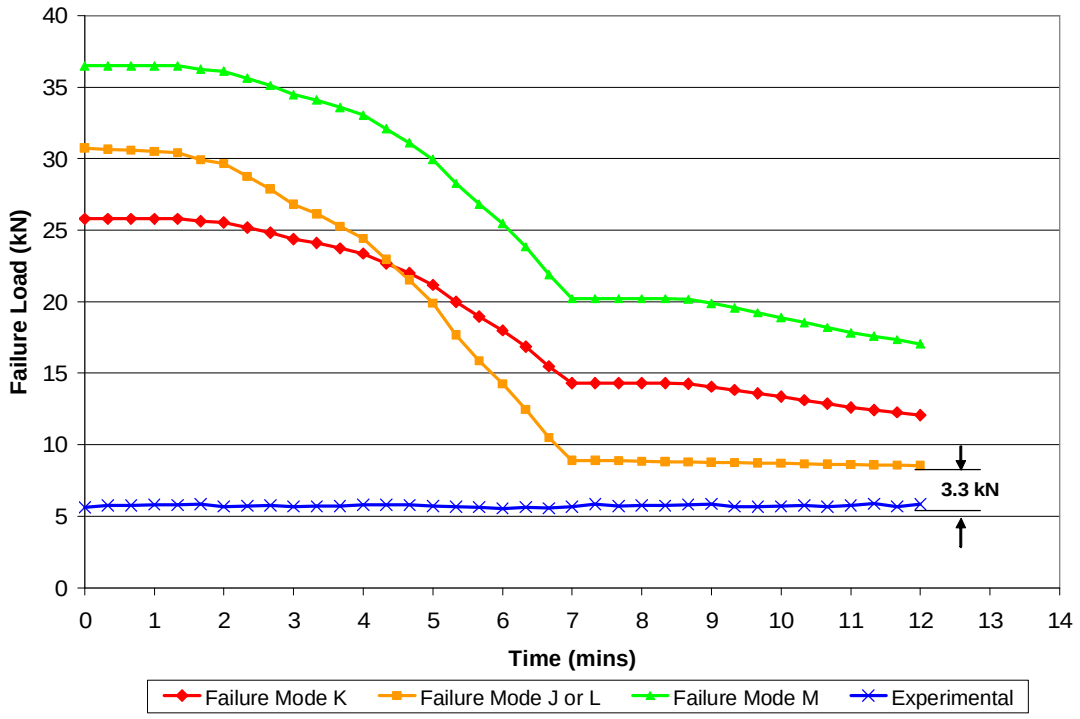

Figure 6-23: Predicted load and failure mode for a fire exposed SWS multi – bolted connection using the standard model.

6.7.3 Modified Model

The predictions of failure for the WWW, WSW and SWS connection after introducing the char rounding effect around the edge of timber adjacent to the bolt are discussed in the following sections.

6.7.3.1 WWW Connections

Using the char rounding model, Figure 6-24 and Figure 6-25 show that the Johansen's Equation predicted failure mode agreed well with the experimental failure mode for a fire exposed WWW connection, i.e. Failure Mode G.

The difference between the predicted failure load and the experimental applied load for a fire exposed singly bolted WWW connection is only 0.3kN. The prediction for WWW multi bolted connection only has a difference of 0.2kN between predicted failure load and experimental failure load. In both cases, the predicted time to failure is approximately 2 minutes earlier than the actual failure time. These predictions are conservative. The summary for fire test WWW connections prediction is summarised as Table 6-11.

Table 6-11: Results summary for the WWW connection calculated using the modified model.

	Predicted Failure Load	**Experimental Failure Load**	**Difference**
	kN	**kN**	**kN (%)**
Singly-bolted WWW	4.3	4.57	0.3 (7%)
Multi-bolted WWW	3.6	*3.78	0.2 (6%)
*** Based on load per bolt.**			

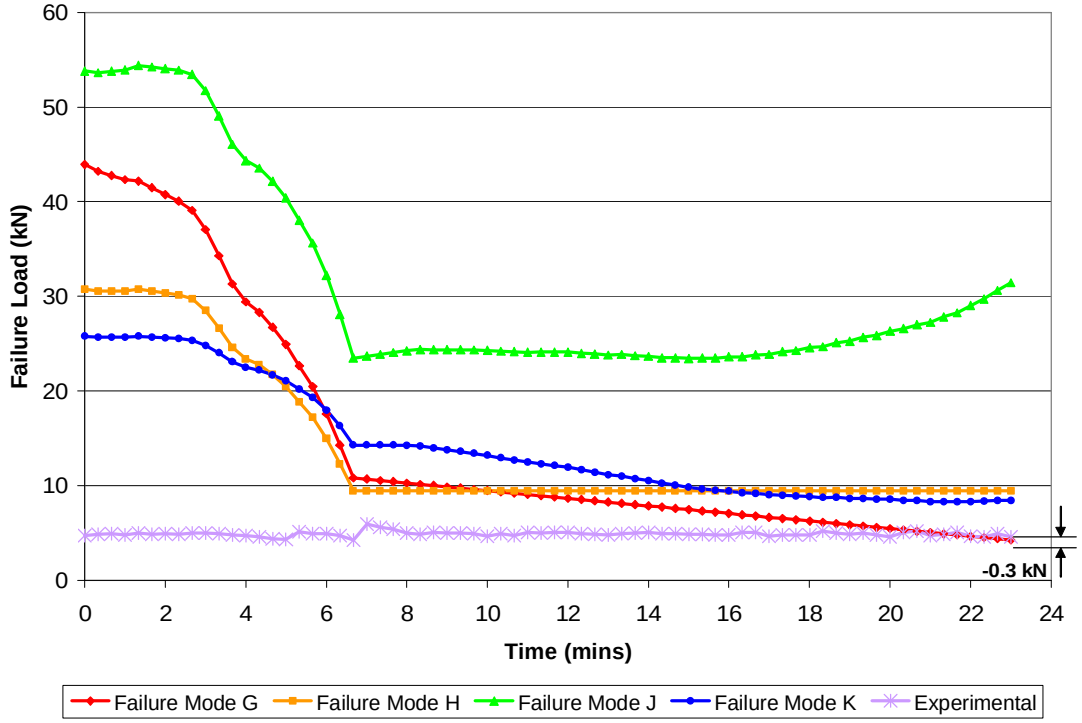

Figure 6-24: Predicted load and failure mode for a fire exposed WWW singly – bolted connection using the modified model.

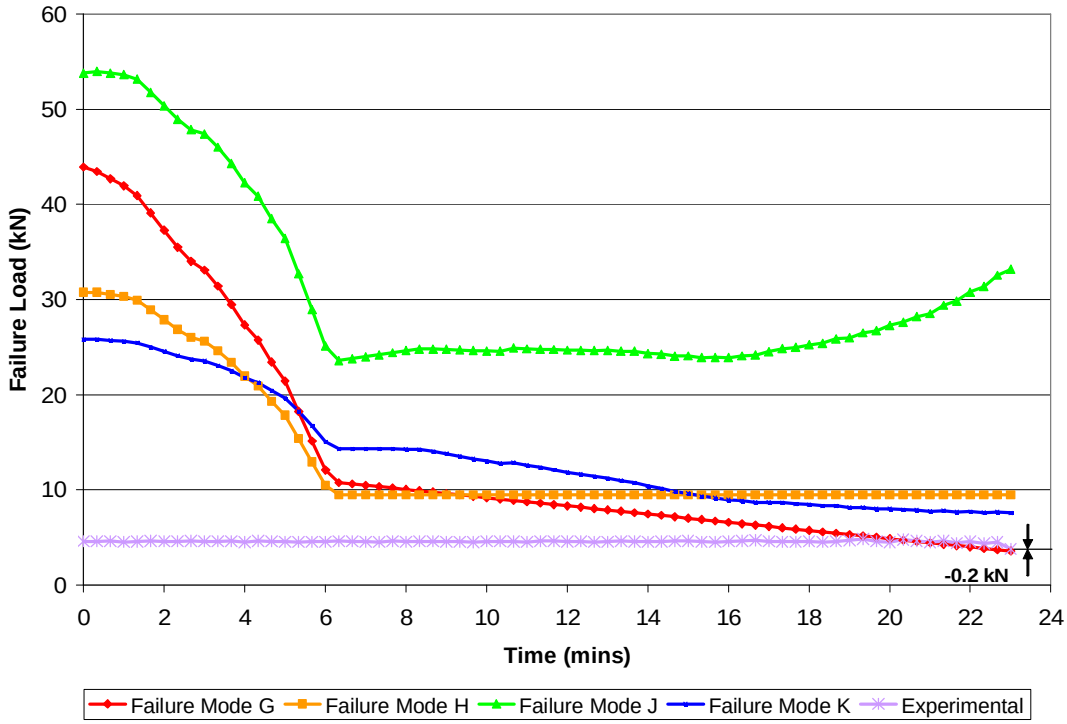

Figure 6-25: Predicted load and failure mode for a fire exposed WWW multi – bolted connection using the modified model.

6.7.3.2 WSW Connections

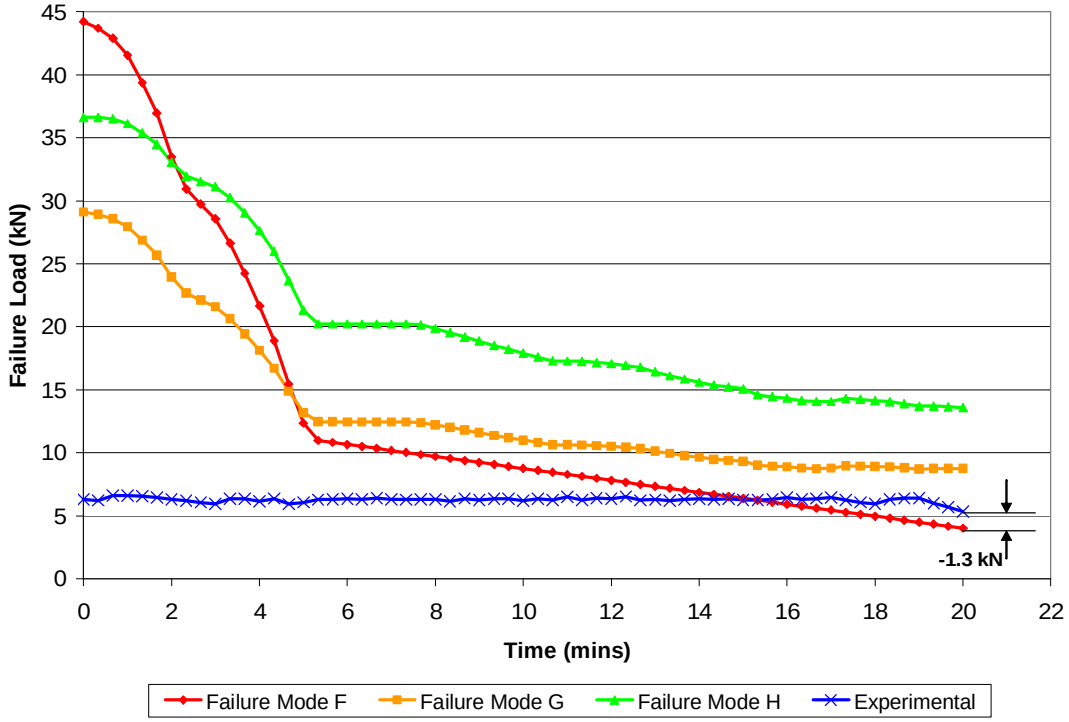

Figure 6-26: Predicted load and failure mode for a fire exposed WSW singly – bolted connection using the modified model.

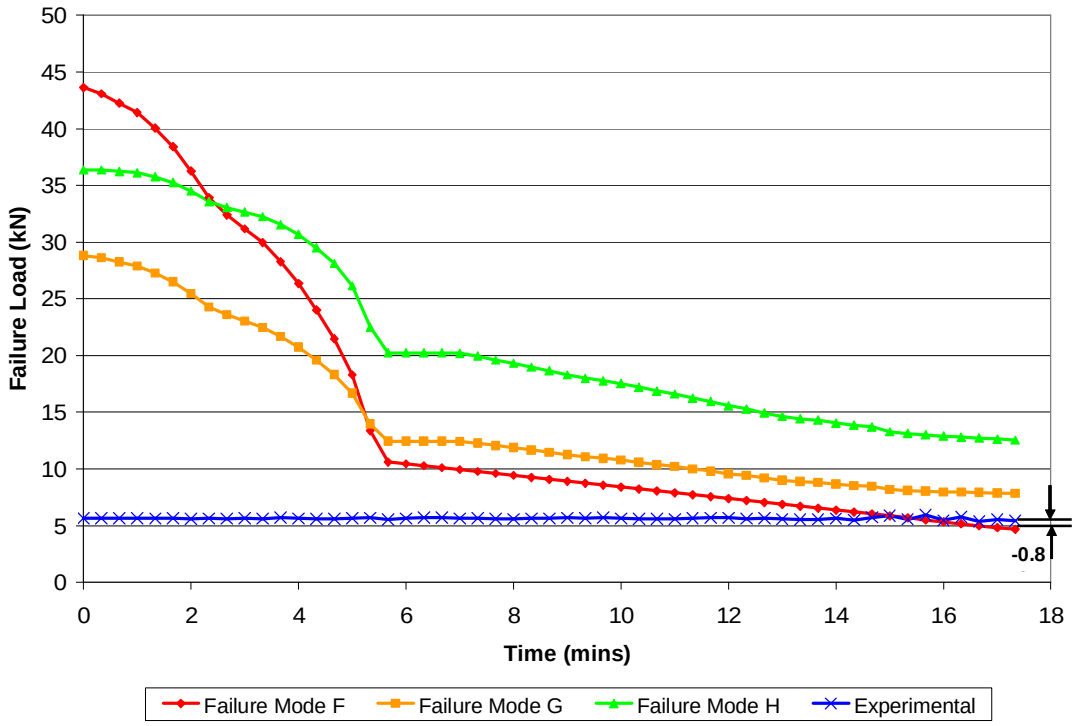

Figure 6-27: Predicted load and failure mode for a fire exposed WSW multi – bolted connection using the modified model.

Figure 6-26 and Figure 6-27 show that the Johansen's Equations under-predicted the WSW connection exposed to fire conditions. The predicted failure time for the singly bolted and multi bolted WSW connections are 15 minutes and 16 minutes respectively after exposure to fire, however the actual failure time is 20 minutes and 17 minutes respectively after exposure to fire.

The predicted failure mode for WSW connections exposed under fire conditions agreed with the experimental failure mode, i.e. Failure Mode F. Table 6-12 below summarises the predicted results for WSW connections exposed to fire conditions.

Table 6-12: Results summary for the WSW connection calculated using the modified model.

	Predicted Failure Load	**Experimental Failure Load**	**Difference**
	kN	**kN**	**kN (%)**
Singly-bolted WSW	4.0	5.33	1.3 (25%)
Multi-bolted WSW	4.7	*5.43	0.8 (14%)
*** Based on load per bolt.**			

6.7.3.3 SWS Connections

The Johansen's Equations again under-predicted the failure load of SWS connection when exposed to fire conditions Figure 6-28 and Figure 6-29. The predicted failure mode was Failure Mode J or L, depending in the thickness of the side member steel plates. This prediction agreed with the experimental failure mode. Table 6-13 summarises the prediction results for SWS connection exposed to fire conditions.

Table 6-13: Results summary for the SWS connection calculated using the modified model.

	Predicted Failure Load	Experimental Failure Load	Difference
	kN	kN	kN (%)
Singly-bolted WSW	7.65	6.84	-0.8 (-12%)
Multi-bolted WSW	7.45	*5.13	-2.3 (-45%)
*** Based on load per bolt.**			

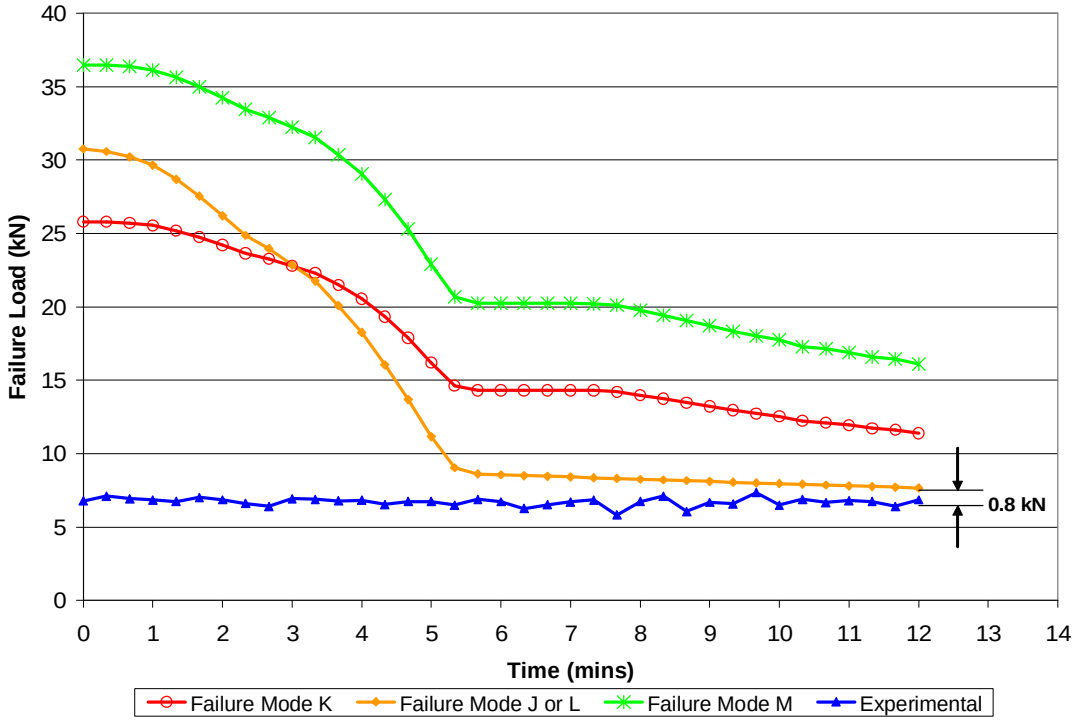

Figure 6-28: Predicted load and failure mode for a fire exposed SWS singly – bolted connection using the modified model.

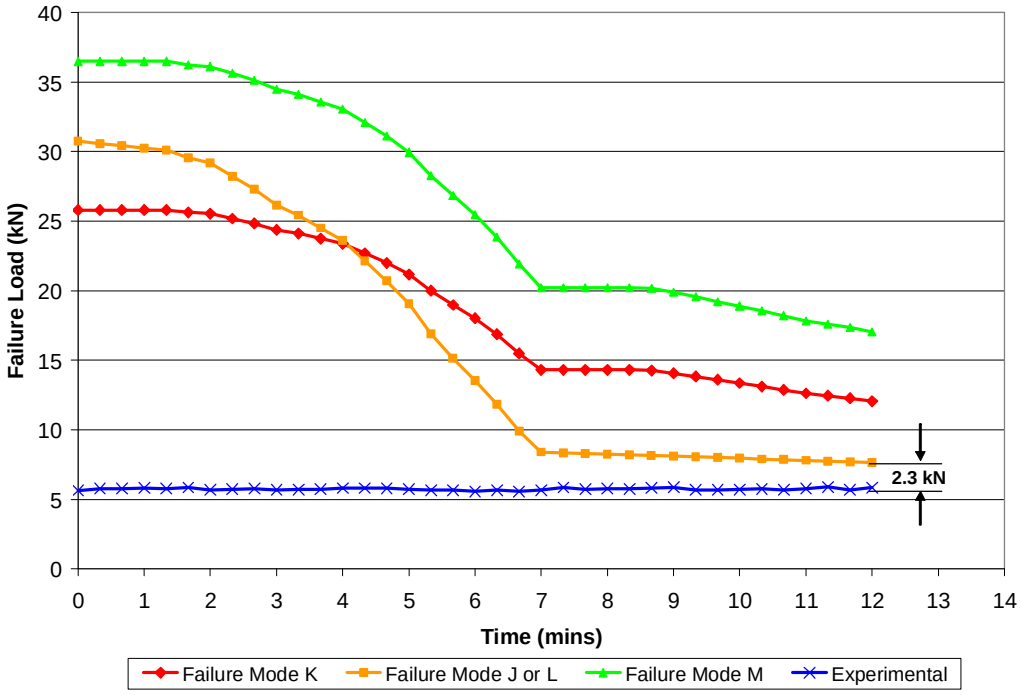

Figure 6-29: Predicted load and failure mode for a fire exposed SWS multi – bolted connection using the modified model.

6.7.4 Summary for Fire Tests

Summarised in Table 6-14 is the percentage difference between the predicted failure load and experimental failure load at the experimental failure time. This shows that the modified model predicts the failure load, hence, the failure time better, compared to the standard model. The modified model also predicts the failure load of multiple fasteners connections better than those with only one bolt.

Table 6-14: Percentage difference between predicted failure load and experimental failure mode using the standard and the modified model.

		Standard Model	Modified Model
		Difference	Difference
One-bolted Connection	WWW	-94%	7%
	WSW	-64%	25%
	SWS	-25%	-12%
Multi-bolted Connection	WWW	-126%	6%
	WSW	-67%	14%
	SWS	-65%	-45%

7 Discussion

7.1 General

Unfortunately due to the limitation of time and material resources, only one specimen was conducted for each of the testing conditions. Therefore the results presented in this research may not necessary be the most representative results. Provided more time and material resources are available, the test conditions should be repeated with multiple tests.

7.2 Repeatability of Tests

In this research, the only repeated test was the 200°C Heated Test for the SWS connection. The modified Load-Displacement curves for these two tests were shown in Figure 7-1. The initial slip when the load was first applied has been ignored.

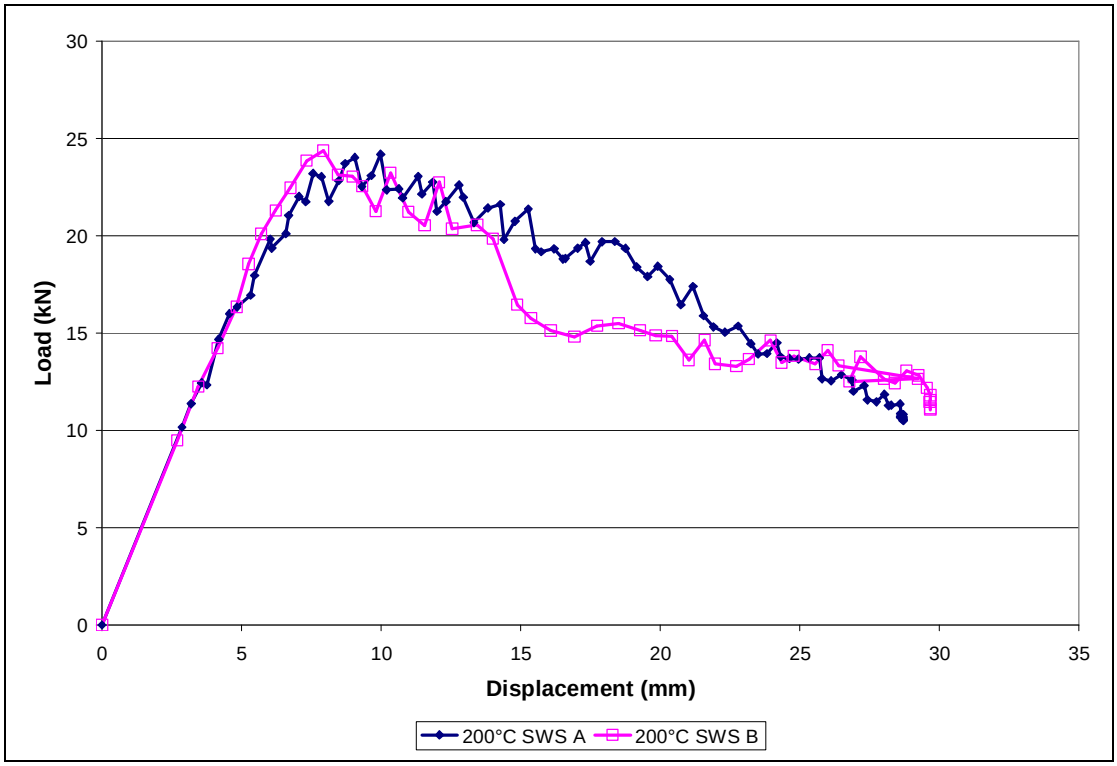

Figure 7-1: Load-Displacement curves for SWS connection tested at 200°C furnace temperature.

The results showed that the tests were highly repeatable. The stiffness of the connection and the maximum load that a SWS connection exposed to 200°C could

resist matched perfectly. Both the curves also showed a similar decaying pattern. Therefore it is reasonable to assume that all the tests could be repeatable.

7.3 Ambient Tests

The WSW connection allows for a larger displacement compared to the WWW and SWS connections. This is because the thin main steel plate member is stiffer than those connections that have timber as the centre member. Besides, the thin member allows the bolt to bend more severely without damaging the member along its cross section.

7.4 Heated Tests

Three types of connection tested under constant temperature showed the expected trend of decreasing load carrying capacity as the exposed temperature becomes higher. This is because as the timber heated up, it lost its load bearing capability, i.e. reducing embedment strength.

Among all the constant temperature tests, neither when the bolts nor the timber members reached 80°C (i.e. the glass transition temperature of lignin as suggested by Chapuis et al (2005)) do the results shows a distinctive drop in load carrying capacity. In this research, the WSW and the SWS connections tend to lose significant load capacity when the average timber member reached approximately 60°C (corresponding to an average bolt temperature of 56°C). For the WWW connection, the load carrying capacity only fell when the average timber member temperature reached approximately 110°C (corresponding to average bolt temperature of 80°C).

Therefore more experiments are required to investigate the timber member and the bolt temperature which caused the connection to lose significant bearing strength.

7.5 Fire Resistance of Connections

The research showed that the WWW connection has the best fire resistance, carrying load for 23 minutes. The SWS connection appeared to have the worst fire resistance, carrying load for only 12 minutes. The WWW and the WSW connections are better for the reason that the timber side members insulate the main members. This is evidenced by the uncharred WWW connection centre timber members.

Table 7-1 below summarises the average experimental fire resistance of WWW, WSW and SWS bolted connections. Included in the table is the average experimental fire resistance for WWW, WSW and SWS bolted connections. The fire resistance conducted for this research was slightly better than that determined by Lau (2006).

Table 7-1: Comparison of fire resistance with Lau's results (2006).

	Experimental Fire Resistance	Lau's Experimental Fire Resistance	Difference
	min	**min**	**min**
WWW	22.9	21.2	1.7 (7.4%)
WSW	18.7	16.3	2.4 (12.8%)
SWS	12.4	9.2	3.2 (25.8%)

7.6 Charring Rate

The average charring rate calculated based on the duration to failure of connection was similar to the other reported charring rates for LVL. However, depending on the type of connection, the charring rate differs slightly. Despite the steel plate side members which accelerate the heat transfer into the timber members, the steel plates limit the amount of ignition of the 63mm timber to flame. Hence, the SWS connection has the lowest charring rate.

The WSW connection has the highest charring rate because the centre steel plate member accelerates the heat transfer into the 45mm side timber members, hence it assists the pyrolysis and flaming process. While the WWW connection side members burned severely during the testing, the char formed insulated the centre members.

Unlike the WSW connections which had a steel plate centre member which has high heat transfer properties, the timber centre members insulate the whole WWW connection.

7.7 Embedment Strength and Fire Tests Prediction

The embedment strength of LVL calculated using the experimental results can be used confidently to predict the failure load of timber connections, even for the fire tested connections. By substituting the bi-linear curves as shown in Figure 6-14 into Johansen's Equations, the predicted failure load was within the range of the experimental failure load.

Even though the failure load prediction using the bi-linear experimental embedment strength is reasonable, more research is required for calculating the embedment strength with bolt temperatures within the range of 120°C to 200°C. The limited available data showed that the embedment strength increased in embedment strength. This may due to the loss of moisture which increases the strength of timber. Therefore, in order to give a conservative prediction, the embedment strength of LVL was assumed to have constant value of 0.025 kN/mm² beyond a bolt temperature of 120°C. König (2005) suggested that for timber in tension, the strength of timber reduced to 40% of initial strength in a linear fashion when the timber reached temperature of 100°C. The timber then continues to reduce its strength to 0% of initial strength when the timber temperature reaches 300°C.

The prediction of the failure mode and the failure load using the bi-linear embedment strength curve together with the experimental charring rate and steel strength reduction factor was excellent. However, the estimation of the failure time was too early compared to the experimental failure time. This is because after the LVL had reached its constant embedment strength, the load carrying capacity of the connection reduces at a minor rate. Therefore, the predicted failure time is very sensitive to the predicted load. More research concentrating at fire condition tests are required to give a reliable result.

7.8 Bending Tests

The direct yield load based on the load-slip curve of a M12 bolt tested under ambient conditions gives a value of 6.6 kN. This corresponds to a yield moment of 165 kNmm. Besides determining the yield moment at ambient temperature, the yield moment of bolt was also determined at elevated temperatures. The load-displacement characteristics for a M12 bolt up to temperature of 200°C are identical (see Appendix C).

The similar bending characteristics of bolts at temperatures less than 200°C can be explained by the yield strength of steel. Yield strength at elevated temperatures is not well defined as stated in Structural Design for Fire Safety (Buchanan, Figure 8.27 and Figure 8.28, 2001). Even different national codes have slightly different recommendations for yield strength of steel at elevated temperatures. The New Zealand steel standard (NZS 3404) suggests steel starts to lose its strength when the temperature reaches 215°C. However, Eurocode 3 suggests the strength starts to reduce at a temperature of 400°C. In the research, the NZS 3404 value was adopted to calculate the strength reduction of bolt at elevated temperatures.

7.9 Comparison between different fastener end distance

For the WSW connection testing carried out by Lau (2006), the distance between the fastener and the end of timber member is 50mm. According to NZS 3603, the minimum end distance must at least be 8d where d is the diameter of bolt for connection in tension action, i.e. 96mm when using Ø12 bolts.

Therefore two WSW connections, one of 50mm end distance and the other with 100mm were tested to compare the load-displacement as well as the failure mode characteristics. The Load-Displacement curves for the tests are shown in Figure 7-2 below.

The loading characteristic did not show any difference between the two connections. However, the failure mode for the connection with 100mm end distance was only

crushing, whereas the failure mode was crushing with shear plug failure for the connection of 50mm end distance.

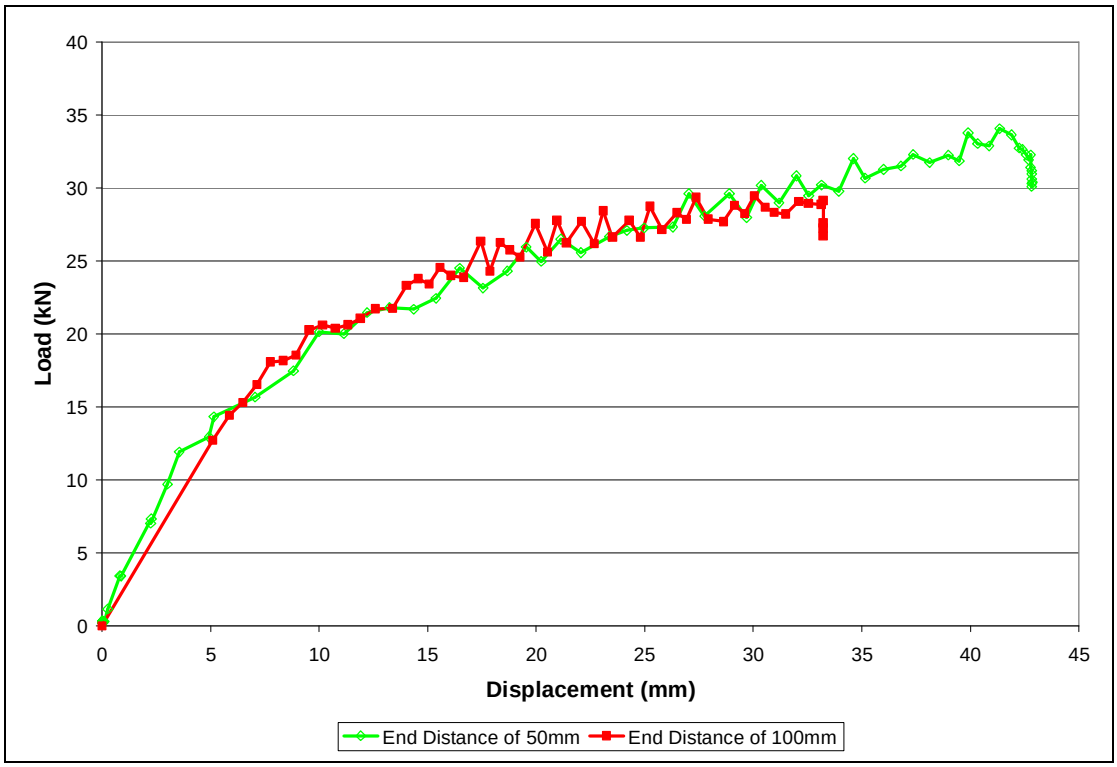

Figure 7-2: Load-slip curves for WSW connection with different timber end distance.

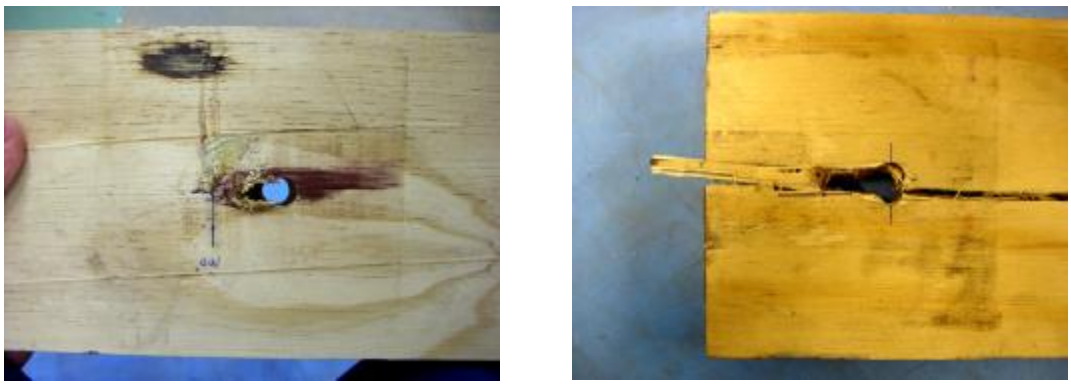

(a) 100mm End Distance **(b) 50mm End Distance**

Figure 7-3: Different failure modes for WSW connections with different end distances.

7.10 Inappropriate Sample Preparation Method

At the start of the research, a 2mm hole was drilled to a certain depth along the shank of bolt to accommodate the thermocouple wire. Thermocouple beads were to be inserted into the holes to measure the bolt temperature. The advantage of drilled holes was to fix the thermocouple beads at the required position.

However, the drilling reduced the strength of the bolt significantly. When the bolt was loaded, it started to yield at this weakest point along the shank of bolt, instead of at the centre of the three-member connection, i.e. the drilling area (see Figure 7-4(b)). As the load continued to be applied, the bolt broke at its weakest point (see Figure 7-4(a)).

This problem was overcome by drilling larger holes in the timber members. The larger holes allowed the thermocouple wires to be inserted to the desired position parallel to the bolt shank.

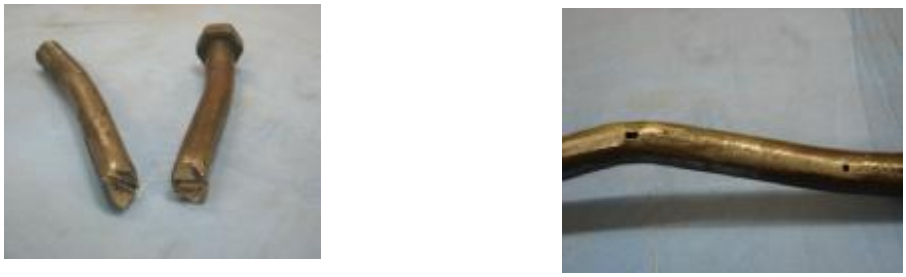

(a) Breakage of bolt **(b) Deformation of bolt**

Figure 7-4: Deformation along bolts caused by drilled holes.

Due to the fact that the furnace opening was too small to allow movement for the WWW connections, the bolts and the nuts were initially machined to a more practical thickness and length (see Figure 7-5). The problem that arose with machining the fasteners to this thickness and length is a reduction of thread to hold the nuts. For a bolted connection, when tensile stress was applied, it will bend the bolt along the shank. Thus, the washer counter-reacted to push the bolt back to its original position through the nut. Due to insufficient thread to hold the nut, the nut will be pushed off, which then loosens each member in the connection. This problem was overcome by widening the furnace opening.

(a) Bolt shortening **(b) Nut thinning**

Figure 7-5: Shortening of bolts and thinning of nuts.

8 Conclusions and Recommendations

8.1 Summary of research

Three different types of connections, a WWW connection, a WSW connection and a SWS connection were tested under various conditions. The timber members were made of either 45mm or 63mm LVL and the steel members were 6mm steel plates. In all the tested connections, M12 galvanised steel bolts were used. As described in the previous chapters, these connections were exposed to ambient, heated and fire conditions. All the tests were conducted in a custom built furnace system in which a tensile load of up to 30kN can be applied.

A side view schematic drawing of all these connections is shown below:

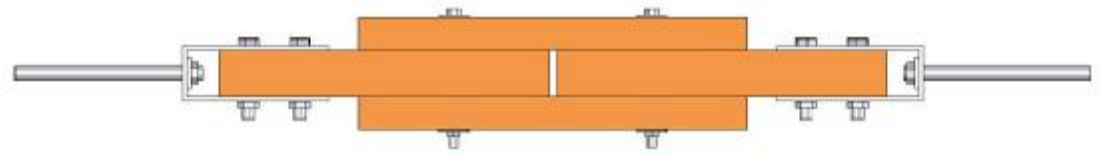

(a) WWW Connection

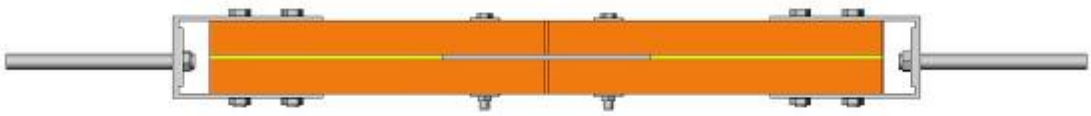

(b) WSW Connection

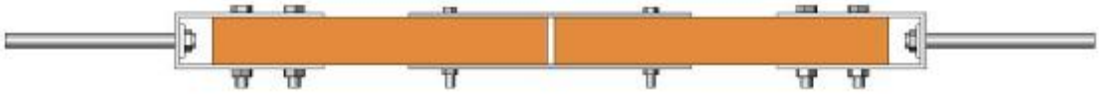

(c) SWS Connection

Figure 8-1: Schematic drawings of connections.

In all tests, the load applied to the connection, the temperature at various locations within the testing specimen and the displacement of the connections were recorded. With the recorded data for the SWS connection under ambient and heated conditions, the embedment strength of the connection at various bolt temperature was calculated using the relevant Johansen's Equations. The experimentally calculated embedment strength was then used to predict the failure load of the WWW and WSW connections in the ambient and heated tests. Finally, it is also used to estimate the failure load and

failure mode of all connections tested in fire conditions. The results from all the tests are summarised in the next section.

8.2 Conclusions

- For singly-bolted connections under ambient conditions, the WWW connection has the lowest ultimate connection strength, i.e. 35kN, among all types of connection. The WSW and SWS connections have a similar ultimate strength of 50kN.

- For singly-bolted connections under ambient conditions, the displacements before failure for the WWW and the SWS connections are similar, i.e. 25mm before splitting occurred. However, the WSW connection undergoes a larger magnitude of displacement.

- For all types of connection, as the heat exposure conditions became more severe, the ultimate strength of the connections dropped. The stiffness of the connection also reduced as the temperature rises. This was expected because the timber and steel strengths reduce as the temperature rises.

- The average experimental charring rate of LVL of 0.76 mm/min was higher than the rate of 0.67 mm/min published by Lau (2006) and 0.72 mm/min by Lane (2004). It is important to notice that different types of connection have different charring rates. The SWS connection had the lowest charring rate even though the side steel plates are encouraging heat into the connection core. This is because the steel plates stopped the pyrolysis gases from burning on the timber side surfaces. The WSW connection has the highest charring rate of 0.82mm/min because the internal steel member absorbs heat directly into the centre between the members being connected enabling the pyrolysis process to take place there as well as at the outside of the connection. The WWW connection has a charring rate of 0.70mm/min.

- The fire resistance of different connections have the following relation:

  SWS Connection < WSW Connection < WWW Connection

  The WWW connections had the longest fire resistance because the side timber members provided some insulation on to the main timber members. Also, the WWW connections had the largest cross-sectional area among the three types of connection. As mentioned already, the steel plate side members of the SWS connections assisted heat transfer into the timber members being joined, thus the SWS connections had the least fire resistance. The SWS connections had the smallest timber cross section among all connections and the double-side charring effect enhanced the reduction of the residual timber cross-section.

- The embedment strength of LVL can be described by a bi-linear relationship. At a bolt temperature of 20°C, the embedment strength of LVL was found to be 0.08 kN/mm². It drops at a constant rate as the bolt temperature increases until 120°C, with a magnitude of 0.025 kN/mm². However, as the bolt temperature continues to rise to 200°C, the experimental results showed the LVL embedment strength as increasing. Due to the limited results and in order to be conservative, the embedment strength of LVL was assumed to remain at magnitude of 0.025 kN/mm² beyond a bolt temperature of 120°C.

- This bi-linear embedment strength obtained experimentally was used to predict the strength of the WWW and WSW connections when exposed to ambient and elevated temperature conditions and the predicted strengths agreed reasonably well with the experimental values.

- Due to the excellent heat conduction properties of steel, there was very little difference in the temperature at various locations in the bolts when heated or exposed to fire conditions. The average timber member temperatures were generally lower than the bolt temperatures due to the poor heat conduction properties of wood, except for the SWS connections where the timber and bolt temperatures are comparable (Appendix D).

- By substituting the bi-linear embedment strength relation into Johansen's Equations to predict the failure mode and the failure load of connections, the results are similar to the experimental results, especially when the reduction of contact area between bolts and timber members were introduced due to the char rounding effect. Excluding the prediction for the SWS connections, all differences are between 1% and 30%. The use of the bi-linear embedment strength in Johansen's Equations gave better agreement with the experimental values in the case of multi-bolted connections and for the WWW connections. The least accuracy occurred in predicting the strength of SWS connections

- In fire conditions, the most significant failure mode for the different types of connection are summarised in Table 8-1.

Table 8-1: Summary of most probable and most significant failure mode for different type of connections.

Type of Connections	Most Probable Failure Mode	Description of Failure Mode
WWW Connection	Failure Mode G	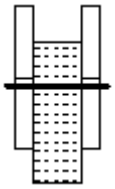
WSW Connection	Failure Mode F	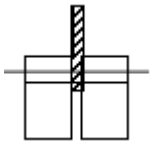
SWS Connection	Failure Mode J or L	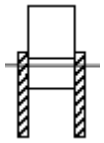

8.3 Recommendations for future research

- Each of the experiments should be repeated to increase the reliability of the results.

- Conduct more experiments at higher temperature exposure conditions. At this stage, the experimental results showed that the ultimate strength of connections increases slightly as the bolt temperature reached 120°C and beyond. However, the magnitude of strength increase, as well as the continuity of the ultimate strength curve with respect to bolt temperature, needs to be verified.

- Finite element analysis of the heat transfer to the core of the connections, either via bolts, steel plates or timber needs to be assessed. The moisture movement within each timber member when exposure to the elevated temperature should also be analysed either experimentally or numerically.

- The proposed embedment strength of LVL using bolted connections should be verified for nailed and screwed timber connections, for both ambient conditions and elevated temperatures.

- The moisture content across the timber member when exposed to fire conditions may vary significantly. Knowing that the embedment strength is influence by the moisture content of the timber member, the relationship between embedment strength and moisture content should also be studied.

- In this research, the embedment strength of timber is studied in respect of bolt temperature, assuming that the timber close to the bolt has identical temperature. It would be interesting to study the temperature difference between the bolt and timber adjacent to the bolt when exposed to fire conditions.

9 References

ASTM International, (2002), '*Annual Book of ASTM Standards*', West Conshohocken, USA.

Blass, H.J., Aune, P., Choo, B.S., Görlacher, R., Griffiths, D.R., Hilson, B.O., Racher, P., Steck, G. (1995), '*Timber Engineering STEP 1 – Basis of design, material properties, structural components and joints*', 1st Edition, Centrum Hout, The Netherlands

Buchanan, A.H. (2001), '*Structural Design for Fire Safety*', John Wiley & Sons Ltd, Chichester, England

Buchanan, A.H. (2002), '*Timber Design Guide*', 2nd Edition, New Zealand Timber Industry Federation Inc, Wellington, New Zealand

Babrauskas, V, (2003), '*Ignition Handbook – principles and applications to fire safety engineering, fire investigation, risk management and forensic science*', Fire Science Publishers.

Carter Holt Harvey Limited (2002), '*Hyspan Structural LVL – Span Tables for Residential Buildings*', 2nd Edition, Futurebuild, Carter Holt Harvey Limited.

Carter Holt Harvey Limited (2002), '*hyBEAM Engineered I-Joists – HJ Series Floors for Houses, Information for Design and Installation*', 2nd Edition, Futurebuild, Carter Holt Harvey Limited.

Carter Holt Harvey Limited (2004), '*hyCHORD – LVL Truss Chords '*, Futurebuild, Carter Holt Harvey Limited.

Carter Holt Harvey Limited (2003), '*hy90 Structural Beams – Hy90 Lintels for Residential Construction, Information for Design and Installation*', 1st Edition, Futurebuild, Carter Holt Harvey Limited.

Carter Holt Harvey Limited (2004), '*hyPLANK LVL Scafford Plan: hyPLANK – Guidelines for Inspection and Maintenance*', Futurebuild, Carter Holt Harvey Limited.

Carter Holt Harvey Limited (2002), '*truFORM LVL Formwork Beam – Shaping the Future of Formwork*', Futurebuild, Carter Holt Harvey Limited.

Carter Holt Harvey Limited (2002), '*LOSP Treated LVL*', Futurebuild, Carter Holt Harvey Limited.

Chapuis, S., Dias de Moraes, P., Rogaume, Y. and Torero, J. (In preparation), '*Evaluation of In-depth Temperature Distributions and Embedding Resistance of Timber in a Fire*'.

Canadian Wood Council (CWC)
http://www.cwc.ca/products/EWP/LVL/introduction.php

EC3 (2003), *Eurocode 3: Design of Steel Structures – Part 1-2: General Rules: Structural Fire Design*', European Committee for Standardization, Brussels, Belgium.

EC5 (2004), *Eurocode 5: Design of Timber Structures. EN 1995-1-1:2004: General – Common Rules and Rules for Buildings*', European Committee for Standardization, Brussels, Belgium.

EC5 (2004), *Eurocode 5: Design of Timber Structures. EN 1995-1-2:2004: General – Structural Fire Design*. European Committee for Standardization, Brussels, Belgium

Erchinger, C. and Frangi, A. (2005), '*Fire Behaviour of Multiple Shear Steel-to-Timber Connections with Dowels*', International Council for research and Innovation

in Building and Construction – Working Commission W18 – Timber Structure, Meeting Thirty-Eight, Karlsruhe, Germany

Frangi, A. and Fontana, M. (2003), '*Charring Rates and Temperature Profiles of Wood Sections*', Fire and Materials, Vol. 27, Page 91-102.

Harris, S. (2004), '*Fire Resistance of Epoxy-grouted Steel Rod Connections in Laminated Veneer Lumber (LVL)*', Master of Engineering (Fire) Thesis, University of Canterbury, New Zealand.

ISO, '*Glossary of Fire Terms and Definations'*, ISO/CD13943, International Standards Organization, Geneva 1996

ISO 834 (2000), '*Fire Resistance Testing*', International Standards Organization, Geneva.

ISO 10984-1 (1999), '*Timber structures — Dowel-type fasteners — Part 1: Determination of yield moment*', International Standards Organization, Geneva.

ISO 10984-2 (1999), '*Timber structures – Dowel-type fasteners – Part 2: Determination of embedding strength and foundation values*', International Standards Organization, Geneva.

König, J., (2005), '*Structural Fire Design of Timber Structures According to Eurocode 5 – design rules and their background*', Fire and Materials, Vol 29, Page 147 – 163, Wiley.

Kodur, V. & Harmathy, T., (2002), '*The SFPE Handbook of Fire Protection Engineering – Section 1, Chapter 10*', 3rd Edition, SFPE and NFPA.

Lane, W., Buchanan, A.H., and Moss, P.J. (2004),'*Fire Performance of Laminated Veneer Lumber (LVL)*', Proceedings of the 18th Australasian Conference on the Mechanics of Structures and Materials, Perth, Australia

Lane, W. (2004), '*Fire Performance of Laminated Veneer Lumber (LVL)*', Master of Engineering (Fire) Thesis, University of Canterbury, New Zealand

Lau, P.H. (2006), '*Fire Resistance of Connections in Laminated Veneer Lumber (LVL)*', Master of Engineering (Fire) Thesis, University of Canterbury, New Zealand

Muller, C. (2000) '*Holzleimbau – Laminated Timber Construction*', Birkhauser – Publishers for Architecture, Basel.

Nelson Pine Industrial Limited
http://www.nelsonpine.co.nz/LVLProd.htm

Nyman, J. (2001), '*Equivalent Fire Resistance Ratings of Construction Elements Exposed to Realistic Fires*', Master of Engineering (Fire) Thesis, University of Canterbury, New Zealand

New Zealand Forest Institute (NZFI), (2006), '*Facts and Figure 2005/2006*', New Zealand Forest Owners Association Inc, Wood Processor Association of NZ and Ministry of Agricultural and Forestry of New Zealand.

NZS 3603: 1994, '*Student Code of Practice for Timber Design'*, Standards New Zealand, Wellington

NZS 3404: Part 1:1997, '*Steel Structures Standard*', Standards New Zealand, Wellington

NZS 4357 (1995), '*Structural Laminated Veneer Lumber (LVL)*', Standards New Zealand, Wellington

NZS 4203:1992, '*Code of Practice for General Structural Design and Design Loadings for Buildings – Volume 1 Code of Practice,*' Standards New Zealand, Wellington.

Quenneville, J. and Mohammad, M., (2000), '*On the failure modes and strength of steel-wood-steel bolted timber connection*', Canadian Journal of Civil Engineering, Vol. 24, No. 4, ProQuest Science Journals.

Reszka, P. and Torero, J. L. (2006), '*In Depth Temperature Measurements of Timber in Fires*', 4th International Workshop << Structures in Fire>>, Aveiro, Portugal.

Scheibmair, D (2003), '*Self-drilling Pin Joints in Laminated Veneer Lumber'*, Master of Engineering Thesis, University of Auckland, New Zealand, July 2003

SNZ (1993), '*Code of Practice for Timber Design'*. NZS 3603: 1993. Standards New Zealand, Wellington, New Zealand

Thelandersson, S. and Hans, J. (2003), '*Timber Engineering*', Wiley, New York.

Walker, J. (1993), '*Primary Wood Processing- principles and practice*', Chapman & Hall, London & New York.

White, R. (2002), '*The SFPE Handbook of Fire Protection Engineering – Section 4, Chapter 11'*, 3rd Edition, SFPE and NFPA.

Appendix A – Original Load-Displacement curves for Heated Tests

Appendix A.1 – Overview

This appendix shows all the unmodified load-displacement curves obtained from the Heated Tests. The load-displacement plot for very low loads was very variable and unpredicted.

Appendix A.2 – SWS Connection Heated Tests

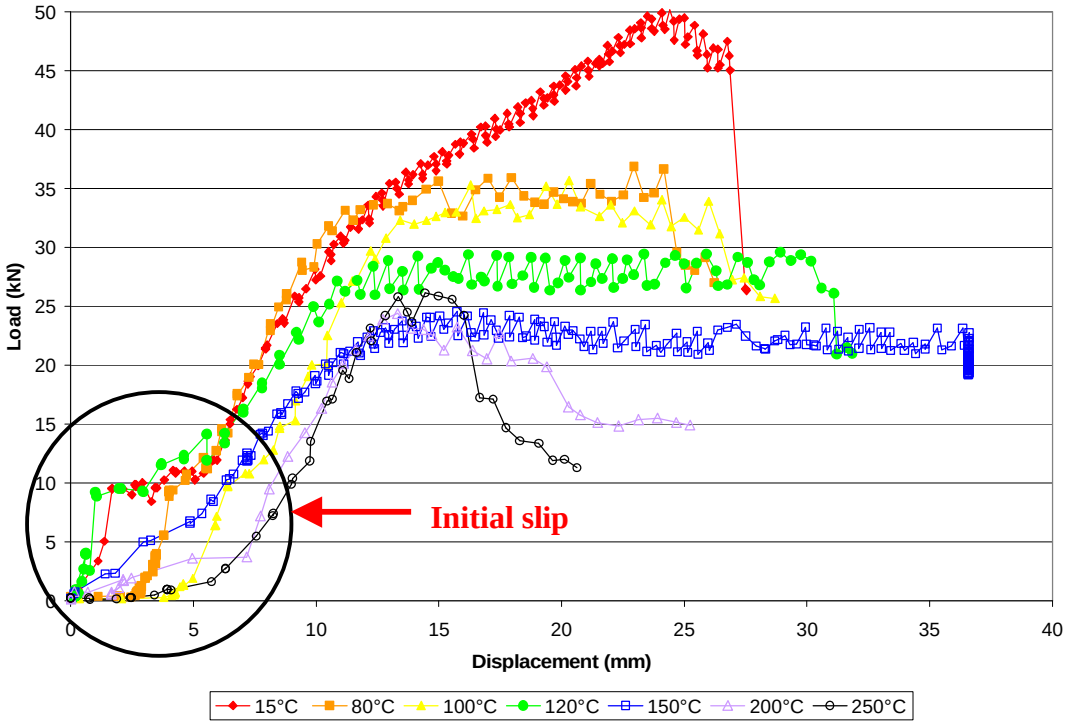

Figure A1: Original Load-Displacement curve for SWS connections Heated Test.

Appendix A.3 – WSW Connection Heated Tests

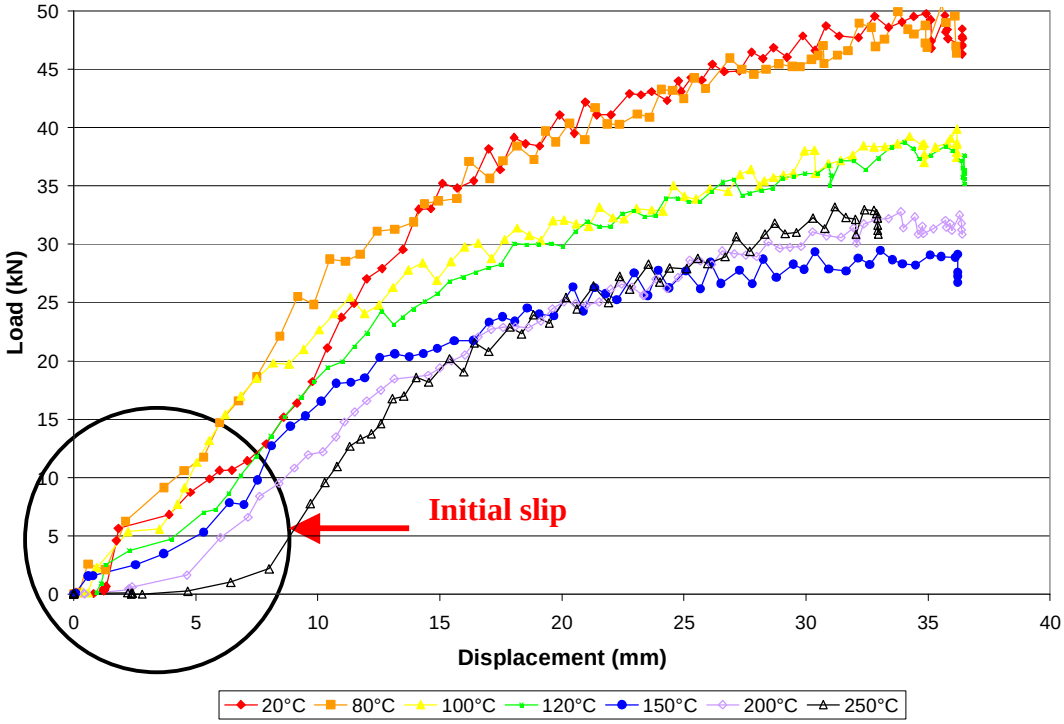

Figure A2: Original Load-Displacement curve for WSW connections Heated Test.

Appendix A.4 – WWW Connection Heated Tests

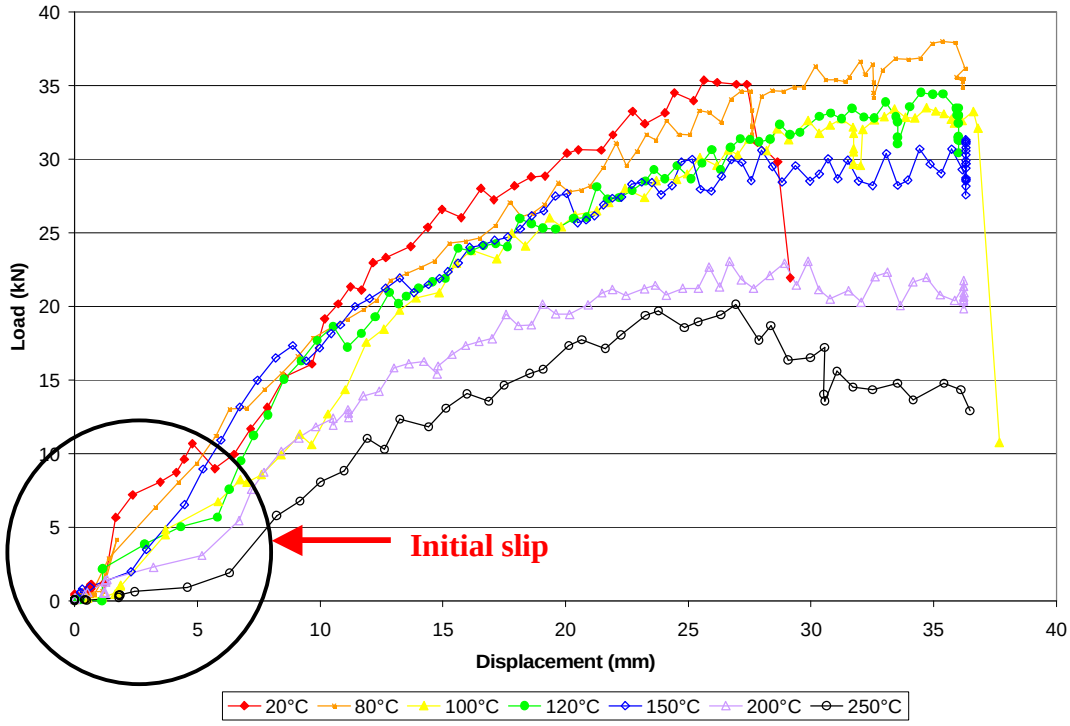

Figure A3: Original Load-Displacement curve for SWS connections Heated Test.

Appendix B – Charring Rate

Appendix B.1 – Overview

This appendix recorded the residual timber thickness after exposure to fire. The charring rate calculations were also included.

Appendix B.2 – SWS Connections

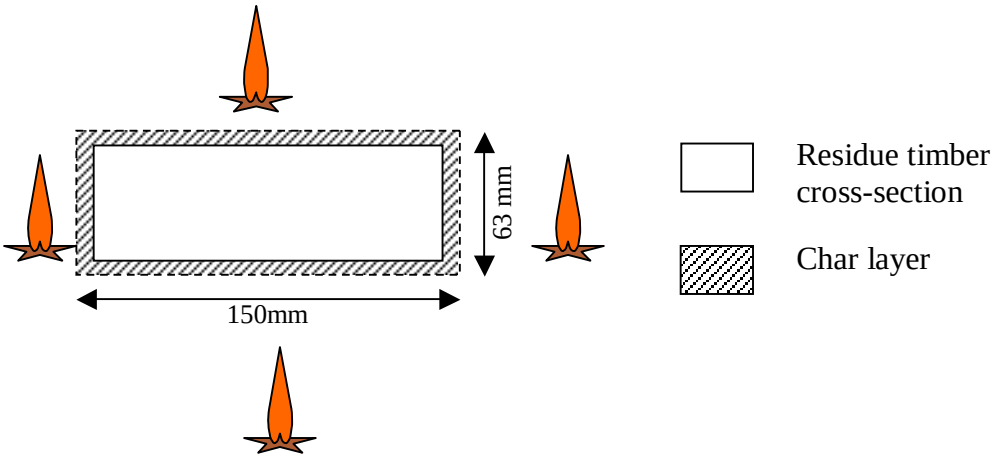

Figure B1: Schematic diagram showing location of fire exposure for SWS connections.

Table B1: Summary of charring rate calculation for SWS connections

No. of Bolts			**1**	**4**
Original Thickness		mm	**65.00**	**65.00**
Residual Thickness	**1**	mm	56.10	55.64
	2	mm	55.53	53.99
	3	mm	56.88	55.76
	4	mm	58.89	56.79
	5	mm	55.49	57.86
	6	mm	57.87	57.59
Average Residual Thickness		mm	**56.79**	**56.27**
Average Charring Thickness		mm	**8.21**	**8.73**
Time of Exposure		min	**12.1**	**12.6**
Number of Exposure Surface		[ ]	**2**	**2**
Charring Rate		mm/min	**0.34**	**0.35**
Average Charring Rate		mm/min	**0.35**	

Appendix B.3 – WSW Connections

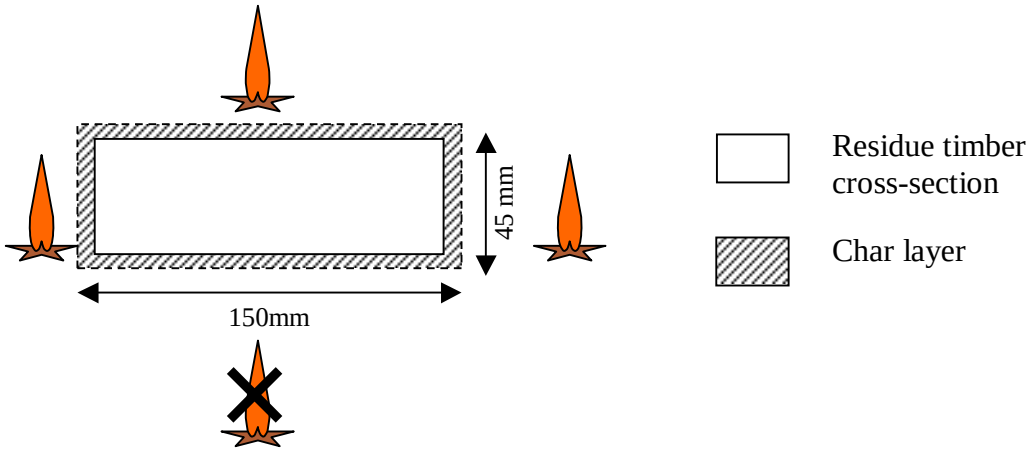

Figure B2: Schematic diagram showing location of fire exposure for WSW connections.

Table B2: Summary of charring rate calculation for WSW connections

No. of Bolts			**1**	**4**
Original Thickness		mm	**45.00**	**45.00**
Residual Thickness	**1**	mm	26.75	28.08
	2	mm	31.99	30.47
	3	mm	28.24	29.62
	4	mm	29.34	27.05
	5	mm	31.18	30.51
	6	mm	30.53	31.34
	7	mm	28.92	29.12
	8	mm	30.71	31.77
	9	mm	28.58	31.83
	10	mm	27.24	29.68
	11	mm	28.63	29.30
	12	mm	28.69	31.91
Average Residual Thickness		mm	**29.23**	**30.06**
Average Charring Thickness		mm	**15.77**	**14.94**
Time of Exposure		min	**19.9**	**17.5**
Charring Rate		mm/min	**0.79**	**0.85**
Average Charring Rate		mm/min	**0.82**	

Appendix B.4 – WWW Connections

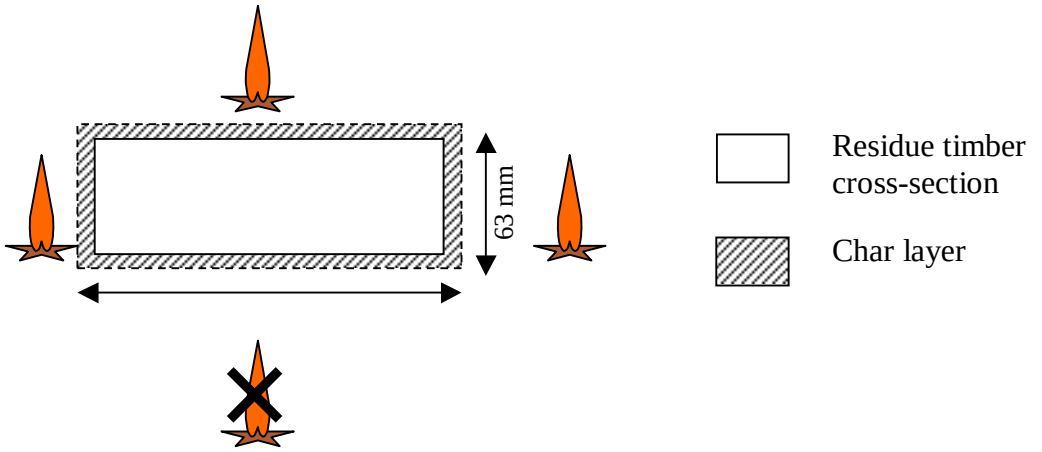

Figure B3: Schematic diagram showing location of fire exposure for WWW connections.

Table B3: Summary of charring rate calculation for WWW connections

No. of Bolts			**1**	**5**
Original Thickness		mm	**45.00**	**45.00**
Residual Thickness	**1**	mm	27.69	27.39
	2	mm	28.30	26.65
	3	mm	27.98	27.78
	4	mm	30.01	29.10
	5	mm	29.13	29.49
	6	mm	30.14	29.08
Average Residual Thickness		mm	**28.88**	**28.25**
Average Charring Thickness		mm	**16.12**	**16.75**
Time of Exposure		min	**22.9**	**23.9**
Charring Rate		mm/min	**0.70**	**0.70**
Average Charring Rate		mm/min	**0.70**	

Appendix B.5 – Summary of Charring rates

The summary of charring rate for each type of connection was summarised below:

Table B4: Summary of experimental calculated charring rate

Type of Connections	**Charring Rates (mm/min)**
SWS	0.35
WSW	0.82
WWW	0.70
Total Average Charring Rate	**0.74**

Appendix C – Bolt Yield Moment at Elevated Temperatures

Appendix C.1 – Overview

This appendix discussed the yield moment of bolt at elevated temperature. The load-displacement curves for the four different temperature tests conducted were included below. A table of bolt yield moment with respect to temperature calculated according to NZS 3404 was also included.

Appendix C.2 – Load-Displacement curves for elevated temperature M12 bolts.

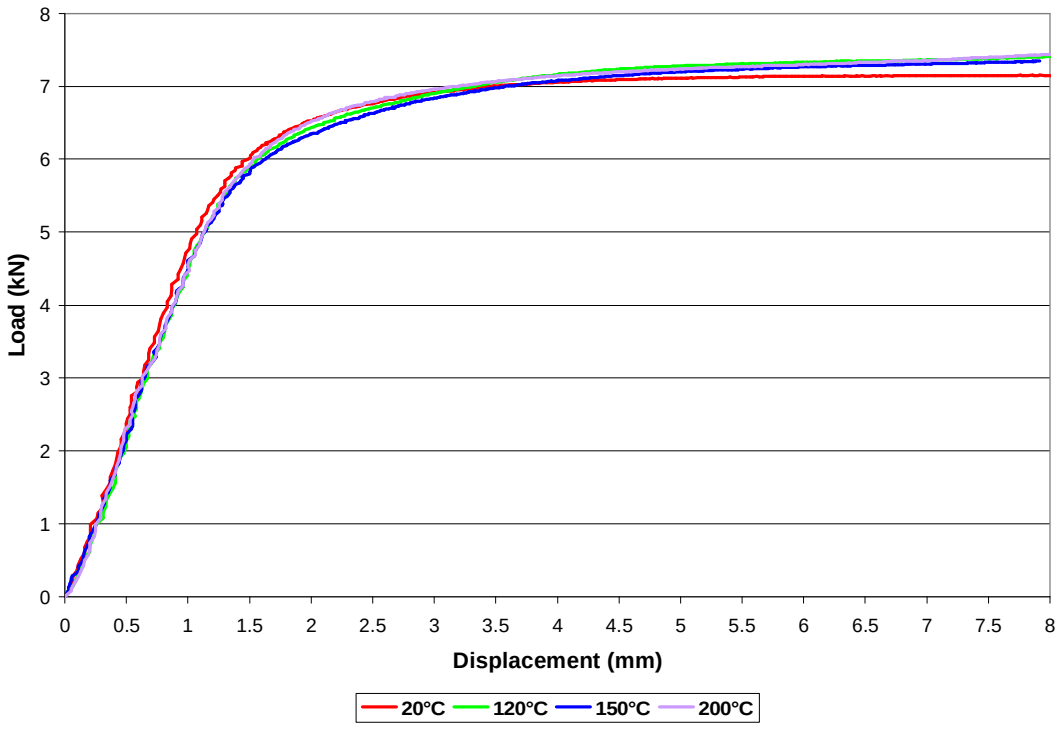

Figure C1: Bending curves for M12 bolts tested at different temperatures.

Appendix C.3 – Calculated Bolt Yield Moment at Elevated Temperature

Table C1: Calculated bolt yield moment at elevated temperature according to NZS 3404.

Temperature	Strength Factor	Yield Load	Yield Moment
°C		kN	kN mm
0	1.0000	6.60	165.00
20	1.0000	6.60	165.00
50	1.0000	6.60	165.00
100	1.0000	6.60	165.00
150	1.0000	6.60	165.00
200	1.0000	6.60	165.00
215	1.0000	6.60	165.00
250	0.9489	6.26	156.57
300	0.8759	5.78	144.53
350	0.8029	5.30	132.48
400	0.7299	4.82	120.44
450	0.6569	4.34	108.39
500	0.5839	3.85	96.35
550	0.5109	3.37	84.31
600	0.4380	2.89	72.26
650	0.3650	2.41	60.22
700	0.2920	1.93	48.18
750	0.2190	1.45	36.13
800	0.1460	0.96	24.09
850	0.0730	0.48	12.04
900	0.0000	0.00	0.00

Appendix D – Temperature Profiles of Specimen in Fire

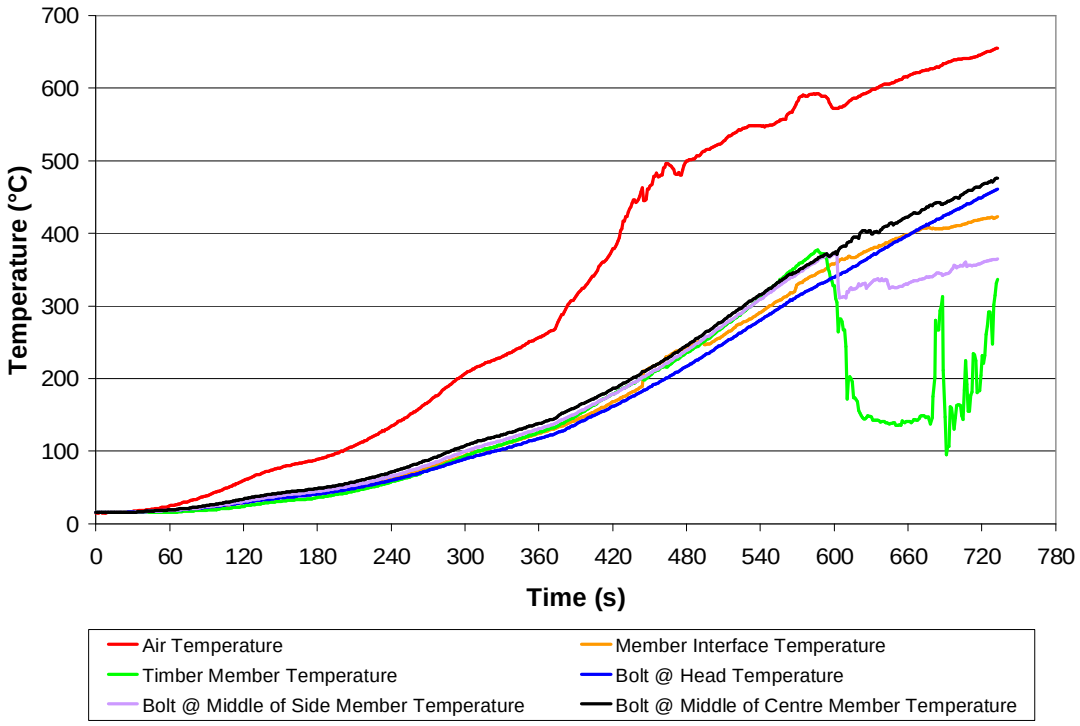

Figure D1: Temperature profiles for singly-bolted SWS connection exposed to fire.

The timber member temperature profile dropped 540 seconds after the furnace was turned on. The crushing on timber that caused the damaged on the thermocouple bead measuring the timber member profile is the most probable reason for the drop in temperature.

Appendix E – Failure load and failure mode prediction for fire exposed connections

Appendix E.1 – Overview

This appendix included the failure load and failure mode prediction calculations for fire exposed connections. The predicted embedment strength LVL was obtained from the bi-linear embedment strength relation and the bolt yield moment was calculated according to the values suggested by NZS 3404. Both the embedment strength and the bolt yield moment depend on the experimental bolt temperature. The residual timber thickness depends on the experimental charring rate.

Appendix E.2 – SWS Connections

Appendix E.2.1 – Singly-bolted SWS connections

TableE1: Prediction failure load and failure mode spreadsheet layout for fire exposed singly-bolted SWS connection.

Time	Bolt Temperature	Predicted Embedment Strength	Bolt Yield Moment	Timber Thickness	Failure Mode K	Failure Mode J/L	Failure Mode M	Applied Load	Difference between Predicted Failure Load of Mode J/L and Applied Load
min	°C	kN/mm²	kNmm	mm	kN	kN	kN	kN	kN
0.0	16.0	0.0813	165.00	63	25.80	30.74	36.48	6.78	23.96
0.3	16.0	0.0813	165.00	62.08	25.80	30.30	36.48	7.09	23.21
0.7	17.0	0.0808	165.00	61.16	25.71	29.65	36.36	6.92	22.73
1.0	19.5	0.0797	165.00	60.24	25.54	28.81	36.12	6.83	21.98
1.3	23.0	0.0775	165.00	59.32	25.19	27.60	35.62	6.73	20.87
1.7	28.0	0.0748	165.00	58.40	24.75	26.22	35.00	7.00	19.22
2.0	34.0	0.0716	165.00	57.48	24.20	24.69	34.23	6.84	17.84

2.3	40.0	0.0683	165.00	56.56	23.65	23.19	33.44	6.61	16.58
2.7	44.5	0.0662	165.00	55.64	23.27	22.09	32.91	6.40	15.69
3.0	49.0	0.0635	165.00	54.72	22.79	20.83	32.23	6.93	13.90
3.3	54.0	0.0608	165.00	53.80	22.30	19.61	31.53	6.87	12.74
3.7	62.0	0.0564	165.00	52.88	21.49	17.90	30.39	6.78	11.12
4.0	71.5	0.0515	165.00	51.96	20.54	16.07	29.04	6.82	9.25
4.3	82.0	0.0456	165.00	51.04	19.31	13.96	27.31	6.52	7.43
4.7	94.5	0.0391	165.00	50.12	17.88	11.75	25.29	6.73	5.02
5.0	107.5	0.0320	165.00	49.20	16.19	9.46	22.90	6.72	2.74
5.3	118.0	0.0261	165.00	48.28	14.61	7.56	20.66	6.49	1.07
5.7	128.0	0.0250	165.00	47.36	14.30	7.10	20.23	6.88	0.22
6.0	138.5	0.0250	165.00	46.44	14.30	6.97	20.23	6.71	0.26
6.3	153.0	0.0250	165.00	45.52	14.30	6.83	20.23	6.25	0.57
6.7	169.5	0.0250	165.00	44.60	14.30	6.69	20.23	6.51	0.18
7.0	186.5	0.0250	165.00	43.68	14.30	6.55	20.23	6.70	-0.14
7.3	203.5	0.0250	164.82	42.76	14.30	6.41	20.22	6.83	-0.42
7.7	224.0	0.0250	162.83	41.84	14.21	6.28	20.09	5.81	0.46
8.0	246.0	0.0250	157.53	40.92	13.98	6.14	19.76	6.73	-0.60
8.3	269.0	0.0250	151.99	40.00	13.73	6.00	19.41	7.10	-1.10
8.7	293.0	0.0250	146.21	39.08	13.46	5.86	19.04	6.06	-0.20
9.0	315.5	0.0250	140.91	38.16	13.22	5.72	18.69	6.67	-0.95
9.3	339.0	0.0250	135.13	37.24	12.94	5.59	18.31	6.57	-0.99
9.7	358.5	0.0250	130.55	36.32	12.72	5.45	17.99	7.35	-1.90
10.0	373.0	0.0250	126.94	35.40	12.55	5.31	17.74	6.49	-1.18
10.3	400.0	0.0250	120.44	34.48	12.22	5.17	17.28	6.87	-1.70
10.7	409.0	0.0250	118.27	33.56	12.11	5.03	17.13	6.66	-1.63
11.0	423.5	0.0250	114.90	32.64	11.94	4.90	16.88	6.80	-1.90
11.3	440.0	0.0250	110.80	31.72	11.72	4.76	16.58	6.72	-1.96
11.7	448.5	0.0250	108.88	30.80	11.62	4.62	16.43	6.39	-1.77
12.0	467.0	0.0250	104.30	29.88	11.37	4.48	16.08	6.84	-2.36

Appendix E.2.2 – Multi-bolted SWS connection

Table E2: Prediction failure load and failure mode spreadsheet layout for fire exposed multi-bolted SWS connection.

Time	Bolt Temperature	Predicted Crushing Strength	Bolt Moment	Timber Thickness	Failure Mode K	Failure Mode J/L	Failure Mode M	Applied Load	Applied Load per bolt	Difference between Predicted Failure Load of Mode J/L and Applied Load
Min	°C	kN/mm²	kNmm	mm	kN	kN	kN	kN	kN	kN
0.0	16.00	0.0813	165.00	63	25.80	30.74	36.48	22.56	5.64	25.10
0.3	16.00	0.0813	165.00	62.17	25.80	30.34	36.48	23.10	5.77	24.57
0.7	16.00	0.0813	165.00	61.35	25.80	29.94	36.48	23.06	5.76	24.17
1.0	16.00	0.0813	165.00	60.52	25.80	29.53	36.48	23.29	5.82	23.71
1.3	16.50	0.0813	165.00	59.69	25.80	29.13	36.48	23.15	5.79	23.34
1.7	18.00	0.0803	165.00	58.87	25.63	28.34	36.24	23.38	5.85	22.50
2.0	19.75	0.0797	165.00	58.04	25.54	27.76	36.12	22.78	5.70	22.06
2.3	23.25	0.0775	165.00	57.21	25.19	26.62	35.62	22.91	5.73	20.89
2.7	27.50	0.0754	165.00	56.39	24.84	25.50	35.12	23.06	5.76	19.74
3.0	32.25	0.0727	165.00	55.56	24.39	24.22	34.49	22.76	5.69	18.54
3.3	35.75	0.0710	165.00	54.73	24.11	23.33	34.10	22.80	5.70	17.63
3.7	39.00	0.0689	165.00	53.91	23.74	22.28	33.57	22.90	5.73	16.55
4.0	43.75	0.0667	165.00	53.08	23.36	21.25	33.04	23.23	5.81	15.44
4.3	50.00	0.0629	165.00	52.25	22.69	19.73	32.09	23.24	5.81	13.92
4.7	57.25	0.0591	165.00	51.43	22.00	18.24	31.11	23.16	5.79	12.45
5.0	65.75	0.0548	165.00	50.60	21.17	16.63	29.95	22.89	5.72	10.91
5.3	76.00	0.0488	165.00	49.77	19.99	14.58	28.27	22.64	5.66	8.92
5.7	85.50	0.0440	165.00	48.95	18.97	12.91	26.82	22.60	5.65	7.26
6.0	93.50	0.0396	165.00	48.12	18.01	11.44	25.47	22.22	5.55	5.89
6.3	102.50	0.0348	165.00	47.29	16.86	9.86	23.85	22.62	5.65	4.21
6.7	112.00	0.0293	165.00	46.47	15.49	8.18	21.91	22.29	5.57	2.60
7.0	126.25	0.0250	165.00	45.64	14.30	6.85	20.23	22.64	5.66	1.19
7.3	142.25	0.0250	165.00	44.81	14.30	6.72	20.23	23.42	5.86	0.87

7.7	158.75	0.0250	165.00	43.99	14.30	6.60	20.23	22.90	5.73	0.87
8.0	176.75	0.0250	165.00	43.16	14.30	6.47	20.23	23.09	5.77	0.70
8.3	195.75	0.0250	165.00	42.33	14.30	6.35	20.23	22.99	5.75	0.60
8.7	216.50	0.0250	164.04	41.51	14.26	6.23	20.17	23.29	5.82	0.40
9.0	238.00	0.0250	159.46	40.68	14.06	6.10	19.88	23.47	5.87	0.23
9.3	259.00	0.0250	154.40	39.85	13.84	5.98	19.57	22.77	5.69	0.29
9.7	281.00	0.0250	149.10	39.03	13.60	5.85	19.23	22.69	5.67	0.18
10.0	302.75	0.0250	144.04	38.20	13.36	5.73	18.90	22.83	5.71	0.02
10.3	324.75	0.0250	138.74	37.37	13.12	5.61	18.55	23.03	5.76	-0.15
10.7	345.75	0.0250	133.69	36.55	12.87	5.48	18.21	22.72	5.68	-0.20
11.0	367.00	0.0250	128.39	35.72	12.62	5.36	17.84	23.06	5.76	-0.41
11.3	382.50	0.0250	124.77	34.89	12.44	5.23	17.59	23.53	5.88	-0.65
11.7	396.25	0.0250	121.40	34.07	12.27	5.11	17.35	22.76	5.69	-0.58
12.0	413.25	0.0250	117.31	33.24	12.06	4.99	17.06	23.36	5.84	-0.85
12.3	430.00	0.0250	113.21	32.41	11.85	4.86	16.75	21.74	5.44	-0.57
12.7	447.00	0.0250	109.12	31.59	11.63	4.74	16.45	20.81	5.20	-0.47
13.0	459.25	0.0250	106.23	30.76	11.48	4.61	16.23	22.56	5.64	-1.03
13.3	473.25	0.0250	102.85	29.93	11.29	4.49	15.97	20.51	5.13	-0.64

Appendix E.3 – WSW Connections

Appendix E.3.1 – Singly-bolted WSW connection

Table E3: Prediction failure load and failure mode spreadsheet layout for fire exposed singly-bolted WSW connection.

Time	Bolt Temperature	Predicted Crushing Strength	Bolt Moment	Timber Thickness	Failure Mode F	Failure Mode G	Failure Mode H	Applied Load	Difference between Predicted Failure Load of Mode F and Applied Load
Min	°C	kN/mm²	kNmm	mm	kN	kN	kN	kN	kN
0.0	15.0	0.0819	165.00	45	44.21	29.13	36.61	6.30	37.91
0.3	15.5	0.0819	165.00	44.47	43.70	28.93	36.61	6.22	37.48
0.7	16.5	0.0813	165.00	43.95	42.89	28.58	36.48	6.60	36.29
1.0	19.5	0.0797	165.00	43.42	41.53	27.94	36.12	6.60	34.93
1.3	25.0	0.0765	165.00	42.89	39.35	26.87	35.37	6.55	32.81
1.7	32.0	0.0727	165.00	42.37	36.94	25.68	34.49	6.45	30.49
2.0	43.0	0.0667	165.00	41.84	33.49	23.94	33.04	6.29	27.20
2.3	51.0	0.0624	165.00	41.31	30.92	22.67	31.95	6.19	24.73
2.7	54.0	0.0608	165.00	40.79	29.73	22.12	31.53	6.07	23.66
3.0	57.0	0.0591	165.00	40.26	28.56	21.58	31.11	5.96	22.60
3.3	63.0	0.0559	165.00	39.73	26.64	20.64	30.24	6.35	20.29
3.7	71.0	0.0515	165.00	39.21	24.25	19.44	29.04	6.34	17.91
4.0	80.5	0.0467	165.00	38.68	21.66	18.13	27.64	6.14	15.52
4.3	90.5	0.0413	165.00	38.15	18.89	16.70	25.98	6.36	12.52
4.7	103.0	0.0342	165.00	37.63	15.45	14.88	23.66	5.92	9.52
5.0	115.0	0.0277	165.00	37.10	12.34	13.19	21.29	6.07	6.27
5.3	122.0	0.0250	165.00	36.57	10.97	12.47	20.23	6.28	4.69
5.7	130.0	0.0250	165.00	36.05	10.81	12.46	20.23	6.32	4.50
6.0	145.0	0.0250	165.00	35.52	10.66	12.45	20.23	6.35	4.30
6.3	158.5	0.0250	165.00	34.99	10.50	12.45	20.23	6.29	4.21
6.7	170.0	0.0250	165.00	34.47	10.34	12.44	20.23	6.40	3.94

7.0	183.0	0.0250	165.00	33.94	10.18	12.44	20.23	6.32	3.87
7.3	198.5	0.0250	165.00	33.41	10.02	12.44	20.23	6.28	3.74
7.7	219.0	0.0250	163.86	32.89	9.87	12.39	20.16	6.32	3.55
8.0	239.5	0.0250	159.22	32.36	9.71	12.22	19.87	6.32	3.39
8.3	261.0	0.0250	153.92	31.83	9.55	12.01	19.54	6.16	3.39
8.7	283.5	0.0250	148.62	31.31	9.39	11.80	19.20	6.38	3.01
9.0	304.5	0.0250	143.56	30.78	9.23	11.60	18.87	6.27	2.97
9.3	326.0	0.0250	138.26	30.25	9.08	11.39	18.52	6.35	2.72
9.7	344.5	0.0250	133.93	29.73	8.92	11.21	18.22	6.34	2.58
10.0	364.5	0.0250	129.11	29.20	8.76	11.00	17.89	6.20	2.56
10.3	382.0	0.0250	124.77	28.67	8.60	10.82	17.59	6.34	2.26
10.7	399.5	0.0250	120.68	28.15	8.44	10.64	17.30	6.25	2.19
11.0	400.5	0.0250	120.44	27.62	8.29	10.63	17.28	6.50	1.79
11.3	401.0	0.0250	120.20	27.09	8.13	10.62	17.26	6.27	1.86
11.7	407.0	0.0250	118.75	26.57	7.97	10.56	17.16	6.41	1.56
12.0	412.0	0.0250	117.55	26.04	7.81	10.51	17.07	6.34	1.47
12.3	419.5	0.0250	115.86	25.51	7.65	10.44	16.95	6.52	1.13
12.7	428.5	0.0250	113.69	24.99	7.50	10.35	16.79	6.23	1.27
13.0	448.5	0.0250	108.88	24.46	7.34	10.13	16.43	6.28	1.06
13.3	465.5	0.0250	104.78	23.93	7.18	9.93	16.12	6.19	0.99
13.7	479.0	0.0250	101.41	23.41	7.02	9.78	15.86	6.28	0.74
14.0	492.5	0.0250	98.28	22.88	6.86	9.63	15.61	6.34	0.52
14.3	505.0	0.0250	95.15	22.35	6.71	9.48	15.36	6.28	0.43
14.7	512.5	0.0250	93.46	21.83	6.55	9.40	15.22	6.34	0.21
15.0	519.0	0.0250	91.77	21.30	6.39	9.32	15.09	6.27	0.12
15.3	543.5	0.0250	85.99	20.77	6.23	9.02	14.60	6.24	-0.01
15.7	550.5	0.0250	84.31	20.25	6.07	8.94	14.46	6.30	-0.23
16.0	556.0	0.0250	82.86	19.72	5.92	8.88	14.33	6.46	-0.55
16.3	565.0	0.0250	80.69	19.19	5.76	8.77	14.15	6.32	-0.56
16.7	568.0	0.0250	79.97	18.67	5.60	8.75	14.08	6.38	-0.78
17.0	568.5	0.0250	79.97	18.14	5.44	8.77	14.08	6.45	-1.01
17.3	557.5	0.0250	82.62	17.61	5.28	8.96	14.31	6.25	-0.97

17.7	560.0	0.0250	81.90	17.09	5.13	8.94	14.25	6.07	-0.94
18.0	565.0	0.0250	80.69	16.56	4.97	8.90	14.15	5.96	-0.99
18.3	569.0	0.0250	79.73	16.03	4.81	8.88	14.06	6.30	-1.49
18.7	577.5	0.0250	77.80	15.51	4.65	8.80	13.89	6.39	-1.74
19.0	585.0	0.0250	75.88	14.98	4.49	8.71	13.72	6.41	-1.92
19.3	585.5	0.0250	75.88	14.45	4.34	8.76	13.72	6.00	-1.66
19.7	588.5	0.0250	75.15	13.93	4.18	8.76	13.65	5.68	-1.50
20.0	591.0	0.0250	74.43	13.40	4.02	8.76	13.59	5.33	-1.31

Appendix E.3.2 – Multi bolted Connection

Table E4: Prediction failure load and failure mode spreadsheet layout for fire exposed multi-bolted WSW connection.

Time	Bolt Temperature	Predicted Crushing Strength	Bolt Moment	Timber Thickness	Failure Mode F	Failure Mode G	Failure Mode H	Applied Load	Applied Load per bolt	Difference between Predicted Failure Load of Mode F and Applied Load
Min	°C	kN/mm²	kNmm	mm	kN	kN	kN	kN	kN	kN
0.0	17.50	0.0808	165.00	45	43.63	28.82	36.36	22.63	5.66	37.97
0.3	17.75	0.0808	165.00	44.47	43.12	28.62	36.36	22.61	5.65	37.46
0.7	18.25	0.0803	165.00	43.95	42.32	28.28	36.24	22.64	5.66	36.66
1.0	19.75	0.0797	165.00	43.42	41.53	27.94	36.12	22.63	5.66	35.87
1.3	22.50	0.0781	165.00	42.89	40.19	27.31	35.75	22.53	5.63	34.56
1.7	26.75	0.0759	165.00	42.37	38.60	26.55	35.25	22.67	5.67	32.93
2.0	32.75	0.0727	165.00	41.84	36.48	25.52	34.49	22.40	5.60	30.89
2.3	39.25	0.0689	165.00	41.31	34.15	24.37	33.57	22.49	5.62	28.52
2.7	43.25	0.0667	165.00	40.79	32.65	23.66	33.04	22.44	5.61	27.04
3.0	46.00	0.0651	165.00	40.26	31.44	23.11	32.64	22.56	5.64	25.80
3.3	49.25	0.0635	165.00	39.73	30.26	22.56	32.23	22.42	5.60	24.65
3.7	54.00	0.0608	165.00	39.21	28.58	21.76	31.53	22.83	5.71	22.87
4.0	60.25	0.0575	165.00	38.68	26.69	20.84	30.68	22.51	5.63	21.06
4.3	68.25	0.0532	165.00	38.15	24.34	19.67	29.50	22.35	5.59	18.76
4.7	77.75	0.0483	165.00	37.63	21.80	18.39	28.11	22.39	5.60	16.21
5.0	89.50	0.0418	165.00	37.10	18.61	16.73	26.15	22.64	5.66	12.95
5.3	109.50	0.0310	165.00	36.57	13.59	14.00	22.51	22.69	5.67	7.91
5.7	129.25	0.0250	165.00	36.05	10.81	12.46	20.23	22.18	5.55	5.27
6.0	147.00	0.0250	165.00	35.52	10.66	12.45	20.23	22.53	5.63	5.02
6.3	167.50	0.0250	165.00	34.99	10.50	12.45	20.23	22.78	5.69	4.80
6.7	189.00	0.0250	165.00	34.47	10.34	12.44	20.23	22.83	5.71	4.63
7.0	211.50	0.0250	164.34	33.94	10.18	12.41	20.19	22.51	5.63	4.55
7.3	234.75	0.0250	160.42	33.41	10.02	12.27	19.94	22.61	5.65	4.37

7.7	257.25	0.0250	154.88	32.89	9.87	12.05	19.60	22.34	5.58	4.28
8.0	276.50	0.0250	150.31	32.36	9.71	11.87	19.31	22.30	5.57	4.13
8.3	298.50	0.0250	145.01	31.83	9.55	11.66	18.96	22.51	5.63	3.92
8.7	318.25	0.0250	140.19	31.31	9.39	11.47	18.64	22.49	5.62	3.77
9.0	339.00	0.0250	135.13	30.78	9.23	11.26	18.31	22.72	5.68	3.55
9.3	358.00	0.0250	130.55	30.25	9.08	11.07	17.99	22.61	5.65	3.42
9.7	372.75	0.0250	127.18	29.73	8.92	10.92	17.76	22.78	5.69	3.22
10.0	387.75	0.0250	123.57	29.20	8.76	10.76	17.50	22.49	5.62	3.14
10.3	405.00	0.0250	119.23	28.67	8.60	10.57	17.19	22.39	5.60	3.01
10.7	424.00	0.0250	114.66	28.15	8.44	10.37	16.86	22.39	5.60	2.85
11.0	438.50	0.0250	111.28	27.62	8.29	10.21	16.61	22.29	5.57	2.71
11.3	458.50	0.0250	106.47	27.09	8.13	9.99	16.25	22.67	5.67	2.46
11.7	475.25	0.0250	102.37	26.57	7.97	9.80	15.93	22.74	5.68	2.29
12.0	495.00	0.0250	97.55	26.04	7.81	9.56	15.55	22.73	5.68	2.13
12.3	509.25	0.0250	94.18	25.51	7.65	9.40	15.28	22.44	5.61	2.05
12.7	527.25	0.0250	89.85	24.99	7.50	9.18	14.93	22.56	5.64	1.86
13.0	542.00	0.0250	86.23	24.46	7.34	8.99	14.62	22.30	5.57	1.76
13.3	552.75	0.0250	83.82	23.93	7.18	8.87	14.42	22.14	5.54	1.64
13.7	558.25	0.0250	82.38	23.41	7.02	8.79	14.29	22.25	5.56	1.46
14.0	570.00	0.0250	79.49	22.88	6.86	8.63	14.04	22.53	5.63	1.23
14.3	579.00	0.0250	77.32	22.35	6.71	8.51	13.85	22.03	5.51	1.20
14.7	586.50	0.0250	75.64	21.83	6.55	8.42	13.69	22.93	5.73	0.82
15.0	605.75	0.0250	71.06	21.30	6.39	8.16	13.27	23.49	5.87	0.52
15.3	612.75	0.0250	69.37	20.77	6.23	8.07	13.12	22.22	5.55	0.68
15.7	617.75	0.0250	68.17	20.25	6.07	8.00	13.00	23.75	5.94	0.14
16.0	622.00	0.0250	66.96	19.72	5.92	7.93	12.89	21.84	5.46	0.46
16.3	625.25	0.0250	66.24	19.19	5.76	7.90	12.82	22.97	5.74	0.02
16.7	629.00	0.0250	65.28	18.67	5.60	7.85	12.72	21.38	5.34	0.26
17.0	633.50	0.0250	64.31	18.14	5.44	7.80	12.63	22.09	5.52	-0.08
17.3	637.25	0.0250	63.35	17.61	5.28	7.75	12.53	21.71	5.43	-0.14

Appendix E.4 – WWW Connections

Appendix E.4.1 – Singly bolted Connection

Table E5: Prediction failure load and failure mode spreadsheet layout for fire exposed singly-bolted WWW connection.

Time	Bolt Temperature	Predicted Crushing Strength	Bolt Moment	Timber Thickness	Failure Mode G	Failure Mode H	Failure Mode J	Failure Mode K	Applied Load	Difference between Predicted Failure Load of Mode G and Applied Load
min	°C	kN/mm²	kNmm	mm	kN	kN	kN	kN	kN	kN
0.0	16.5	0.0813	165.00	45	43.92	30.74	53.81	25.80	4.71	39.21
0.3	17.5	0.0808	165.00	44.53	43.18	30.54	53.64	25.71	4.87	38.31
0.7	17.5	0.0808	165.00	44.07	42.72	30.54	53.79	25.71	4.91	37.81
1.0	17.5	0.0808	165.00	43.60	42.27	30.54	53.94	25.71	4.82	37.45
1.3	16.5	0.0813	165.00	43.13	42.10	30.74	54.41	25.80	5.01	37.09
1.7	17.5	0.0808	165.00	42.67	41.37	30.54	54.25	25.71	4.84	36.52
2.0	18.0	0.0803	165.00	42.20	40.64	30.33	54.10	25.63	4.91	35.72
2.3	19.0	0.0797	165.00	41.73	39.92	30.13	53.96	25.54	4.83	35.09
2.7	21.5	0.0786	165.00	41.27	38.94	29.72	53.50	25.37	5.01	33.92
3.0	27.5	0.0754	165.00	40.80	36.90	28.49	51.79	24.84	4.99	31.92
3.3	36.5	0.0705	165.00	40.33	34.12	26.65	49.13	24.02	4.91	29.21
3.7	46.0	0.0651	165.00	39.87	31.14	24.60	46.14	23.08	4.82	26.32
4.0	52.5	0.0618	165.00	39.40	29.23	23.37	44.43	22.49	4.73	24.50
4.3	55.5	0.0602	165.00	38.93	28.13	22.76	43.67	22.20	4.58	23.55
4.7	60.0	0.0575	165.00	38.47	26.54	21.74	42.27	21.69	4.42	22.12
5.0	66.0	0.0543	165.00	38.00	24.74	20.51	40.55	21.07	4.33	20.41
5.3	74.0	0.0499	165.00	37.53	22.48	18.87	38.17	20.21	5.16	17.32
5.7	82.0	0.0456	165.00	37.07	20.28	17.23	35.79	19.31	4.93	15.35
6.0	93.0	0.0396	165.00	36.60	17.40	14.98	32.39	18.01	4.91	12.49
6.3	106.0	0.0326	165.00	36.13	14.13	12.32	28.26	16.33	4.72	9.41
6.7	129.0	0.0250	165.00	35.67	10.70	9.45	23.66	14.30	4.25	6.45

7.0	152.5	0.0250	165.00	35.20	10.56	9.45	23.86	14.30	5.95	4.61
7.3	170.0	0.0250	165.00	34.73	10.42	9.45	24.07	14.30	5.59	4.83
7.7	190.0	0.0250	165.00	34.27	10.28	9.45	24.28	14.30	5.40	4.88
8.0	206.0	0.0250	164.64	33.80	10.14	9.45	24.48	14.29	5.03	5.11
8.3	223.0	0.0250	163.07	33.33	10.00	9.45	24.63	14.22	4.85	5.15
8.7	244.0	0.0250	158.01	32.87	9.86	9.45	24.60	14.00	5.05	4.81
9.0	261.0	0.0250	153.92	32.40	9.72	9.45	24.62	13.81	4.99	4.73
9.3	278.5	0.0250	149.82	31.93	9.58	9.45	24.64	13.63	5.03	4.55
9.7	297.0	0.0250	145.25	31.47	9.44	9.45	24.62	13.42	4.94	4.50
10.0	316.5	0.0250	140.67	31.00	9.30	9.45	24.61	13.21	4.67	4.63
10.3	338.5	0.0250	135.37	30.53	9.16	9.45	24.54	12.96	4.94	4.22
10.7	358.0	0.0250	130.55	30.07	9.02	9.45	24.50	12.72	4.75	4.27
11.0	378.0	0.0250	125.74	29.60	8.88	9.45	24.45	12.49	5.06	3.82
11.3	393.5	0.0250	122.12	29.13	8.74	9.45	24.47	12.31	4.99	3.75
11.7	407.5	0.0250	118.75	28.67	8.60	9.45	24.50	12.13	5.10	3.50
12.0	423.0	0.0250	114.90	28.20	8.46	9.45	24.50	11.94	5.05	3.41
12.3	444.5	0.0250	109.84	27.73	8.32	9.45	24.41	11.67	4.93	3.39
12.7	462.5	0.0250	105.50	27.27	8.18	9.45	24.36	11.44	4.89	3.29
13.0	483.0	0.0250	100.45	26.80	8.04	9.45	24.24	11.16	4.82	3.22
13.3	493.0	0.0250	98.04	26.33	7.90	9.45	24.33	11.02	4.91	2.99
13.7	512.0	0.0250	93.46	25.87	7.76	9.45	24.23	10.76	5.00	2.76
14.0	529.0	0.0250	89.36	25.40	7.62	9.45	24.16	10.53	5.06	2.56
14.3	549.0	0.0250	84.55	24.93	7.48	9.45	24.02	10.24	4.94	2.54
14.7	561.5	0.0250	81.66	24.47	7.34	9.45	24.05	10.06	4.94	2.40
15.0	576.5	0.0250	78.04	24.00	7.20	9.45	23.99	9.84	4.89	2.31
15.3	585.0	0.0250	75.88	23.53	7.06	9.45	24.08	9.70	4.87	2.19
15.7	597.5	0.0250	72.99	23.07	6.92	9.45	24.09	9.51	4.79	2.13
16.0	603.5	0.0250	71.54	22.60	6.78	9.45	24.25	9.42	4.79	1.99
16.3	614.5	0.0250	68.89	22.13	6.64	9.45	24.28	9.24	5.09	1.55
16.7	617.5	0.0250	68.17	21.67	6.50	9.45	24.54	9.19	5.07	1.43
17.0	627.0	0.0250	65.76	21.20	6.36	9.45	24.60	9.03	4.65	1.71

17.3	628.5	0.0250	65.52	20.73	6.22	9.45	24.94	9.01	4.80	1.42
17.7	635.5	0.0250	63.83	20.27	6.08	9.45	25.10	8.90	4.79	1.29
18.0	636.5	0.0250	63.59	19.80	5.94	9.45	25.47	8.88	4.78	1.16
18.3	644.0	0.0250	61.66	19.33	5.80	9.45	25.62	8.74	5.17	0.63
18.7	642.5	0.0250	62.15	18.87	5.66	9.45	26.13	8.78	4.98	0.68
19.0	649.5	0.0250	60.46	18.40	5.52	9.45	26.33	8.66	4.84	0.68
19.3	649.5	0.0250	60.46	17.93	5.38	9.45	26.82	8.66	4.99	0.39
19.7	655.0	0.0250	59.01	17.47	5.24	9.45	27.10	8.55	4.78	0.46
20.0	655.5	0.0250	59.01	17.00	5.10	9.45	27.63	8.55	4.56	0.54
20.3	660.5	0.0250	57.81	16.53	4.96	9.45	27.99	8.47	5.09	-0.13
20.7	662.5	0.0250	57.33	16.07	4.82	9.45	28.50	8.43	5.17	-0.35
21.0	668.0	0.0250	55.88	15.60	4.68	9.45	28.86	8.32	4.74	-0.06
21.3	667.0	0.0250	56.12	15.13	4.54	9.45	29.59	8.34	4.83	-0.29
21.7	670.5	0.0250	55.40	14.67	4.40	9.45	30.16	8.29	5.05	-0.65
22.0	667.5	0.0250	56.12	14.20	4.26	9.45	31.09	8.34	4.68	-0.42
22.3	666.5	0.0250	56.36	13.73	4.12	9.45	31.98	8.36	4.61	-0.49
22.7	662.5	0.0250	57.33	13.27	3.98	9.45	33.10	8.43	4.93	-0.95
23.0	661.0	0.0250	57.57	12.80	3.84	9.45	34.15	8.45	4.57	-0.73

Appendix E.4.2 – Multi bolted Connection

Table E6: Prediction failure load and failure mode spreadsheet layout for fire exposed multi-bolted WWW connection.

Time	Bolt Temperature	Predicted Crushing Strength	Bolt Moment	Timber Thickness	Failure Mode G	Failure Mode H	Failure Mode J	Failure Mode K	Applied Load	Applied Load per Bolt	Difference between Predicted Failure Load of Mode G and Applied Load
min	°C	kN/mm²	kNmm	mm	kN	kN	kN	kN	kN	kN	kN
0.0	16.0	0.0813	165.00	45	43.92	30.74	53.81	25.80	22.98	4.60	39.32
0.3	16.5	0.0813	165.00	44.53	43.46	30.74	53.96	25.80	22.97	4.59	38.87
0.7	17.5	0.0808	165.00	44.07	42.72	30.54	53.79	25.71	23.02	4.60	38.12
1.0	18.0	0.0803	165.00	43.60	41.99	30.33	53.62	25.63	22.63	4.53	37.46
1.3	20.5	0.0792	165.00	43.13	40.98	29.93	53.15	25.45	22.78	4.56	36.42
1.7	25.0	0.0765	165.00	42.67	39.15	28.90	51.74	25.01	23.23	4.65	34.50
2.0	30.0	0.0738	165.00	42.20	37.35	27.88	50.32	24.57	22.93	4.59	32.76
2.3	35.0	0.0710	165.00	41.73	35.58	26.85	48.91	24.11	22.89	4.58	31.00
2.7	39.0	0.0689	165.00	41.27	34.11	26.03	47.82	23.74	23.10	4.62	29.49
3.0	41.5	0.0678	165.00	40.80	33.19	25.63	47.36	23.55	22.97	4.59	28.60
3.3	46.5	0.0651	165.00	40.33	31.50	24.60	45.96	23.08	22.98	4.60	26.90
3.7	52.5	0.0618	165.00	39.87	29.58	23.37	44.24	22.49	23.02	4.60	24.98
4.0	59.5	0.0580	165.00	39.40	27.44	21.94	42.20	21.79	22.41	4.48	22.96
4.3	64.5	0.0553	165.00	38.93	25.85	20.92	40.79	21.28	23.14	4.63	21.22
4.7	72.0	0.0510	165.00	38.47	23.54	19.28	38.42	20.43	22.94	4.59	18.95
5.0	79.0	0.0472	165.00	38.00	21.53	17.84	36.35	19.65	22.73	4.55	16.98
5.3	91.5	0.0407	165.00	37.53	18.34	15.39	32.64	18.25	22.62	4.52	13.81
5.7	103.5	0.0342	165.00	37.07	15.22	12.93	28.87	16.73	22.75	4.55	10.67
6.0	115.5	0.0277	165.00	36.60	12.17	10.47	25.01	15.06	22.74	4.55	7.62
6.3	130.0	0.0250	165.00	36.13	10.84	9.45	23.47	14.30	23.08	4.62	6.22
6.7	146.0	0.0250	165.00	35.67	10.70	9.45	23.66	14.30	22.88	4.58	6.12
7.0	159.5	0.0250	165.00	35.20	10.56	9.45	23.86	14.30	22.67	4.53	6.03
7.3	175.5	0.0250	165.00	34.73	10.42	9.45	24.07	14.30	22.62	4.52	5.90

7.7	192.0	0.0250	165.00	34.27	10.28	9.45	24.28	14.30	23.03	4.61	5.67
8.0	206.5	0.0250	164.64	33.80	10.14	9.45	24.48	14.29	22.77	4.55	5.59
8.3	222.5	0.0250	163.31	33.33	10.00	9.45	24.64	14.23	22.93	4.59	5.41
8.7	242.5	0.0250	158.50	32.87	9.86	9.45	24.63	14.02	22.95	4.59	5.27
9.0	262.5	0.0250	153.68	32.40	9.72	9.45	24.61	13.80	22.68	4.54	5.18
9.3	287.5	0.0250	147.66	31.93	9.58	9.45	24.52	13.53	22.68	4.54	5.04
9.7	310.5	0.0250	142.12	31.47	9.44	9.45	24.45	13.27	22.51	4.50	4.94
10.0	332.0	0.0250	136.82	31.00	9.30	9.45	24.38	13.02	22.94	4.59	4.71
10.3	351.5	0.0250	132.24	30.53	9.16	9.45	24.35	12.80	22.90	4.58	4.58
10.7	347.0	0.0250	133.20	30.07	9.02	9.45	24.66	12.85	22.78	4.56	4.46
11.0	369.5	0.0250	127.91	29.60	8.88	9.45	24.58	12.59	22.60	4.52	4.36
11.3	389.5	0.0250	123.09	29.13	8.74	9.45	24.53	12.35	22.99	4.60	4.14
11.7	409.0	0.0250	118.27	28.67	8.60	9.45	24.47	12.11	22.99	4.60	4.00
12.0	429.0	0.0250	113.45	28.20	8.46	9.45	24.40	11.86	22.80	4.56	3.90
12.3	446.0	0.0250	109.36	27.73	8.32	9.45	24.37	11.64	22.97	4.59	3.73
12.7	463.5	0.0250	105.26	27.27	8.18	9.45	24.34	11.42	22.60	4.52	3.66
13.0	478.0	0.0250	101.65	26.80	8.04	9.45	24.33	11.23	22.73	4.55	3.49
13.3	497.0	0.0250	97.07	26.33	7.90	9.45	24.25	10.97	23.04	4.61	3.29
13.7	513.0	0.0250	93.22	25.87	7.76	9.45	24.21	10.75	22.79	4.56	3.20
14.0	538.5	0.0250	87.20	25.40	7.62	9.45	23.97	10.40	22.69	4.54	3.08
14.3	555.0	0.0250	83.10	24.93	7.48	9.45	23.89	10.15	22.82	4.56	2.92
14.7	577.5	0.0250	77.80	24.47	7.34	9.45	23.68	9.82	22.99	4.60	2.74
15.0	589.5	0.0250	74.91	24.00	7.20	9.45	23.68	9.64	23.22	4.64	2.56
15.3	608.5	0.0250	70.34	23.53	7.06	9.45	23.50	9.34	22.74	4.55	2.51
15.7	619.0	0.0250	67.69	23.07	6.92	9.45	23.52	9.16	22.65	4.53	2.39
16.0	632.5	0.0250	64.55	22.60	6.78	9.45	23.47	8.95	22.90	4.58	2.20
16.3	638.5	0.0250	63.11	22.13	6.64	9.45	23.61	8.85	23.12	4.62	2.02
16.7	646.5	0.0250	61.18	21.67	6.50	9.45	23.70	8.71	23.52	4.70	1.80
17.0	647.5	0.0250	60.94	21.20	6.36	9.45	24.00	8.69	22.92	4.58	1.78
17.3	649.5	0.0250	60.46	20.73	6.22	9.45	24.29	8.66	22.74	4.55	1.67
17.7	657.0	0.0250	58.53	20.27	6.08	9.45	24.39	8.52	22.68	4.54	1.54

18.0	661.0	0.0250	57.57	19.80	5.94	9.45	24.63	8.45	22.89	4.58	1.36
18.3	669.5	0.0250	55.64	19.33	5.80	9.45	24.74	8.31	22.63	4.53	1.27
18.7	669.5	0.0250	55.64	18.87	5.66	9.45	25.15	8.31	22.93	4.59	1.07
19.0	678.0	0.0250	53.47	18.40	5.52	9.45	25.24	8.14	23.31	4.66	0.86
19.3	678.0	0.0250	53.47	17.93	5.38	9.45	25.69	8.14	24.29	4.86	0.52
19.7	685.5	0.0250	51.79	17.47	5.24	9.45	25.87	8.01	22.97	4.59	0.65
20.0	685.5	0.0250	51.79	17.00	5.10	9.45	26.37	8.01	22.53	4.51	0.59
20.3	691.5	0.0250	50.34	16.53	4.96	9.45	26.62	7.90	23.80	4.76	0.20
20.7	692.0	0.0250	50.10	16.07	4.82	9.45	27.13	7.88	23.21	4.64	0.18
21.0	699.5	0.0250	48.42	15.60	4.68	9.45	27.37	7.75	22.56	4.51	0.17
21.3	696.5	0.0250	49.14	15.13	4.54	9.45	28.14	7.81	23.12	4.62	-0.08
21.7	702.0	0.0250	47.69	14.67	4.40	9.45	28.49	7.69	21.97	4.39	0.01
22.0	700.5	0.0250	48.18	14.20	4.26	9.45	29.30	7.73	22.78	4.56	-0.30
22.3	705.0	0.0250	46.97	13.73	4.12	9.45	29.77	7.63	21.78	4.36	-0.24
22.7	702.0	0.0250	47.69	13.27	3.98	9.45	30.76	7.69	22.46	4.49	-0.51
23.0	708.5	0.0250	46.25	12.80	3.84	9.45	31.26	7.57	18.91	3.78	0.06

Appendix F – Photo Gallery of Testing Specimens

Appendix F.1 – SWS Connection Heated Tests

20°C SWS

80°C SWS

100°C SWS

120°C SWS

150°C SWS

200°C SWS

250°C SWS

250°C Pre

250°C Post

Figure F1: Dissembled SWS connections tested under constant temperature.

Appendix F.2 – WSW Connection Heated Tests

20°C WSW

80°C WSW

100°C WSW

120°C WSW

150°C WSW

200°C WSW

250°C WSW

Figure F2: Dissembled WSW connections tested under constant temperature.

Appendix F.3 – WWW Connection Heated Tests

20°C WWW

80°C WWW

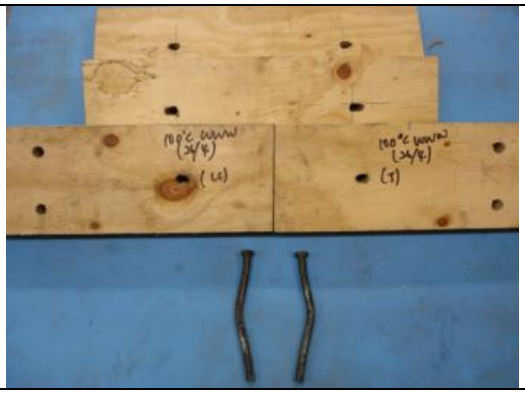

100°C WWW

120°C WWW

150°C WWW

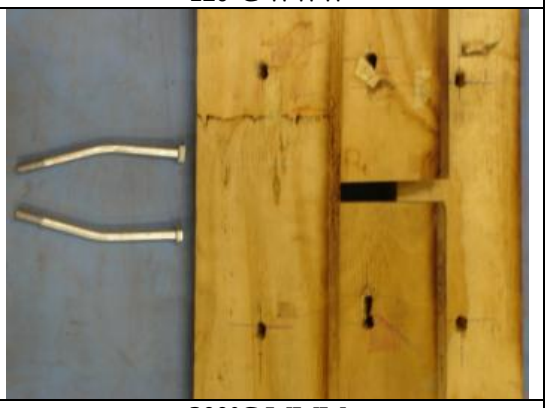

200°C WWW

250°C WWW

Figure F3: Dissembled WWW connections tested under constant temperature.

Appendix F.4 – Fire Tests

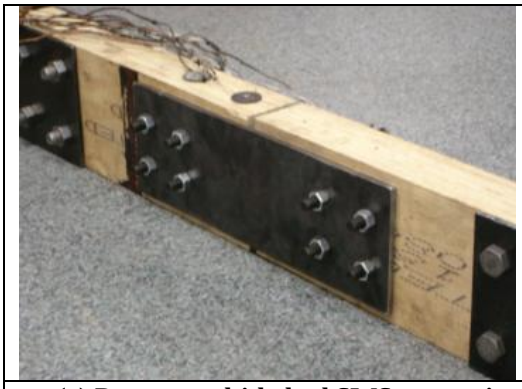

(a) Pre test multi-bolted SWS connection

(b) Post test multi-bolted SWS connection

(c) Pre test multi-bolted WSW connection

(d) Post test multi-bolted WSW connection

(e) Pre test multi-bolted WWW connection

(f) Post test multi-bolted WWW connection

Figure F4: Dissembled connection tested under fire conditions.

Appendix G – Cumulated Energy Calculation for ISO 834 Fire Curve

Table G1: Cumulated energy calculations for ISO 834 fire curve.

Time		Temperature		Energy	Cumulated Energy	
sec	min	°C	K	J/m²	J/m²	kJ/m²
0	0.0	15.00	288.0	0.00E+00	0.00E+00	0.00E+00
30	0.5	256.1	529.1	2.22E+03	2.22E+03	2.22E+00
60	1.0	344.2	617.2	4.11E+03	6.34E+03	6.34E+00
90	1.5	399.3	672.3	5.79E+03	1.21E+04	1.21E+01
120	2.0	439.5	712.5	7.31E+03	1.94E+04	1.94E+01
150	2.5	471.2	744.2	8.69E+03	2.81E+04	2.81E+01
180	3.0	497.3	770.3	9.98E+03	3.81E+04	3.81E+01
210	3.5	519.5	792.5	1.12E+04	4.93E+04	4.93E+01
240	4.0	538.9	811.9	1.23E+04	6.16E+04	6.16E+01
270	4.5	556.0	829.0	1.34E+04	7.50E+04	7.50E+01
300	5.0	571.4	844.4	1.44E+04	8.94E+04	8.94E+01
330	5.5	585.4	858.4	1.54E+04	1.05E+05	1.05E+02
…	…	…	…	…	…	…
…	…	…	…	…	…	…
1500	25.0	809.6	1082.6	3.89E+04	1.24E+06	1.24E+03
1530	25.5	812.6	1085.6	3.94E+04	1.27E+06	1.27E+03
1560	26.0	815.5	1088.5	3.98E+04	1.31E+06	1.31E+03
1590	26.5	818.3	1091.3	4.02E+04	1.35E+06	1.35E+03
1620	27.0	821.1	1094.1	4.06E+04	1.40E+06	1.40E+03
1650	27.5	823.8	1096.8	4.10E+04	1.44E+06	1.44E+03
1680	28.0	826.5	1099.5	4.14E+04	1.48E+06	1.48E+03
1710	28.5	829.1	1102.1	4.18E+04	1.52E+06	1.52E+03
1740	29.0	831.7	1104.7	4.22E+04	1.56E+06	1.56E+03
1770	29.5	834.3	1107.3	4.26E+04	1.60E+06	1.60E+03
1800	30.0	836.8	1109.8	4.30E+04	1.65E+06	1.65E+03

Appendix H – Experimental LVL Embedment Strength Calculation Spreadsheet

This appendix is a copy of experimental embedment strength calculation spreadsheet for ambient and heated SWS connections. The bolt temperature, the experimental failure mode, and the experimental load at total displacement of 10mm were obtained from the ambient and heated test results. The centre timber member thickness, bolt diameter and the rope effect factor were assumed to be 63mm, 12mm and 1.25 respectively. The bolt yield moment was the experimental result from the conducted bending test.

Table H1: Experimental LVL embedment strength calculation.

Environment Temperature	°C	**20**	**80**	**100**	**120**	**150**	**200**	**250**
Bolt Temperature	°C	18	59	73	90	114	153	199
Experimental Failure Mode	[-]	**M**	**M**	**M**	**M**	**M**	**K**	**K**
Experimental Resistance at total displacement of 10mm	kN	36.3	33.35	32.71	26.86	22.01	22.58	23.17
Experimental Bolt Yield Moment	kNmm	165	165	165	165	165	165	165
Centre Timber Member Thickness	mm	63	63	63	63	63	63	63
Side Steel Member Thickness	mm	6	6	6	6	6	6	6
Bolt Diameter	mm	12	12	12	12	12	12	12
Rope Effect Factor	[-]	1.25	1.25	1.25	1.25	1.25	1.25	1.25
Experimental Calculated Embedment Strength	kN/mm²	0.0805	0.0680	0.0654	0.0441	0.0296	0.0623	0.0656
Using Experimental Embedment Strength,								
Resistance for Failure Mode J or L	kN	30.43	25.69	24.71	16.66	11.19	23.55	24.80
Resistance for Failure Mode K	kN	25.67	23.58	23.13	18.99	15.56	22.58	23.17
Resistance for Failure Mode M	kN	36.30	33.35	32.71	26.86	22.01	31.93	32.77